

Supplementary Information

Paleolithic DNA from the Caucasus reveals core of West Eurasian ancestry

Table of Contents

SI 1 – Archaeological description of Dzudzuana Cave and origin of specimens used for ancient DNA	1–12
SI 2 – An admixture graph model of Upper Paleolithic West Eurasians	13–35
SI 3 – Quantifying admixture in ancient populations without an explicit phylogenetic model	36–47
SI 4 – Ancestral proportions of West Eurasians and North Africans	48–65
SI 5 – Dilution of Neandertal ancestry in West Eurasians	66–75

Archaeological description of Dzudzuana Cave and origin of specimens used for ancient DNA

Dzudzuana cave is located in the Chiatura region, western Georgia, in the foothills of the Caucasus Mountains, close to other recently excavated Palaeolithic sites (e.g., Ortvale Klde, Bondi, Satsurbli, and see below). Two series of excavations were conducted on site. The first took place between 1966–75, directed by D. Tushabramishvili (Tbilisi National Museum, Georgia). It covered an area of ca. 40m² near the cave entrance which was excavated down to the bedrock. The excavations were carried out using the methodologies of that time without sediment sieving. The stratigraphy exposed comprised two main components: an Upper Eneolithic sequence on top of an Upper Palaeolithic one (Liubin 1989). The second series of excavations, part of an international project of exploring Middle and Upper Palaeolithic in Georgia, was directed by T. Mesheveliani (Tbilisi National Museum), O. Bar-Yosef (Harvard University) and A. Belfer-Cohen (The Hebrew University of Jerusalem) took place in 1996–2008 exposing a similar sequence of Upper Palaeolithic occurrences capped by Eneolithic ones (for a detailed description of the excavations see Bar-Yosef et al. 2011).

A special effort was made to correlate the results from the two campaigns of excavations, the later excavations using the same grid as that of Tushabramishvili, and confronted the differences that arose through different techniques of recovery and scale of excavation. Two areas were excavated: the first, an extension of Tushabramishvili's excavations near the entrance of the cave (squares F–I 9–7 and J–K 12–11), termed the 'lower area' (LA) and the second, an 'upper area' (UA), comprising squares G–H 24–21, 19–15. The total excavated surface was c. 24m². The depth of the excavated deposits in LA was 4.5m while that at UA was 3.25m. The basic units of excavation were 50mm-thick quadrants of 0.5 × 0.5m, within a 1×1m grid. The excavated deposits were wet-sieved, dried and later hand-picked in order to retrieve the smallest archaeological components.

The Upper Palaeolithic (UP) archaeological sequence in the LA was subdivided into four main stratigraphic units (A–D). In the UA we could observe only part of this sequence, namely Units D and C with rare residues of B at the top.

Overall, the sediments in the cave consist of differing proportions of silty clay that vary locally in bedding, colour or rock content. There was a general shift in the type of sediment from Units D and C (mudflow deposits) into Unit B (secondary clay accumulations due to dripping water or groundwater). Studies suggest that the deposit derived from both the inside of the cave (some rockfall and clay) and the outside, from streams (rounded gravel and sandy ‘foreign’ lithologies, as well as some clay).

The teeth which provided the genetic data discussed in the present paper (and published in Margherita et al. 2017) derive from Unit C (Extended Data Fig. 1), one from the UA (sub-unit C4) and the other from the LA, which stratigraphically overlies Unit D (dated to 34-32 ka cal BP) and is overlain by Unit B (dated to 16.5-13.2 ka cal BP). Both teeth are deciduous molars (Margherita et al. 2017). Dzu 2 (I2949), recovered from square H16b (390-395cm), is an upper right 2nd molar (Rdm²) and Dzu 3 (I2963), recovered from square I8b (585-600cm), is a lower right 2nd molar (Rdm2). They both represent just a part of the tooth, namely a complete crown and a cervical quarter of the root. Both are heavily worn and through detailed testing (see *ibid.*) it is quite clear that they do not belong to the same individual. Unit C is dated to 27-24 ka cal BP based on 12 radiocarbon determinations (see Bar-Yosef et al. 2011). Additional radiocarbon determinations were obtained from The Penn State Radiocarbon 14C laboratory, and are reported in Table S1. Extended Data Fig. 1 provides the calibrated OxCal results for the new dates (upper part) and compared to the calibrated reported dates for Unit C (Bar-Yosef et al. 2011). These dates have a max-min range (2 SD, calibrated), of 25,560-23,279 cal BP.

Unit C was subdivided, on the basis of changes in the nature of its clayey deposit and the inclusions of small limestone fragments in the UA, into five sub-units numbered from top to bottom as C1 to C5. Still, archaeologically, there is no difference between the assemblages of these sub-units as well as between the assemblages of LA and UA. One should note that no distinct spatial distribution was observed in Unit C in both areas as well as any remains other than those described below, namely lithics, bone tools, some ornaments, flax fibers and faunal remains.

Table S1. New radiocarbon determinations for Dzudzuana Cave, Layer C/C4 Lower and Upper Areas.

PSUAMS#	Sample ID	Description	Material	¹⁴ C age (BP)	±	δ ¹³ C (‰)	δ ¹⁵ N (‰)	%C	%N	C:N
4041	DC97	Lower area Sq I9C, 590-595, Layer C, Basket #97	Animal bone	21690	180	-19.24	6.32	42.24	15.32	3.22
4042	DC206	Lower area, Sq I8a, 585-600, Layer C, Basket #206	Animal bone	21690	180	-18.43	6.39	41.25	14.79	3.25
4043	DC207	Lower area, Sq I8a, 600-605, Layer C, Basket 207	Animal bone	21720	180	-18.93	6.92	37.16	13.28	3.26
4044	DC226	Lower area, Sq I8b, 600-605, Layer C, Basket 226	Animal bone	22790	210	-19.50	4.92	39.77	14.36	3.23
4045	DC202	Upper area, Sq H16b, 390-395, Layer C4, Basket202	Animal bone	21410	180	-19.04	5.48	20.80	7.60	3.19
4046	DC259	Upper area, Sq H16c, 395-400, Layer C4, Basket 259	Animal bone	21560	180	-20.03	6.23	39.60	14.10	3.28
4047	DC260	Upper area, Sq H16d, 395-400, Layer C, Basket 260	Animal bone	21400	170	-18.99	5.70	22.06	8.08	3.19
4048	DC217	Upper area, Sq H16d, 390-395, Layer C4, Basket 217	Animal bone	21260	170	-19.16	5.64	42.55	15.36	3.23

Most of the findings comprise lithic artefacts, the majority made of local chert (radiolarite) and a minority – of obsidian. Here there is a difference between the LA and UA areas as in LA obsidian tools comprise ca. 4% of the assemblage versus ca. 1% in the UA, though there is no obvious difference between the areas in the numbers of obsidian cores and debitage. The lithic assemblage, comprising cores, production debitage, chips, chunks and tool, is the largest of its kind currently known in the Caucasus, comprising ca. 10,000 tools and ca. 80,000 debitage and cores, not to mention the chunks and chips categories (and see Bar-Yosef et al. 2011). The lithic technology is mainly characterised by a reduction sequence based on narrow carinated cores, producing small blades and bladelets. Carinated cores were often seen as an Aurignacian characteristic; however, there is no justification (either technological or typological) for associating this assemblage with the Aurignacian tradition of western Europe (and see further below). Indeed, in the past UP industries similar to that of Unit C were mistakenly referred to as Aurignacian. Detailed lithic studies, as well as the absolute dating, preclude such an association. The majority of tools are retouched bladelets, comprising more than 40%. It is of interest to note that up to ca. 32% of those from the UA are of the narrow variety — less than 3 mm in width and ca. 18% are 3–5 mm wide.

A unique characteristic of Unit C (mainly sub-units C2–4) in the UA is the Sakajia point (Bader 1965). This is an arched/curved pointed blade with abrupt retouch (never bipolar) along the straight edge and a proximal retouched truncation. The blanks were removed from unidirectional cores. Although their shape is reminiscent of Gravette points they differ technologically. Though they are present in small numbers (ca. 1%) one can actually observe in the assemblages of the following Unit B the transformation of the Sakajia point into microgravettes (to be later, chronologically, replaced by asymmetric triangles). All of

these tool types exhibit a straight lateral edge shaped by varieties of abrupt retouch combined with basal truncation.

Endscrapers are quite numerous (ca. 19%) and outnumber burins. They greatly vary in form and type, as well as in their blank types.

Unit C is also the richest, among the archaeological units identified in Dzudzuana, in more unique finds, such as flax fibers (Kvavadze et al. 2009) used most probably for clothing, incorporating dyed (blue, green and pink) fibers as well as knitted string with numerous knots.

Other unique finds incorporate stone, bone and teeth pendants (Bar-Yosef et al. 2011). There are also other decorated items, incised pieces, sometimes with elaborate patterns. There is quite a number of bone artefacts (200<), most of which are awl/point varieties made by a shaving technique, mostly on splinters, with polishing as the last phase of shaping. Of interest are antler bipoints which are much thicker and robust than the ones made on bone. Other categories are represented by single specimens, such as a bone needle with an ‘eye’, a polisher made of a bovid rib, a rib spatula, and a ‘retoucher’ made on a bone splinter (13x3 cm).

The pollen spectra of Unit C are indicative of warm and wet conditions (more than Unit D), as the arboreal pollen is dominated by trees adapted to warm and wet conditions. This is further supported by the presence of forest ferns and fungi spores, which actually negates the assignment of Unit C on the whole to the Last Glacial Maximum (LGM) (E. Kvavadze in Bar-Yosef et al. 2011) (but see the conclusions drawn from the fauna).

The small mammal assemblage of Unit C overall confirms the paleo-botanical reconstruction and points to a mosaic habitat of open grassland with the presence of closed woodland vegetation. Yet it seems that already during the accumulation of Unit C1 forest coverage and local wetland habitat around the cave diminished, as indicated by reduction of species diversity and increase of taxa that are affiliated with grassland and cooler and dryer environment (Belmaker et al. 2016).

Though the larger mammal are rough indicators to the paleo-ecological settings it is worth mentioning that in Unit C the large bovids, aurochs (*Bos primigenius*) and steppe bison

(*Bison priscus*), outnumber the Caucasian tur (*Capra caucasica*). On the other hand, in the earlier phase in the cave (Unit D), the proportions of the Caucasian tur are higher, while in the later occupation phase (Unit B) the proportions of large bovids and tur are even. The presence of tur and to some extent the steppe bison is indicative of cool and more open landscape; the presence of aurochs indicates a more temperate and temperate forest conditions. Still, however, the species frequency did not seem to change profoundly overtime (Bar-Oz et al. 2004). Comparison with the nearby Late Middle Palaeolithic (LMP) and UP layers at Ortvale Klde reveal species representation similar to the earlier phase of Dzudzuana (Unit D), with Caucasian tur being the most abundant prey species in the LMP and Early UP layers (Bar-Oz & Adler, 2005; Adler et al., 2006). Comparison with a contemporaneous site nearby, the Satsurbliia Cave (Pinhasi et al. 2014) suggests a high spatial-temporal mosaic habitat in the region. A somewhat similar breakdown of taxa was also identified in the Mesolithic site of Kotias Klde (Bar-Oz et al. 2009).

Comparisons: The two Georgian assemblages traditionally assigned to the early UP are Sagvardjile cave layer V and the assemblage from Samerzkhle Klde site (Liubin 1989). Still it seems that the lithics of these assemblages comprise a mixture of earlier and later UP material and indeed the carinated cores ('rabots') from Sagvardjile layer V as well as the date obtained on a bone from the same assemblage of ca. 24 ka cal BP (Nioradze & Otte 2000) indicate a possible contemporaneity with Unit C at Dzudzuana, though there are also other indications for a similarity between this assemblage and Dzudzuana Unit B. Thus it seems that no comparisons are possible with assemblages excavated before the introduction of modern excavation methodologies (Meshevlani et al. 2004).

Still it is of interest to note the presence of UP assemblages which were excavated early in the 20th century, lacking radiocarbon dates and differ in their techno-typological properties from the Dzudzuana assemblages, as perhaps they do illustrate both regional variation as well as possibly fill-in the chronological gaps observed in Dzudzuana. One example is the assemblage from Svanta Savane, a site in the lowlands, rich in scrapers with scalariform retouch and high frequencies of burins on truncations. This assemblage resembles similar industries reported from Levantine sites which date to ca. 25–20 ka cal BP (Belfer-Cohen & Goring-Morris 2003).

As for sites excavated more recently with updated methodologies and excavation technique the most comparable are two sites, unfortunately, in both cases the relevant material is as yet unpublished fully. The first is **Kotias Klde** cave (Mesheveliani et al. 2007) which comprises a sequence of Eneolithic-Mesolithic-UP occurrences. Though there is some overlap between the dates of Dzudzuana (Dzu) Unit C and Kotias Klde Layer C (26.8-29.0 ka cal BP), which was exposed only to a limited extent, it seems that overall the lithic material is more similar to that of Dzu Unit D. There are some carinated cores but they differ from those of Dzu C. Also there is a difference with the blanks being more elongated, there are no Sakajia points, and the burins outnumber the endscrapers. Also, the bone industry, though still in small numbers (as the excavated area is quite small) does not comprise bipoints as compared with the bone inventory in Dzu C. It is of interest to note that there is a time gap in the occupations at Kotias Klde between Layer C and the overlying Layer B, indicating most probably that the cave was not occupied during the LGM and for quite some time after the LGM.

The other site is **Satsurblia Cave** where on-going excavations revealed a long sequence of human occupations which is still expanding as the excavations progress, from the Eneolithic through the Mesolithic and unto the UP. There are two areas of excavations (A and B) (Pinhasi et al. 2014) differing in the presence and thickness of the ~~different~~ various archaeological layers. Yet it appears that in both areas, at the levels of Layer A/III and Layer B/III the lithic industry is very similar to that of Dzudzuana Unit C. In both areas the dominant core type is the carinated variety, the majority of tools comprises retouched and to a lesser extent backed bladelets, the endscrapers outnumber the burins and there are a few Sakajiya points. Also among the worked bone artefacts there are variants similar to those observed in the bone industry of Dzu C, namely thick points (sometimes made on antler), needles, tooth pendants, and incised pieces in numbers higher than in the previous and proceeding levels. Moreover, the dating of these layers fits well with that of Dzu C.

Other sites, in close vicinity to Dzudzuana, with layers contemporaneous to Dzu C, are very poor in lithic materials which preclude comparison between them. Such is the case for **Ortvale Klde** where layers 2-3 are dated to 25-26 ka cal BP (Adler et al. 2008; Moncel et al. 2013), but the UP findings are rather ephemeral. The same can be said concerning **Bondi Cave** (Plerdeau et al. 2016). Layer IV therein was dated to ca. 27 ka cal BP, and there are high quantities of flax fibers (though there is no details as regards their distribution within the UP layers II-V), yet its lithic inventory incorporates but 6 cores, and 49 tools while the whole

UP sequence yielded 391 tools. Only five bone artefacts were recovered through the whole UP sequence. Still, Pleurdeau et al. (2016:91) state that “...within layer II and IV, besides the presence of the same “UP-like” tendency of blade technology, a few carinated cores are present”. Moreover, it appears that most of the tools are retouched bladelets with some endscrapers, burins, retouched blades and a few backed bladelets.

In the neighboring **Armenia** the situation is quite similar, with single sites dating to the UP and so far no assemblage similar to that of Dzu Unit C was identified. The site of **Hovk 1** yielded mostly MP remains (levels 8-6) while the UP levels (4-5) are too poor to provide any comparative information and the dates obtained indicate an age more comparable to that of Dzu Unit D (Pinhasi et al. 2012).

Another site, **Kalavan 1** (Mentoya et al. 2013) provided assemblages which compare better with Dzu Unit B and even more so with Satsurbliya layers A/II and B/II which also accords with their dates of ca. 17 ka cal BP.

A more appropriate assemblage for comparison with Dzu Unit C is that deriving from the upper most UP layer, AH III, at the site of Aghitu 3 Cave (Kandel et al. 2017) and dated to 29-24 ka cal BP. It is a relatively rich assemblage comprising ca. 90% of the lithic finds of the whole local UP sequence (starting at 39 ka cal BP). Still it is much poorer than Dzu Unit C comprising but 110 cores and 745 tools. No mention is made of carinated cores, retouched bladelets comprise the majority of the tools, and burins outnumber endscrapers, with the latter ~~are~~ recorded only on flakes (Kandel et al. 2017: table 9), while ca. 18% of the burins are on bladelets, a unique phenomenon in the Caucasus Palaeolithic (*ibid.*). Of the 12 bone implements recorded from the UP sequence at Aghitu 3, three were reported from AH III including a broken ‘eyed’ needle. Another obvious difference is the proportion of obsidian in the lithic assemblages which comprises the majority of the raw material. Thus though Kandel et al. (2017) claim that Units C and D in Dzudzuana offer perhaps the best comparison to Aghitu-3, and that “starting at ~ 29,ka cal BP, we note a degree of cultural convergence between the two regions” it is quite obvious that Dzu Unit C and AH III of Aghitu-3 represent two contemporaneous yet different facies of UP mainly sharing the dominance of retouched and to a lesser degree backed bladelets. The detailed comparison shows that though both sites shared some characteristics in their contemporaneous lithic industries they do differ in their raw material, techniques of production, proportions of various tool types, the

bone tool industry, etc. They do have in common the dominance of bladelets, bladelet tools and lack of 'classical' Aurignacian characteristics. Kandel et al. (2017:64) note that perhaps the differences observed had to do with the different geographical circumstances as "Much of the territory of Armenia lies between 1000 and 2000 m, whereas the Georgian sites are much lower at ~300-500 m. Thus, Georgian UP populations might have had access to a more stable variety of locally available resources which reduced their need for long-distance mobility and/or social networks."

Further afield is **Mezmaiskaya Cave** (Golovanova et al. 2005, 2014) located in the Russian northern Caucasus. A MP sequence is topped by UP layers. The one contemporaneous with Dzu Unit C is 1-4 (dated by two dates to 25-19 ka cal BP, MIS 2) which unfortunately is comprised of reworked deposits and filled pits and hollows that intrude into an earlier UP layer (1A) and the lithics recovered are too meagre to provide comparative data to the Dzu Unit C assemblage. It is of interest to note that the upper layer, 1-3 brings to the mind of the excavators the assemblage of Dzu Unit B, though it is a bit earlier than the latter.

Conclusions

It seems that the beginnings of the UP in western Georgia are relatively late, compared with the earliest UP in the Near East and southeastern Europe and they appear to be already dominated by the production of bladelets (e.g., Dzudzuana Unit D). Another important observation is that while the Caucasus served as a geographic barrier between two MP Neanderthal populations (the Mousterian of the southern flanks which closely resembles the Mousterian of the Taurus and the Zagro, and the Late Mousterian of the northern Caucasus, similar to the northern European Micoquian Mousterian (Meignen & Tushabramishvili 2006), the early UP assemblages on both sides of the Caucasus Mountains demonstrate similarities, indicating the dispersal of modern humans throughout the whole region.

The proceeding cultural traditions (e.g., Dzudzuana Unit C) do not follow the UP sequence of western Europe or the Near East as previously claimed. In particular, the 'carinated core' industries found all over the Caucasus region lack any evidence for the presence of the west European 'classical' Aurignacian (and see Belfer-Cohen & Grosman 2007; Goring-Morris & Belfer-Cohen 2006, vis à vis carinated artefacts).

The presence of carinated cores in some sites may indicate a general contemporaneity among sites in western Georgia, as with the site of Gubs (Amirkhanov 1986) located on the northern slopes of the Caucasus. Yet, there are no typical Aurignacian tool types either among the lithics or among the bone artefacts. The bone and antler implements in Dzu Unit C (as in other UP assemblages in the Caucasus) do not comprise artefacts such as the split-base point, the hall-mark of the west European early Aurignacian. Bone awls, needles, points and the like were recovered from UP contexts all over the Old World and the same is true for the rare bone beads and decorations. The same is true also for the other sites in Georgia dating to the early UP (and see Moncel 2013; Pleardeau et al. 2016) as well as sites in the neighboring Armenia and northern Caucasus (and see above).

All in all the UP in the Caucasus retains its own local characteristics, differing both from Europe (no Aurignacian industry) and the Levant (no el Wad points, yet with rich bone artefacts industries) (and see Golovanova et al. 2014).

It seems that Dzu Unit C and its contemporaneous entities elsewhere in the Caucasus dissolved with the advance of the LGM. Still it is of interest to note that the following archaeological entities (e.g., Unit B in Dzudzuana, Layer B in Kotias Klde, Layers A/II and B/II in Satsurblia) exhibit some continuity in the basic concepts of lithic technomorphological characteristics as detailed above (and see Pleardeau et al. 2016 for the same observation in the UP sequence of Bondi cave).

Bibliography

Amirkhanov, H.A. 1986 *The Upper Paleolithic of the Kuban valley*. Moscow: Nauka (in Russian).

Adler, D.S., G Bar-Oz, A. Belfer-Cohen, and O. Bar-Yosef 2006 Ahead of the Game. Middle and Upper Palaeolithic Hunting Behaviors in the Southern Caucasus. *Current Anthropology* 47(1):89-118.

Adler, D. S., O. Bar-Yosef, A. Belfer-Cohen, N. Tushabramishvili, E. Boaretto, N.

Mercier, H. Valladas, and W. J. Rink 2008 Dating the demise: Neandertal extinction and the establishment of modern humans in the southern Caucasus. *Journal of Human Evolution* 55(5):817-833.

Bader, N.O. 1965 Cultural variability at the end of the Upper Palaeolithic and Mesolithic of the Caucasus. *Sovetskaya Arkheologiya* 4:141-156 (in Russian).

Bar-Oz, G., D. S. Adler, A. Vekua, T. Meshveliani, N. Tushabramishvili, A. Belfer-Cohen, and O. Bar-Yosef 2004 Faunal Exploitation Patterns along the Southern Slopes of the Caucasus During the Late Middle and Early Upper Palaeolithic. In *Colonisation, Migration and Marginal Areas. A Zooarchaeological Approach*. M. Mondini, S. Munoz, and S. Wickler, eds. Pp. 46-54. Oxford: Oxbow Books.

Bar-Oz, G., and D.S. Adler 2005 Taphonomic History of the Middle and Upper Palaeolithic Faunal Assemblage from Ortvale Klde, Georgian Republic, *Journal of Taphonomy* 3(4):185-211.

Bar-Oz, G., A. Belfer-Cohen, T. Meshveliani, N. Jakeli, Z. Matskevich, and O. Bar-Yosef 2009 Bear in Mind: Bear Hunting in the Mesolithic of the Southern Caucasus. *Archaeology Ethnology and Anthropology of Eurasia* 37(1):15-24.

Bar-Yosef, O., A. Belfer-Cohen, T. Mesheviliani, N. Jakeli, G. Bar-Oz, E. Boaretto, P. Goldberg, E. Kvavadze, and Z. Matskevich, 2011 Dzudzuana: an Upper Palaeolithic cavesite in the Caucasus foothills (Georgia). *Antiquity* 85:331–349.

Belfer-Cohen, A., and A. N. Goring-Morris 2003 Current Issues in Levantine Upper Palaeolithic Research. In: *More Than Meets the Eye: Studies on Upper Palaeolithic Diversity in the Near East*. A.N. Goring-Morris and A. Belfer-Cohen, eds. Pp. 1-12. Oxford: Oxbow.

Belfer-Cohen, A., and L Grosman 2007 Tools or Cores? Carinated Artifacts in Levantine Late Upper Paleolithic Assemblages and Why Does It Matter. In: *Tools versus Cores Alternative Approaches to Stone Tool Analysis*. S.P. McPherron, ed. Pp. 143-163. Cambridge: Cambridge Scholars Publishing.

Belmaker, Miriam, O. Bar-Yosef, A. Belfer-Cohen, T. Meshveliani, and N. Jakeli 2016 The environment in the Caucasus in the Upper Paleolithic (Late Pleistocene): Evidence from the small mammals from Dzudzuana cave, Georgia. *Quaternary International* 425:4-15.

Golovanova, L.V., and V. B. Doronichev 2005 New data on the Late Paleolithic from Mezmayaskaya Cave. *IVth Conference on Kuban Archaeology*, pp. 69-72, Krasnodarsk (in Russian)

Golovanova, L.V., V. B. Doronichev, N. E. Cleghorn, M. A. Koulikova, T. V. Sapelko, M. S. Shackley, and Y. N. Spasovskiy 2014 The Epipaleolithic of the Caucasus after the Last Glacial Maximum. *Quaternary International* 337: 189-224.

Kandel, A. W., B. Gasparyan, E. Allué, G. Bigga, A. A. Bruch, V. L. Cullen, E. Frahm, R. Ghukasyan, B. Gruwier, F. Jabbour, C. E. Miller, A. Taller, V. Vardazaryan, D. Vasilyan, and L. Weissbrod 2017 The earliest evidence for Upper Paleolithic occupation in the Armenian Highlands at Aghitu-3 Cave. *Journal of Human Evolution* 110:37-68.

Kvavadze, E., O. Bar-Yosef, A. Belfer-Cohen, E. Boaretto, N. Jakeli, Z. Matskevich, and T. Meshveliani 2009 30,000-Year-Old Wild Flax Fibers. *Science* 325(5946):1359

Liubin, V.P. 1989 The Palaeolithic of the Caucasus. In *The Palaeolithic of the Caucasus and Northern Asia*. P.I. Boriskovski, ed. Pp. 9-142. Moscow: Institute of Archaeology.

Margherita, C., G. Oxilia, V. Barbi, D. Panetta, J.- J. Hublin, D. Lordkipanidze, T. Meshveliani, N. Jakeli, Z. Matskevich, O. Bar-Yosef, A. Belfer-Cohen, R. Pinhasi, and S. Benazzi 2017 Morphological description and morphometric analyses of the Upper Palaeolithic human remains from Dzudzuana and Satsurblia caves, western Georgia. *Journal of Human Evolution* 113(Supplement C):83-90.

Meignen, L., and N. Tushabramishvili 2006 Paleolithique Moyen Laminaire sur les Flancs Sud du Caucase: Productions Lithiques et Fonctionnement du Site de Djrchula (Georgie). *Paleorient* 32(2):81-104.

- Meshveliani, T., O. Bar-Yosef, and A. Belfer-Cohen 2004 The Upper Palaeolithic in Western Georgia. In: *The Early Upper Paleolithic Beyond Western Europe*. P.J. Brantingham, S.L. Kuhn, and K.W. Kerry, eds. Pp. 129-143. Berkeley: University of California Press.
- Meshveliani, T., G. Bar-Oz, O. Bar-Yosef, A. Belfer-Cohen, E. Boaretto, N. Jakeli, I. Koridze, and Z. Matskevich 2007 Mesolithic Hunters at Kotias Klde, Western Georgia: Preliminary results. *Paléorient* 33 (2):47-58.
- Moncel, M. H., D. Pleurdeau, N. Tushubramishvili, R. Yeshurun, T. Agapishvili, R. Pinhasi, and T. F. G. Higham 2013 Preliminary results from the new excavations of the Middle and Upper Palaeolithic levels at Ortvale Klde-north chamber (South Caucasus Georgia). *Quaternary International* 316:3-13.
- Nioradze, M.G., and M. Otte 2000 Paleolithique superieur de Georgie. *L'Anthropologie* 104:265-300.
- Pinhasi, R., M. Nioradze, N. Tushabramishvili, D. Lordkipanidze, D. Pleurdeau, M.-H. Moncel, D. S. Adler, C. Stringer, and T. F. G. Higham 2012 New chronology for the Middle Palaeolithic of the southern Caucasus suggests early demise of Neanderthals in this region. *Journal of Human Evolution* 63(6):770-780.
- Pinhasi, R., T. Meshveliani, Z. Matskevich, G. Bar-Oz, L. Weissbrod, C. E. Millerm, K. Wilkinson, D. Lordkipanidze, N. Jakeli, E. Kvavadze, T. F. G. Higham, and A. Belfer-Cohen 2014 Satsurbli: New Insights of Human Response and Survival across the Last Glacial Maximum in the Southern Caucasus. *PLoS ONE* 9(10):e111271.
- Pleurdeau, D., M.-H. Moncel, R. Pinhasi, R. Yeshurun, T. F. G. Higham, T. Agapishvili, M. Bokeria, A. Muskhelishvili, F.-X. Le Bourdonnec, S. Nomade, G. Poupeau, H. Bocherens, M. Frouin, D. Genty, M. Pierre, E. Pons-Branchu, D. Lordkipanidze, and N. Tushabramishvili 2016 Bondi Cave and the Middle-Upper Palaeolithic transition in western Georgia (south Caucasus). *Quaternary Science Reviews* 146:77-98.

Supplementary Information 2

An admixture graph model of Upper Paleolithic West Eurasians

In this section we develop an ADMIXTUREGRAPH¹ model of Upper Paleolithic West Eurasians whose purpose is (i) to provide insight about possible histories of these populations, (ii) to identify histories which are inconsistent with the genetic data, (iii) to quantify the minimum complexity (number of admixture events) that an admixture graph model must have, and (iv) to provide an explicit phylogenetic model counterpart to the modeling using *qpAdm* in Supplementary Information section 3, thereby mutually checking whether the two approaches produce similar inferences.

ADMIXTUREGRAPH allows the analyst to manually specify a model and test its fit. In the past, we have used it in a semi-automated way² by grafting populations onto a user-specified model. The advantage of doing so is to remove the subjectivity of the analyst who makes modeling decisions based on background knowledge or examination of relevant *f*-statistics that allow him to quickly “guess” where a population must be placed.

Some computational considerations

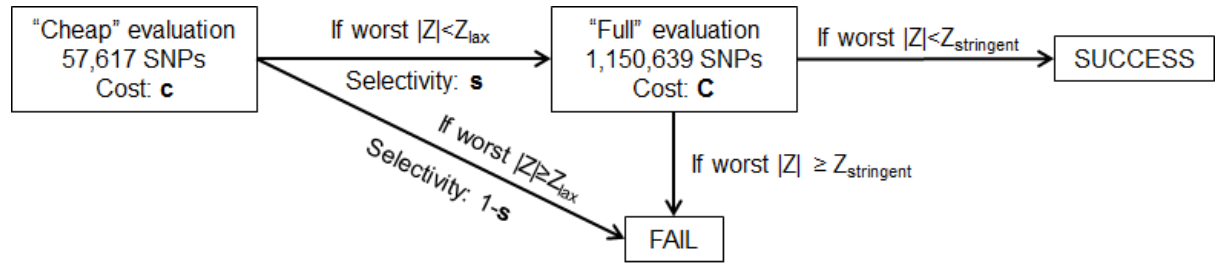
In the current section we adopt an automated brute force procedure with minimal user input; this is useful both to remove the subjectivity of the analyst, and also, practically, to explore models with many included populations.

The downside of an automated approach is computational, so before we explain our approach, we note a few heuristics that allow us to evaluate tens of thousands graphs relatively efficiently, as these may be useful to other practitioners who wish to use a similar approach.

1. When evaluating a graph, a substantial amount of time may be spent loading the dataset into memory. It is recommended that the dataset be in the PACKEDANCESTRYMAP format, and also that a subset of it which includes only the populations of interest be used. One can do both by using *convertf* in EIGENSOFT^{3,4} to create a dataset in this manner.
2. Many graphs are phylogenetically equivalent. We use a hash function implemented in *qpreroot* that allows us to avoid evaluating multiple equivalent copies of the same graph.
3. When evaluating graphs in an automated way, many of them do not fit, i.e., the difference between the estimated (based on the graph topology and branch lengths) vs. fitted (based on actual data) values of some *f*-statistics is more than a set number of standard errors (Z-score). We thus use a staged approach in which we first evaluate a graph in a subset of 1/20th of the SNPs (Fig. S2.1). By reducing the number of SNPs we drastically reduce the time needed to

load the data to memory and to compute f -statistics. We expect a loss of power by the reduction of the number of SNPs, so that the worst Z-score (in absolute value) computed using the filtering subset of SNPs will tend to be lower than the worst Z-score when using the full SNP set. Thus, a graph that would be rejected using the full set of SNPs may sometimes be accepted using the SNP subset. Occasionally, the worst Z-score in the SNP subset might be greater than in the full SNP set, which would lead us to erroneously reject a model. To reduce the chance that we miss plausible models, we apply a more lax filtering threshold of $|Z|=Z_{\text{lax}}$; models that fail the filtering stage by $|Z|>Z_{\text{lax}}$ are likely to also fail the evaluation at the full SNP set at a more stringent threshold $Z_{\text{stringent}}<Z_{\text{lax}}$. Thus we can reject many models cheaply by evaluating them only with the SNP subset. For the relatively fewer models that pass the filtering stage ($|Z|<Z_{\text{lax}}$), we re-evaluate with the full set (thus paying the cost of both evaluations). This is an optimization problem in which we can adapt the SNP subset fraction (which we set to $1/20^{\text{th}}$); making it smaller results in cheaper rejection of bad models, but allows more models to pass the filtering stage (and thus evaluated twice).

Figure S2.1: Staged evaluation of admixture graphs. The total cost of evaluation of an admixture graph using this approach is $c+sC$. This can be much less than the cost of performing only the evaluation on the full set of SNPs (C). Formally, $c+sC<C$ iff $s<1-c/C$. Thus, a benefit is realized if most graphs are rejected with the cheap evaluation ($s\rightarrow 0$) or if the cheap evaluation is much cheaper than the full one (small c/C).



Identifying a graph with no admixture

Given N populations which we aim to place on the admixture graph, there will be some number M which are unadmixed and will be related to each other as a simple graph with no admixture (this is similar to the idea of a “scaffold tree” used in MixMapper⁵). At the beginning of our automated procedure we place each of the N populations on the graph, then each of the $N-1$ remaining ones, and so on. Since order does not matter, we do not consider multiple permutations of the same elements.

The following simple example illustrates how this works. Suppose we begin with the following order of populations:

Order: ABCDE

We consider “pools” of models with 1, 2, 3, etc. populations. A pool consists of all possible models without admixture given the number of populations. We do not make any assumptions about which populations are unadmixed, but rather seek to find the maximum number of such populations that can be so related to each other, and then we attempt to graft the remainder as admixtures.

The original pool includes models in which only a single population has been grafted **Pool₁**: (A, B, C, D, E). To each of these models, we then graft any of the remaining ones. However, we avoid different permutations of the same elements by only considering populations that come after all the elements of the **Order**.

Thus, **Pool₂**: (AB, AC, AD, AE, BC, BD, BE, CD, CE, DE), and **Pool₃**: (ABC, ABD, ABE, ACD, ACE, ADE, BCD, BCE, BDE, CDE), and so on.

In the above ABC is the set of all possible models that include populations A, B, C. It may be that there are multiple ways in which these populations can be related to each other, and we consider all.

Whenever a graph fails, we stop and do not consider graphs that include it as a component. For example, if BCD fails, we do not need to evaluate BCDE, since a simple graph that includes BCDE has a BCD simple graph as a component (which has failed).

Minimum graph complexity

The pool is exhausted if either all populations have been grafted, or all models are rejected. If all models of **Pool_{i+1}** are rejected, this means that the set of populations has i populations that can fit without admixture, and thus there must be as many as $N-i$ admixed *populations*. There may be more than $N-i$ admixture *events*, if some of the admixed populations are derived from 3-way or higher admixture. Conversely, there may in fact be fewer admixture events if there exist at least two admixed populations that form a post-admixture clade within the graph.

Grafting populations onto a graph

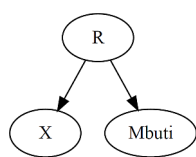
A population C may be grafted onto an existing graph at any edge. If there is an edge $A \rightarrow B$, we perform a split-and-graft operation, by replacing it with three edges $A \rightarrow X$, $X \rightarrow B$, $X \rightarrow C$. It is possible also that C may be placed at the root R. This is done by introducing a new root R' and two new edges

$R' \rightarrow R$, $R' \rightarrow C$. Thus, for a graph with e edges, a new population can be grafted in $e+1$ positions, and the new graph has $e+2$ edges.

If a population is grafted as a 2-way mixture, two edges are split, thus adding 2 edges to the graph, one admixture event is added, and a new post-admixture drift edge is added. Thus, for a graph with e edges, a graph with $e+3$ edges is formed. It is possible, however, that a population is a mixture of a new basal population to the existing root (+2 new edges) and another from an existing edge, thus with a total of $e+4$ new edges.

For completeness, we mention the possibility of 3-way mixtures; these are formed by splitting 3 edges (or making a new root and splitting 2 edges). However, in 3-way admixture events, a total of 3 new graphs are generated for each choice of edges to be split, depending on the order in which the new population is grafted onto the chosen edges. If E_1 , E_2 , E_3 are the three edges, we may form a 2-way mixture of E_1 , E_2 followed by a second mixture with E_3 , and two other choices (depending on how the mixtures are ordered). When considering a single grafted population, the order does not matter, as the grafted population traces a fraction of its ancestry to all of the chosen edges, regardless of the order in which these mixtures take place. However, the order does matter in subsequent grafting operations. As a concrete example, one may form Late Neolithic/Bronze Age Europeans as a mixture of Anatolia_N, WHG, and Yamnaya. If one chooses the order ((Anatolia_N, WHG), Yamnaya), then one makes available an Anatolia_N+WHG mixed population for subsequent grafting operations (corresponding to what we know about Middle Neolithic Europeans). If the order (Anatolia_N, (WHG, Yamnaya)) had been chosen, such a population would not have been available for subsequent grafting operations.

Figure S2.2: Base model.



Base model

We begin with the simple model of Fig. S2.2 where X is any population taken from the following set E which includes Upper Paleolithic Europeans, Siberians (Ust'Ishim and MA1), and the only published sample from East Asia (Tianyuan):

E: Ust_Ishim⁶, GoyetQ116-1⁷, Vestonice16⁷, Kostenki14⁷, MA1⁸, Sunghir3⁹, Tianyuan¹⁰, Villabruna⁷

Thus the original pool **Pool**₀ includes 8 models, all of which obviously fit; the reason to begin from such a simple model is that it allows us to consider all populations from **E** as unadmixed.

Table S2.1 shows the number of models for successive graftings. Notice that there is a “growth phase” in this procedure, with the number of considered models growing as the number of combinations of populations increases, followed by a “shrink phase”: there are more possible models for a larger number of populations, but it becomes increasingly difficult to fit most of them in a simple graph. We limit the growth phase by adopting a very stringent $Z_{\text{stringent}}=2$ initially and $Z_{\text{stringent}}=3$ from **Pool**₄ onwards; we keep $Z_{\text{lax}}=4$ throughout. The shrink phase ends when an attempt to graft an additional population fails, and thus the maximum number of populations in the simple graph is reached; henceforth, we abandon the attempt to graft populations as simple clades and begin grafting them as 2-way mixtures.

The final pool consists of 9 models with worst $|Z|$ between 2.69-2.74 which differ subtly in the placement of Tianyuan, as there is uncertainty about the branching pattern of the trio (Ust’Ishim, Tianyuan, Western Eurasians)¹¹. In order to avoid evaluating multiple very similar models with similar fit going forward, we choose the nominally best model (Fig. S2.3). This model includes an admixture event of Vestonice16 as a mixture of the Villabruna and Sunghir3 lineages which was also the model favored by Sikora *et al.* who introduced Sunghir3 and fit it into a phylogenetic relationship for Upper Paleolithic Europeans⁹. The second admixture event models Tianyuan as a mixture of GoyetQ116-1 and an early diverging lineage (nominally placed as a clade with Ust’Ishim, but with no shared genetic drift, reflecting the quasi-trifucation mentioned above). The relationship between GoyetQ116-1 and Tianyuan, crossing the West Eurasian/eastern non-African split has been observed before¹⁰ where it was noted that it is difficult to simultaneously model these two individuals in an admixture graph framework. The solution presented in Fig. S2.3 is tentative and should not be interpreted as strong evidence for the direction of gene flow between the two populations.

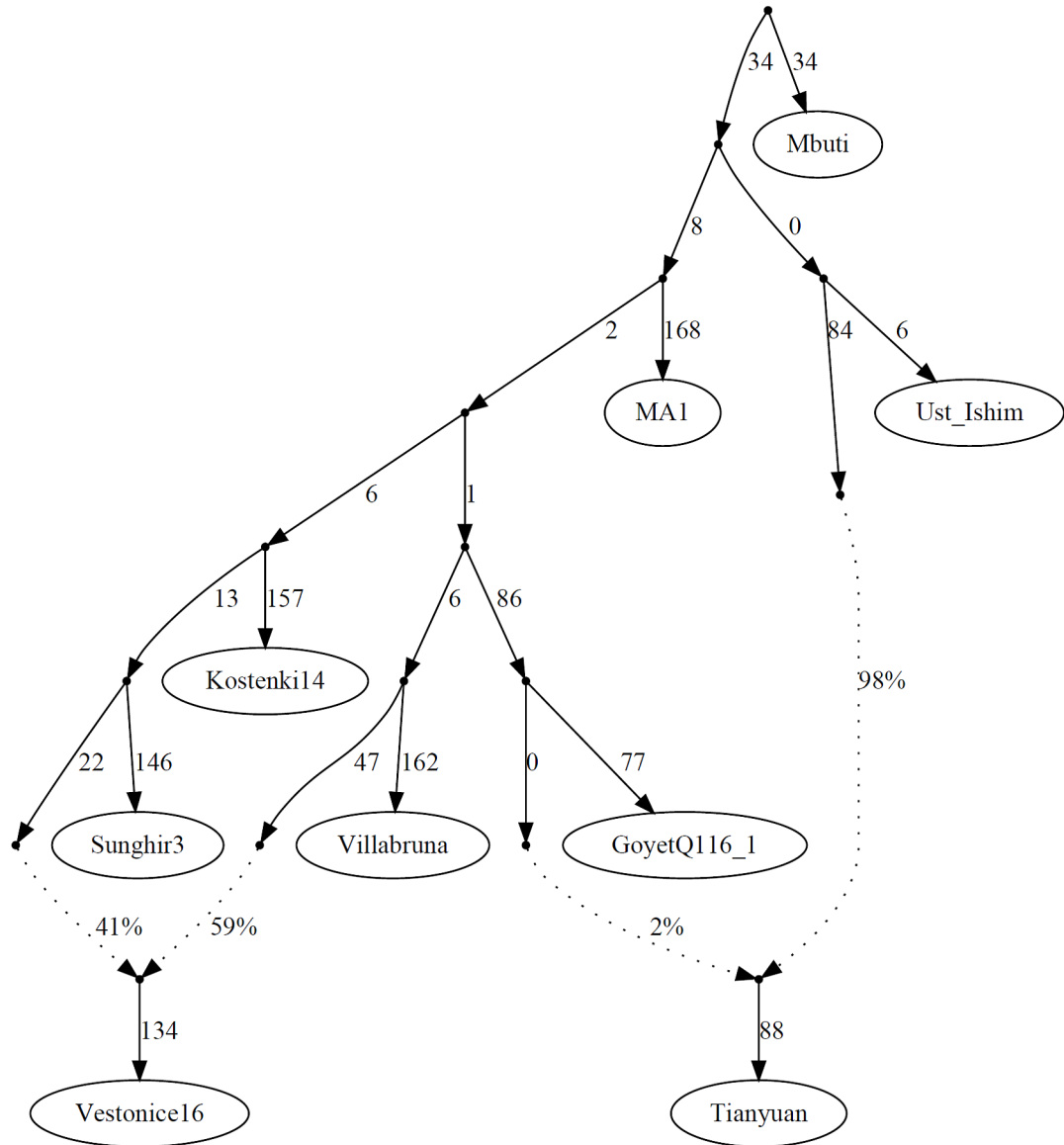
Inspecting the worst-fitting f -statistic of the graph of Fig. S2.3 we observe that it underestimates shared drift between Tianyuan and MA1. Presence of eastern non-African ancestry in MA1 has been proposed before^{8,11}, although MA1 nominally fits as unadmixed in previous analyses^{12,13} as in this one. Following ref.¹¹ we decided to model it as a 2-way mixture, a manual modification to our automated process: we removed MA1 from the graph of Fig. S2.3 and re-fit it as a 2-way mixture. The best 2-way mixture model is shown in Fig. S2.4 and models MA1 as a mixture of a deep West Eurasian lineage and ~24% of Tianyuan-related ancestry.

Table S2.1: Grafting non-African, non-Near Eastern populations from set E. The table should be read as follows. Pool₀ consists of the 8 models of Fig. S2.2 for each of the 8 populations of set E. Pool_{*i*} consists of feasible models with *i* additional grafted populations. We add the *i*+1th population as an *n*-way mixture (either as a simple clade, or a 2-way mixture). The number of generated models is listed, as is the Lowest maximum |Z| of these models. Note, for example, that for Pool₅ we first attempt to add the 6th population as a simple clade, but the best model has |Z|=4, we thus continue by adding the 6th population as a 2-way mixture, which results in 21 feasible models with |Z| as low as 2.2. In the end, we are able to add all members of **E** with only 2 mixture events; there is a total of 9 feasible models with |Z| as low as 2.7.

Stage	Number of feasible models	<i>n</i>-way mixture	Number of generated models	Lowest maximum Z
Pool ₀	8	1	28	0.1
Pool ₁	28	1	168	0.2
Pool ₂	62	1	365	0.4
Pool ₃	57	1	336	1.2
Pool ₄	16	1	90	2.2
Pool ₅	6	1	33	4.0
Pool ₅	6	2	792	2.2
Pool ₆	21	2	2847	2.7
Pool ₇	9			

Figure S2.3: A model of Upper Paleolithic Eurasians without Basal Eurasian admixture.

Job.6J.pool.1263 :: Kos MA1 Kos Tia 0.165549 0.168597 0.003048 0.001132 2.693



Job.L.pool.99 ::	Ust	Vil	Goy	Vil	0.168209	0.170717	0.002508	0.001131	2.218
------------------	-----	-----	-----	-----	----------	----------	----------	----------	-------



Paleolithic populations from the Caucasus/Levant/North Africa

We graft populations with Basal Eurasian admixture onto the admixture graph of Fig. S3.4. We refer to these populations as “Near Eastern” for ease of reference, although they come from the Caucasus/Levant/North Africa.

NE.cand: Taforalt, Natufian, Dzudzuana

We set one of the sources to stem from Basal Eurasians, and vary the other in a 2-way mixture. It would be possible to treat them as unconstrained 2-way mixtures, but it is clear from f -statistics that these populations must derive some of their ancestry from within the West Eurasian population radiation, to account for the fact that they are asymmetrically related to different West Eurasian populations. However, they cannot derive *all* of it from within the West Eurasian population radiation, to account for the asymmetry of Near Eastern and European populations with Ust’Ishim and Tianyuan. By constraining one of the 2 sources to be basal to Eurasians, we are severely cutting back on the number of models that need to be evaluated without missing any of the plausibly fitting ones, because provably any models without Basal Eurasian admixture fail for these populations.

A priori it might seem reasonable that Dzudzuana, being older than the others, should be fit first, as it is more likely that it should serve as a source for the others than vice versa. However, we treat all 3 populations equally. Similarly, we do not consider Taforalt as a mixture of Africans and West Eurasians¹⁴. Rather, we attempt to graft each of the 3 populations on the graph in the 1st step, then the second population as a mix of the first and an unconstrained other (2nd step), and finally the third population as a mix of the second and an unconstrained other (3rd step). Thus, all orders of the 3 populations are considered.

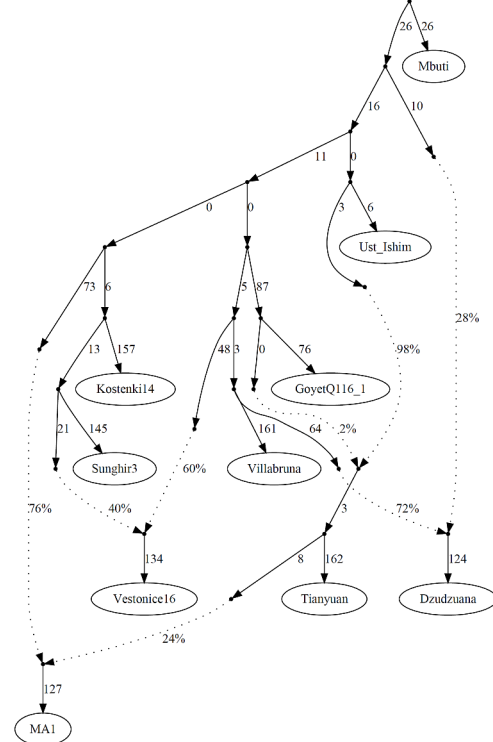
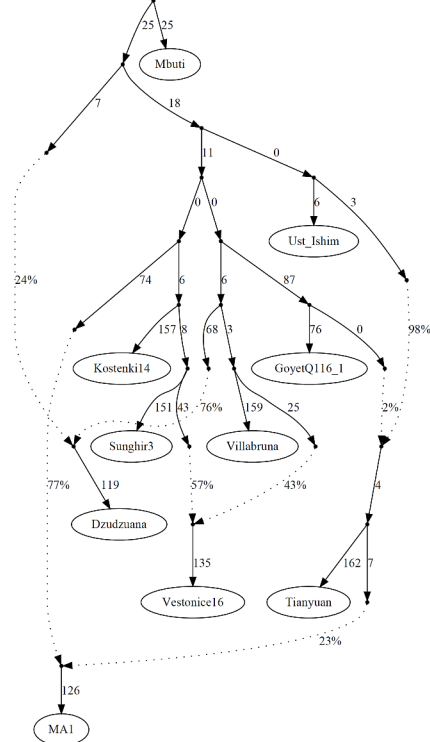
In the 1st step, three models fit, with the non-Basal Eurasian ancestry of the Near Eastern populations derived from any of (i) the edge leading to Villabruna, (ii) its sister edge contributing ancestry to Vestonice16, or (iii) the ancestral edge of (i) and (ii). This makes sense, as Near Eastern populations share more alleles with Villabruna than with other European populations. In Fig. S3.5 we show the three models for Dzudzuana, all of which give Dzudzuana ~24-28% Basal Eurasian admixture.

A total of 59 models fit in the 2nd step. We show the six best ones in Fig. S3.6, for each choice of 1st and 2nd grafted population.

Only 2 models fit in the 3rd step (shown in Fig. S3.7), both of which derive Natufians as a mix of Dzudzuana and Taforalt; the two models differ subtly in how the non-Basal Eurasian component of Dzudzuana is derived, with the best model ($|Z|=2.4$) deriving it from a sister group of Villabruna.

Figure S3.5: Grafting Dzudzuana onto the model of Fig. S2.4.

Job.1La.pool.9 :: Ust Dzu Goy Vil 0.004498 0.007201 0.002702 0.001135 2.382 Job.1La.pool.12 :: Kos Ves Vil Dzu -0.000793 -0.003486 -0.002693 0.001170 -2.301



Job.1La.pool.13 :: Kos Ves Vil Dzu -0.000861 -0.003486 -0.002625 0.001170 -2.243

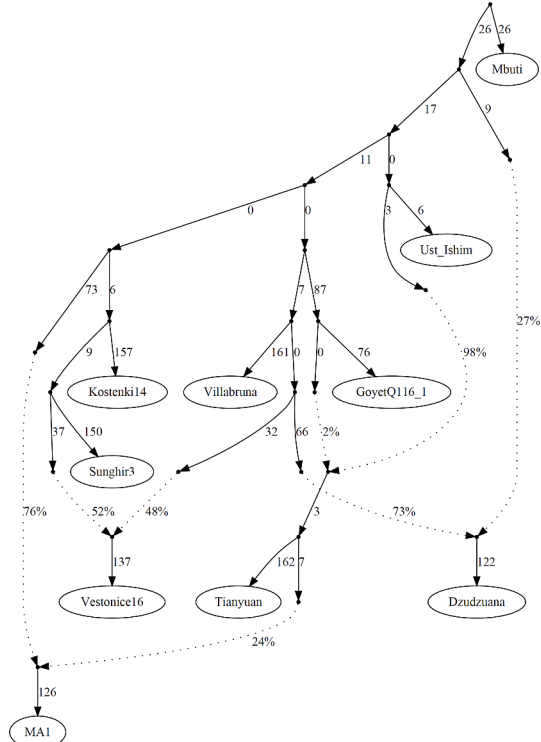


Figure S3.6: Best models with two Near Eastern populations.

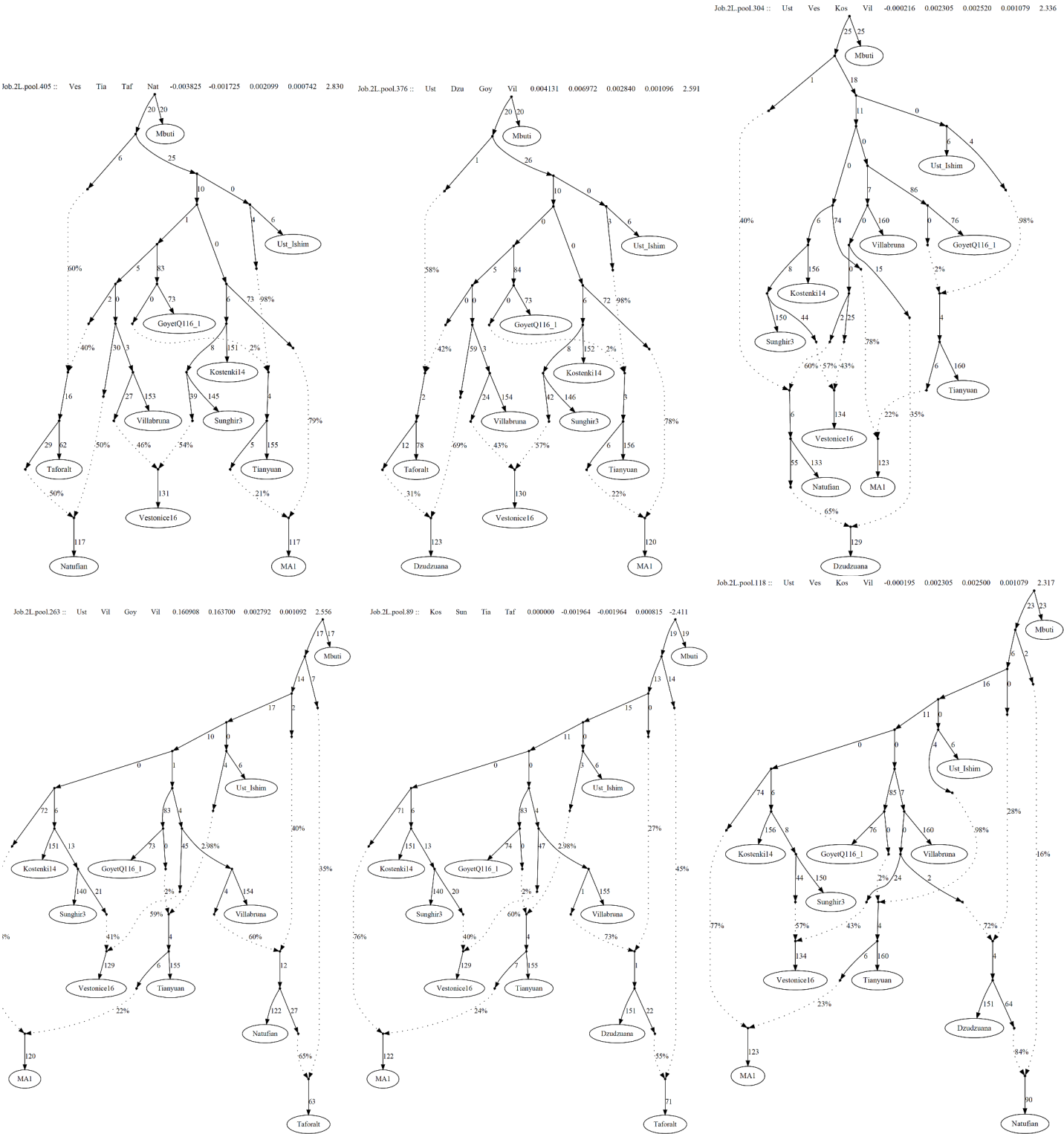
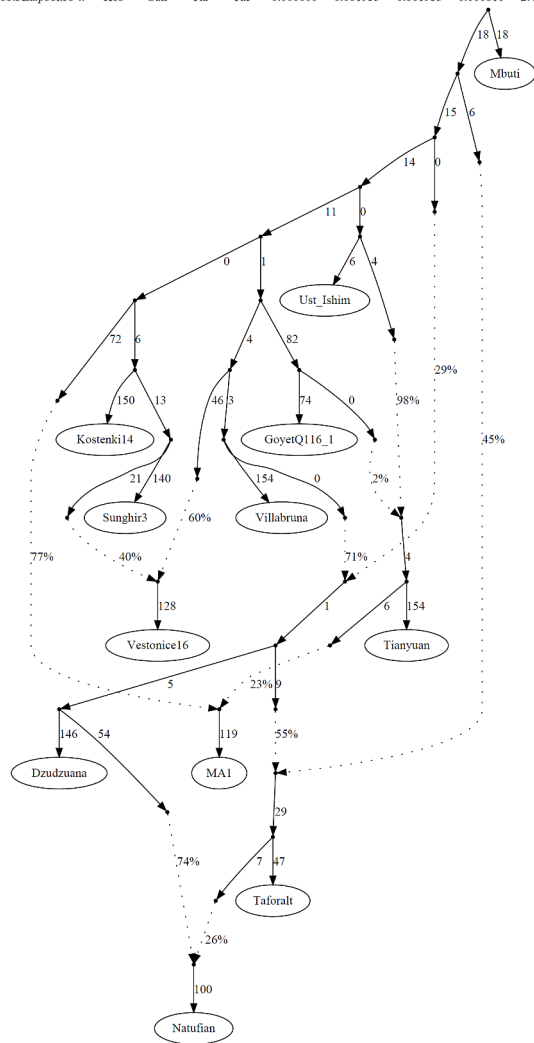
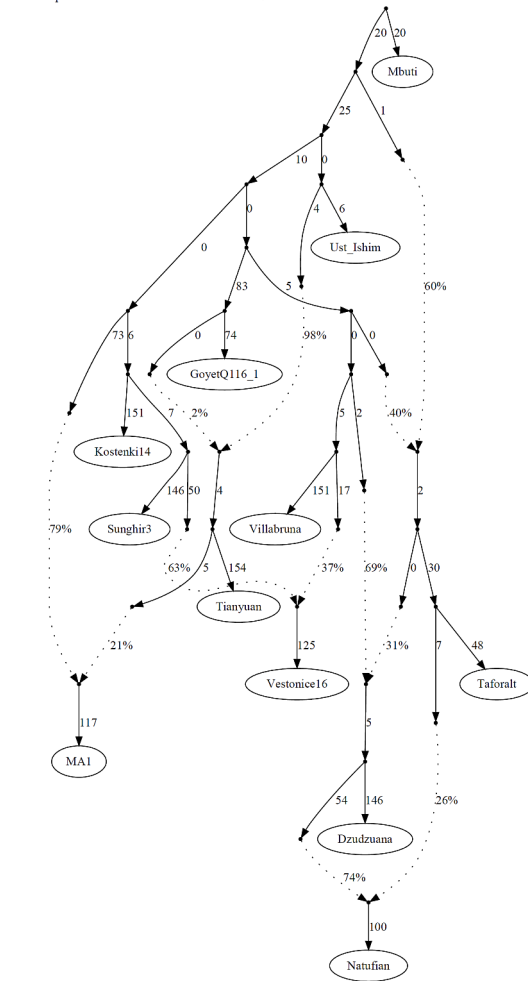


Figure S3.7: Models with three Near Eastern populations

Job.3La.pool.33 :: Kos Sun Tia Taf 0.000000 -0.001953 -0.001953 0.000810 -2.412



Job.3La.pool.169 :: Kos Tia Kos Nat 0.159554 0.162209 0.002655 0.000938 2.830



African populations

Finally, we attempt to fit Sub-Saharan African populations onto the models of Fig. S2.7, motivated by the observation¹⁴ that West Africans share more alleles with Taforalt than with Natufians, which was interpreted as evidence that Taforalt is a mixture of a Sub-Saharan lineage and Natufians. The models of Fig. S2.7 suggest that Natufians are not a source for Taforalt, but the reverse, a conclusion also supported by the independent *qpAdm* analysis of Supplementary Information section 3. Thus, we wanted to see what the implications are of this is on the relationship of Taforalt with other African populations.

We use the following set of African populations from East, South, and West Africa.

A: Mota¹⁵, South_Africa_HG¹⁶, Yoruba¹⁷

We can only fit Mota as a simple clade onto both models of Fig. S2.7; the results are shown in Fig. S2.8. Mota is placed as an earlier split than the Basal Eurasian ancestry that goes into Near Eastern populations. Neither Yoruba nor South_Africa_HG fit as a simple clade, with $|Z|$ down to 4.2 and 3.3 respectively. The best position for Yoruba and South_Africa_HG involves the same placement as with Mota (an earlier split than the Basal Eurasians).

We next try to fit Yoruba and South_Africa_HG as 2-way mixtures. Only Yoruba fits as such a mixture (Fig. S2.9) with one edge derived from an African split earlier than Mota (as in Fig. S2.8) and the second edge derived from a Taforalt-related population.

Finally, we fit South_Africa_HG as a 2-way mixture (Fig. S2.10); this is a mixture of a Mota-related population and a deeper branch within the African phylogeny. This is the “final” model of Fig. 1. We refit this model for the two Dzudzuana individuals separately, obtaining similar proportions of Basal Eurasian ancestry of 26.4% (I2949) and 29.1% (I2963).

We also refit the model of Fig. 1 a hundred times deleting equally sized blocks of the genome to obtain standard errors of the mixture proportions using a block jackknife¹⁸. Our estimates are shown in Table S2.2.

We think that the model of Fig. 1 is useful because it includes diverse African and Eurasian populations, and may provide some insight into the history of the included populations. In Supplementary Information section 3 we compare its predictions with that of *qpAdm* which does not make strong phylogenetic assumptions but which does not produce any strong insight about the deep evolutionary relationships among the different populations.

Figure S2.8: Fitting Mota

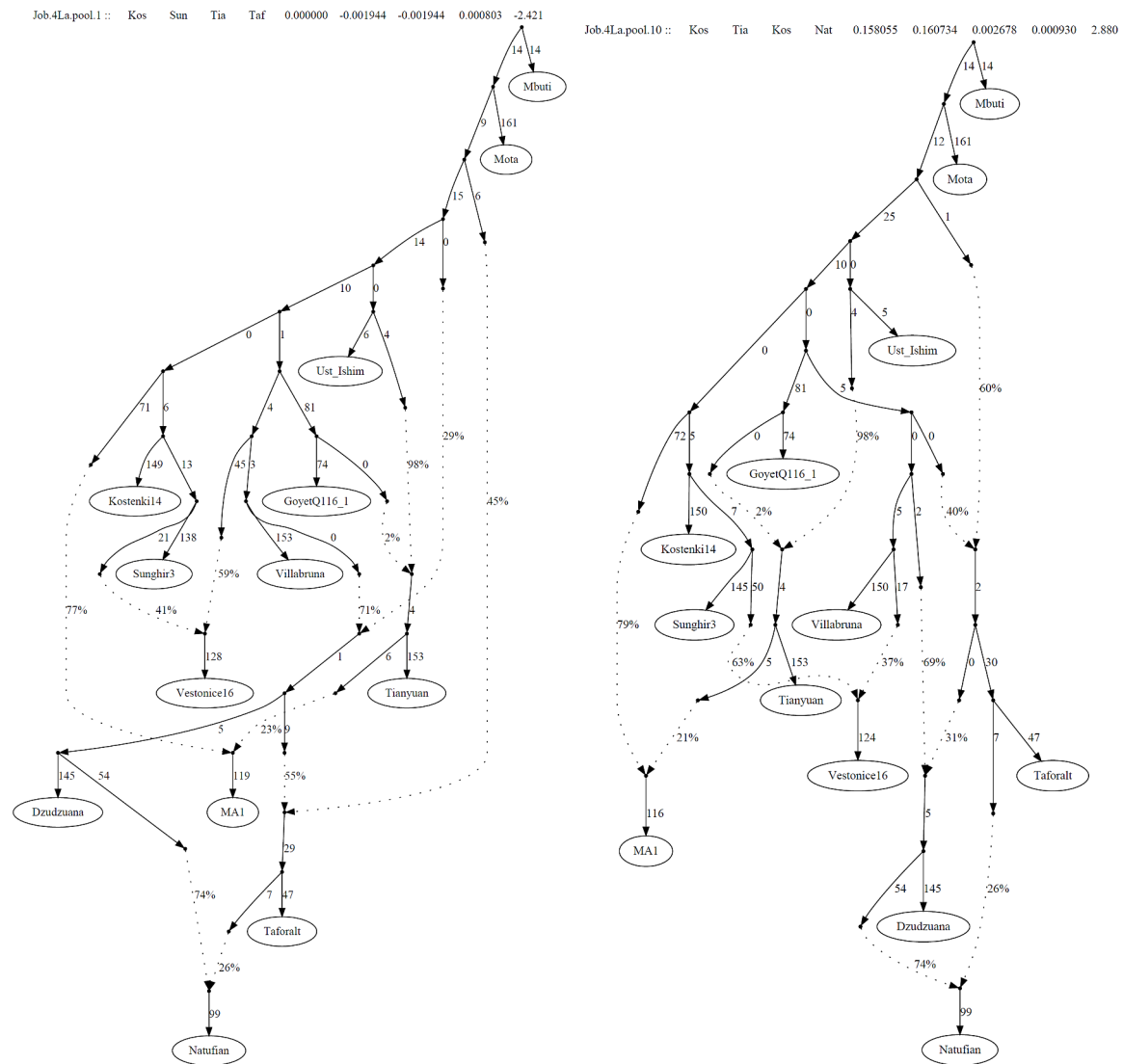


Figure S2.9: Fitting Yoruba. We show a single model, the models where the Taforalt-related ancestry in Yoruba is derived from the sister clade of Taforalt, or of the ancestral clade of the Taforalt/Natufian pair have the same fit.

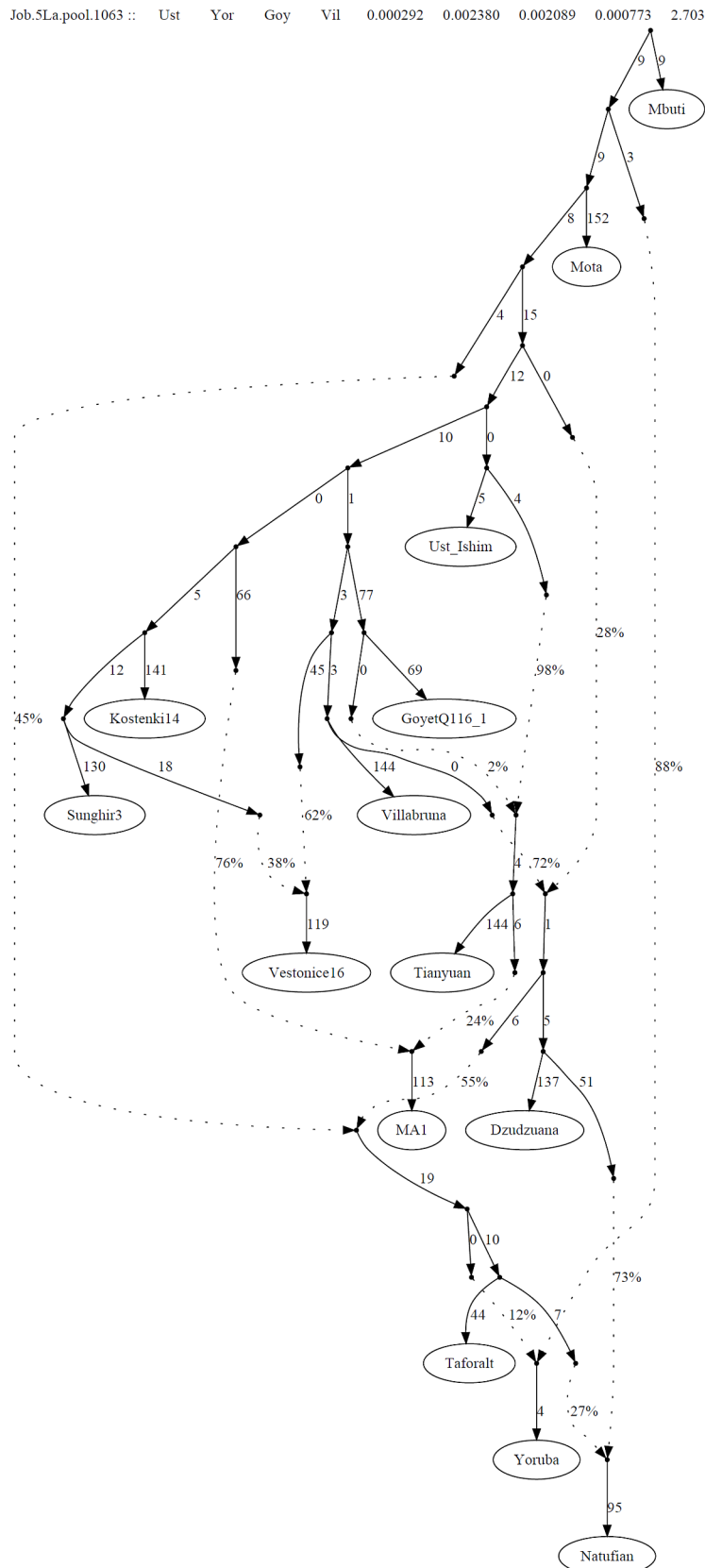


Figure S2.10: Final model (fitting South_Africa_HG)

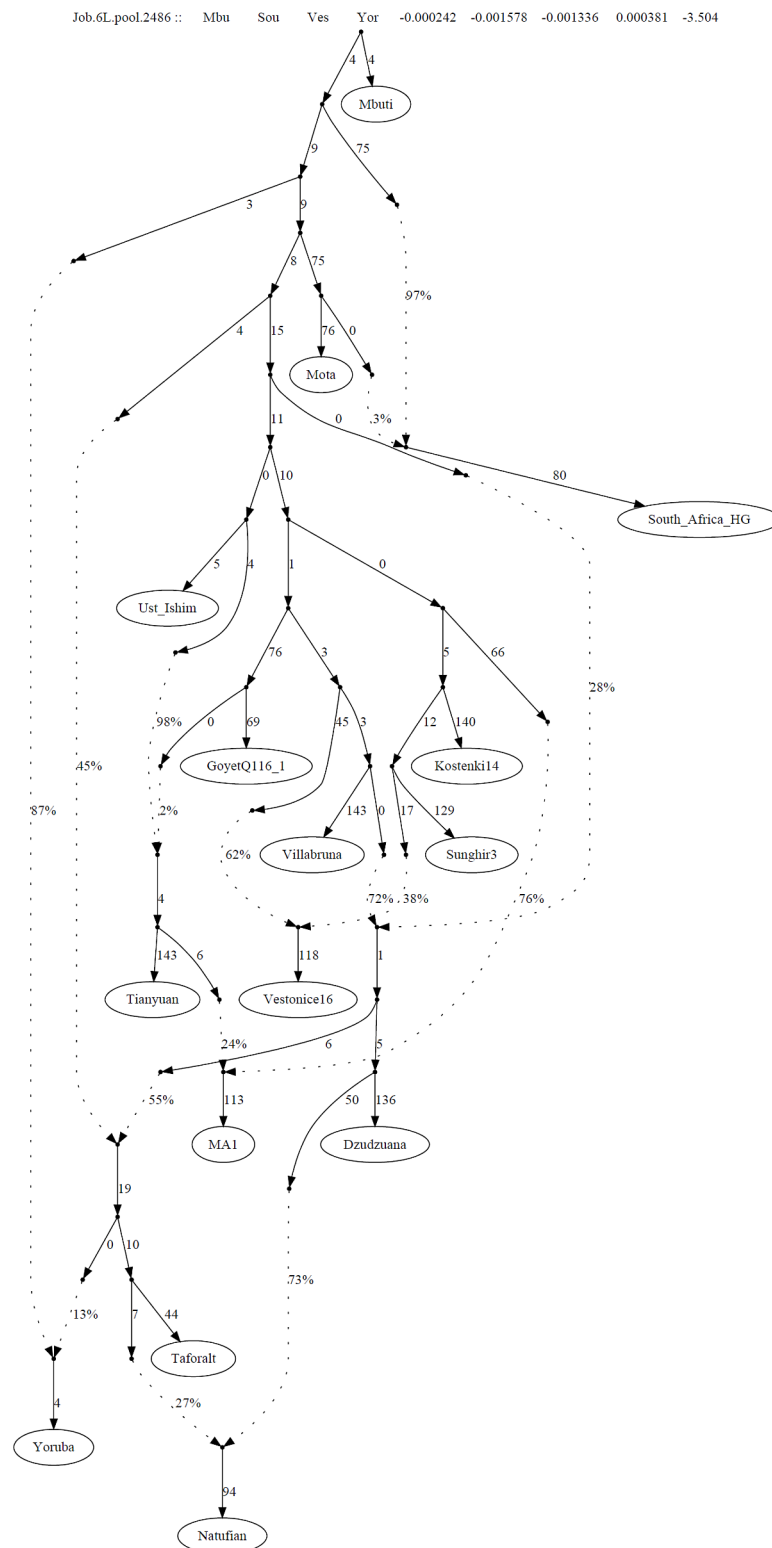


Table S2.1: Block jackknife estimates of mixture proportions of model of Fig. S2.10

Fig. S2.10 estimate	Jackknife estimate		Description
	All data	Damage-restricted data	
0.968	0.968 \pm 0.004	0.967 \pm 0.004	Deep Ancestry in South_Africa_HG
0.875	0.875 \pm 0.011	0.883 \pm 0.011	Deep Ancestry in Yoruba
0.451	0.451 \pm 0.044	0.488 \pm 0.085	Deep ancestry in Taforalt
0.283	0.284 \pm 0.042	0.292 \pm 0.085	Deep (basal Eurasian) ancestry in Dzudzuana
0.978	0.978 \pm 0.009	0.978 \pm 0.009	Eastern non-African ancestry in Tianyuan
0.763	0.764 \pm 0.050	0.801 \pm 0.054	Western Eurasian ancestry in MA1
0.729	0.729 \pm 0.032	0.657 \pm 0.060	Dzudzuana ancestry in Natufians
0.381	0.387 \pm 0.138	0.402 \pm 0.133	Sunghir3 ancestry in Vestonice16

Fitting CHG and Iran_N

In Supplementary Information section 3 we infer that these populations can be fit as 4-way mixtures and may thus be too complicated to fit as 2-way mixtures, a result which we confirm also in the admixture graph framework here.

We take as our starting point the final model of Fig. S2.10/Fig. 1. Because it is computationally difficult to exhaustively enumerate 3/4-way mixtures for a graph of Fig. 1's complexity, we adopt a greedy approach in which we take the “best” model for each number N of sources and then seek the best $N+1$ source.

Neither Iran_N nor CHG fit as clades with Dzudzuana (worst $|Z| > 5$; Fig. S2.11). Allowing a second source (from anywhere in the graph) improves the fit (Fig. S2.12) for CHG with MA1-related ancestry. Such ancestry is inferred for the two populations as an important component in the *qpAdm* analysis of Supplementary Information section 3.

We then allow for a 3rd ancestry component, taking the models of Fig. S2.12 as a starting point. The nominally best model of Fig S2.13 shows that in addition to Dzudzuana- and MA1-related ancestry, CHG/Iran acquires also some ‘Deep’ ancestry from either a node related to Basal Eurasians or Taforalt.

Figure S2.11: Iran_N and CHG do not fit as clades with Dzudzuana.

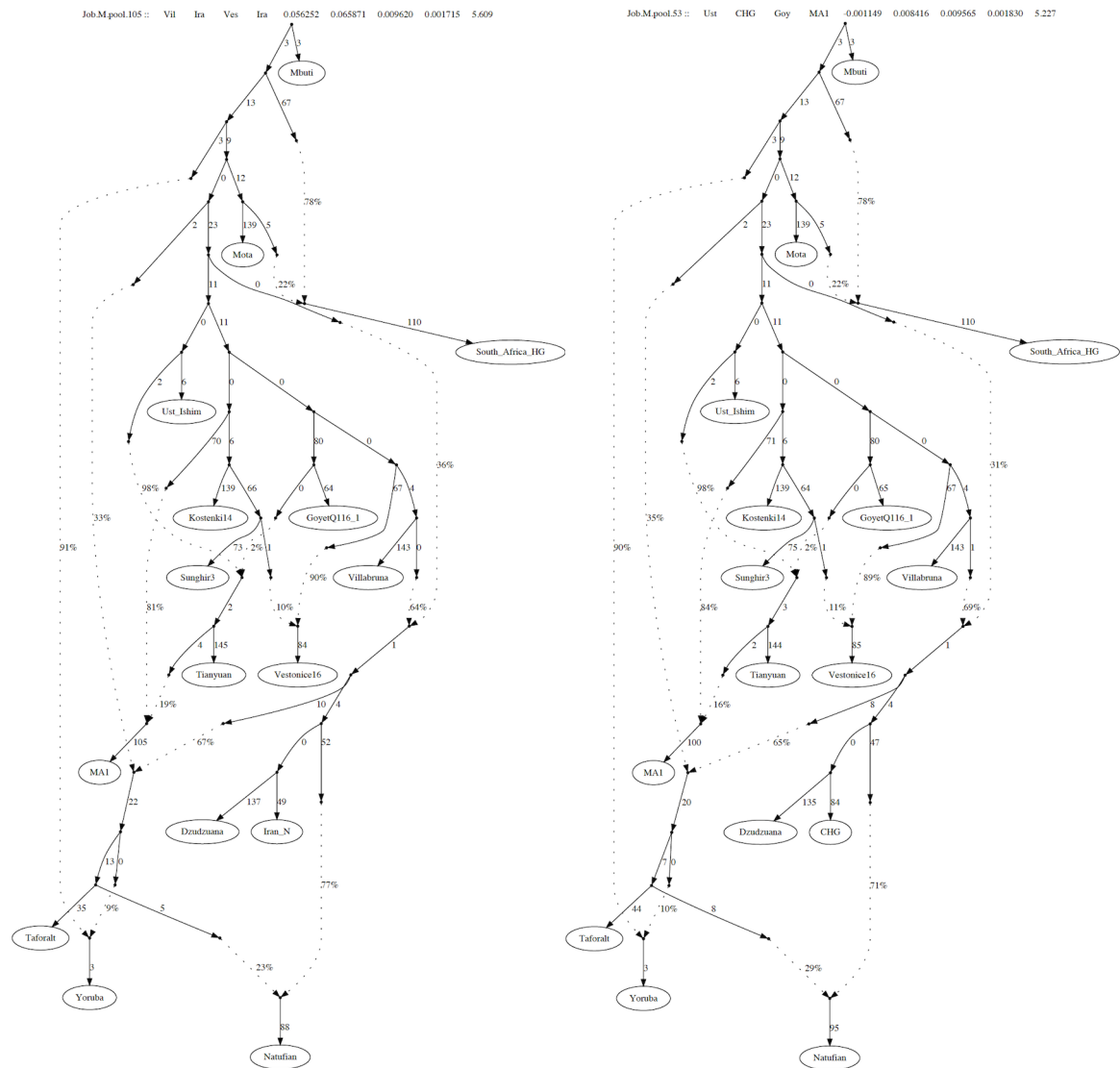


Figure S2.12: Adding a 2nd source.

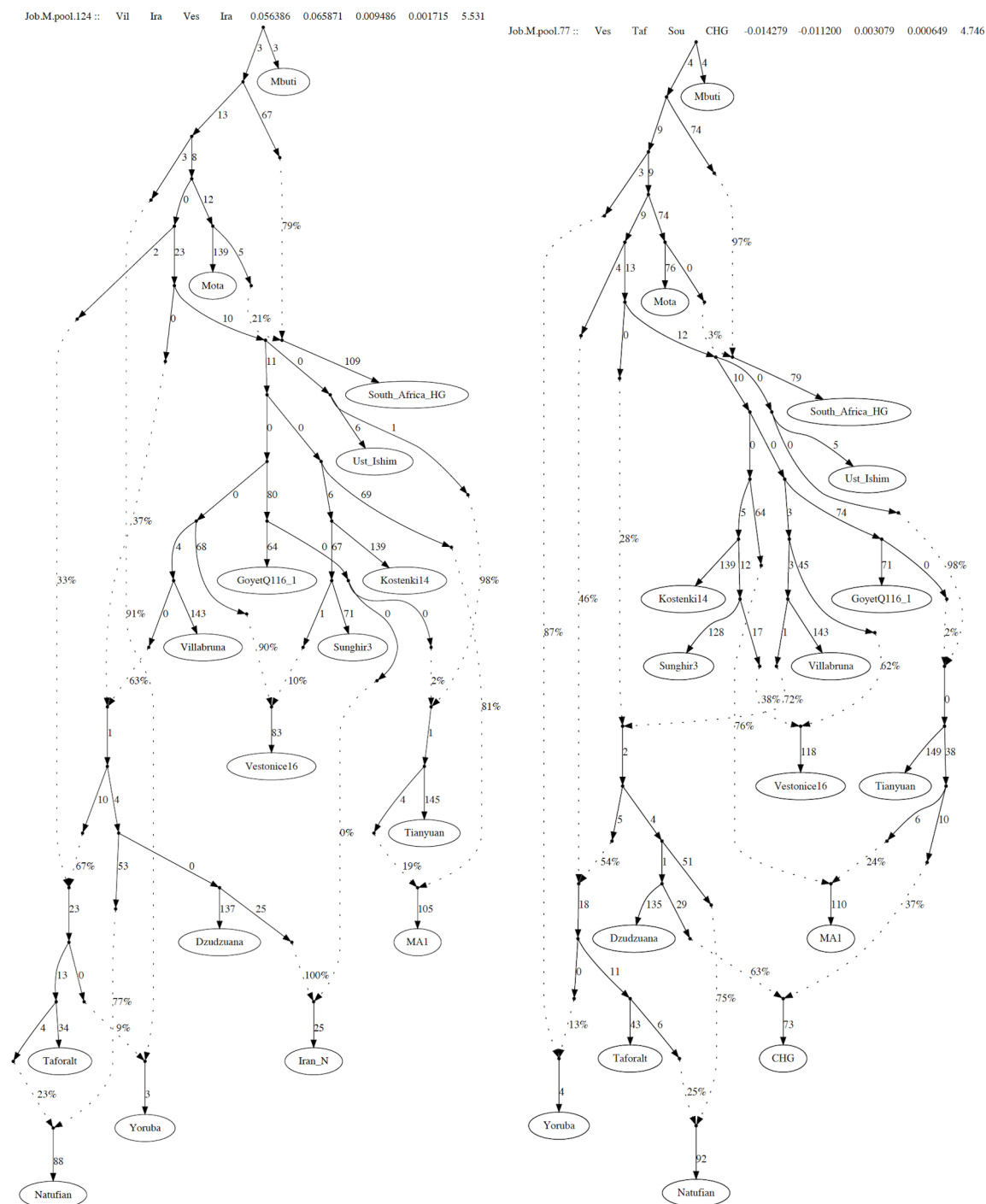
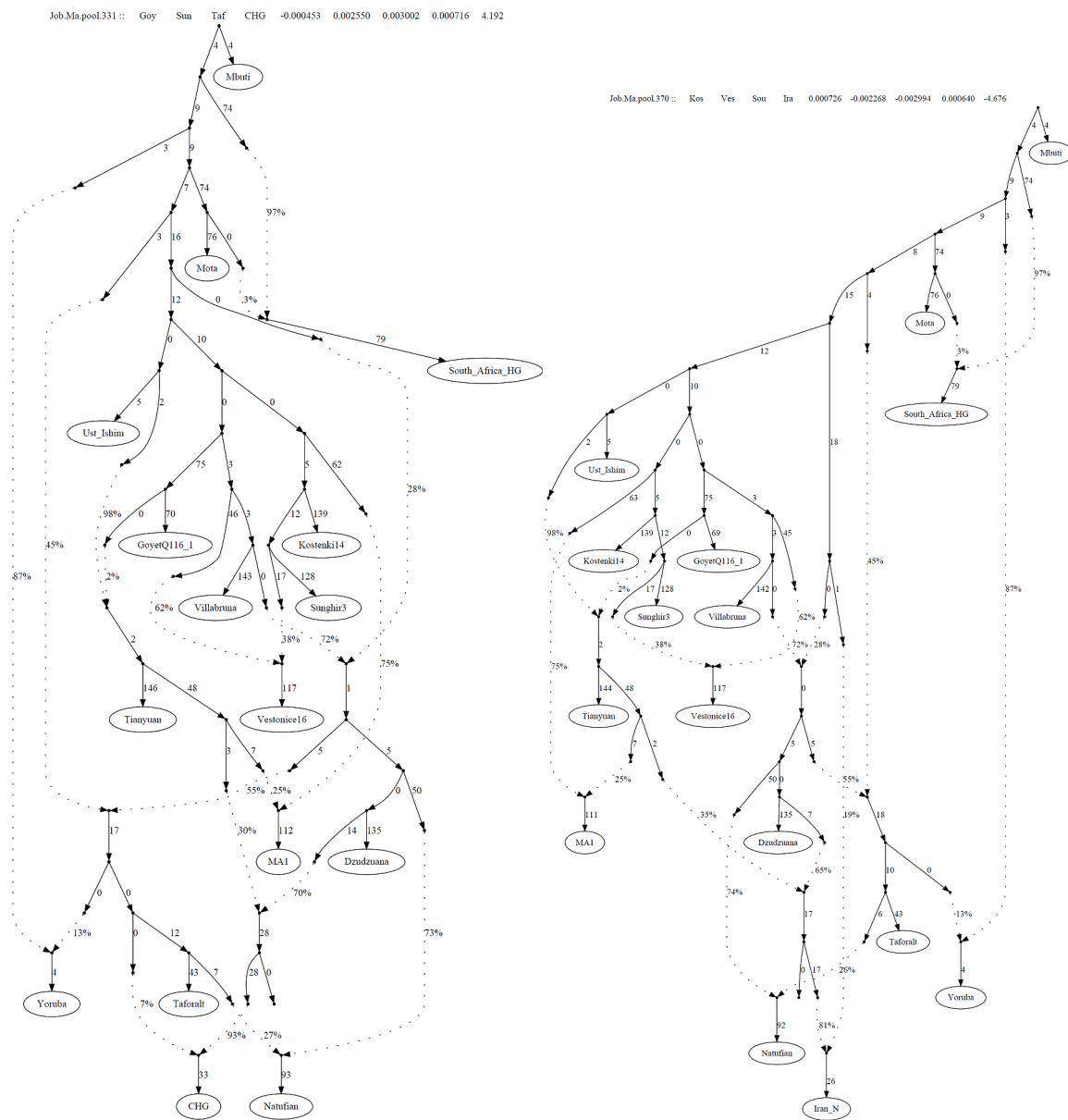


Figure S2.13: Adding a 3rd source.

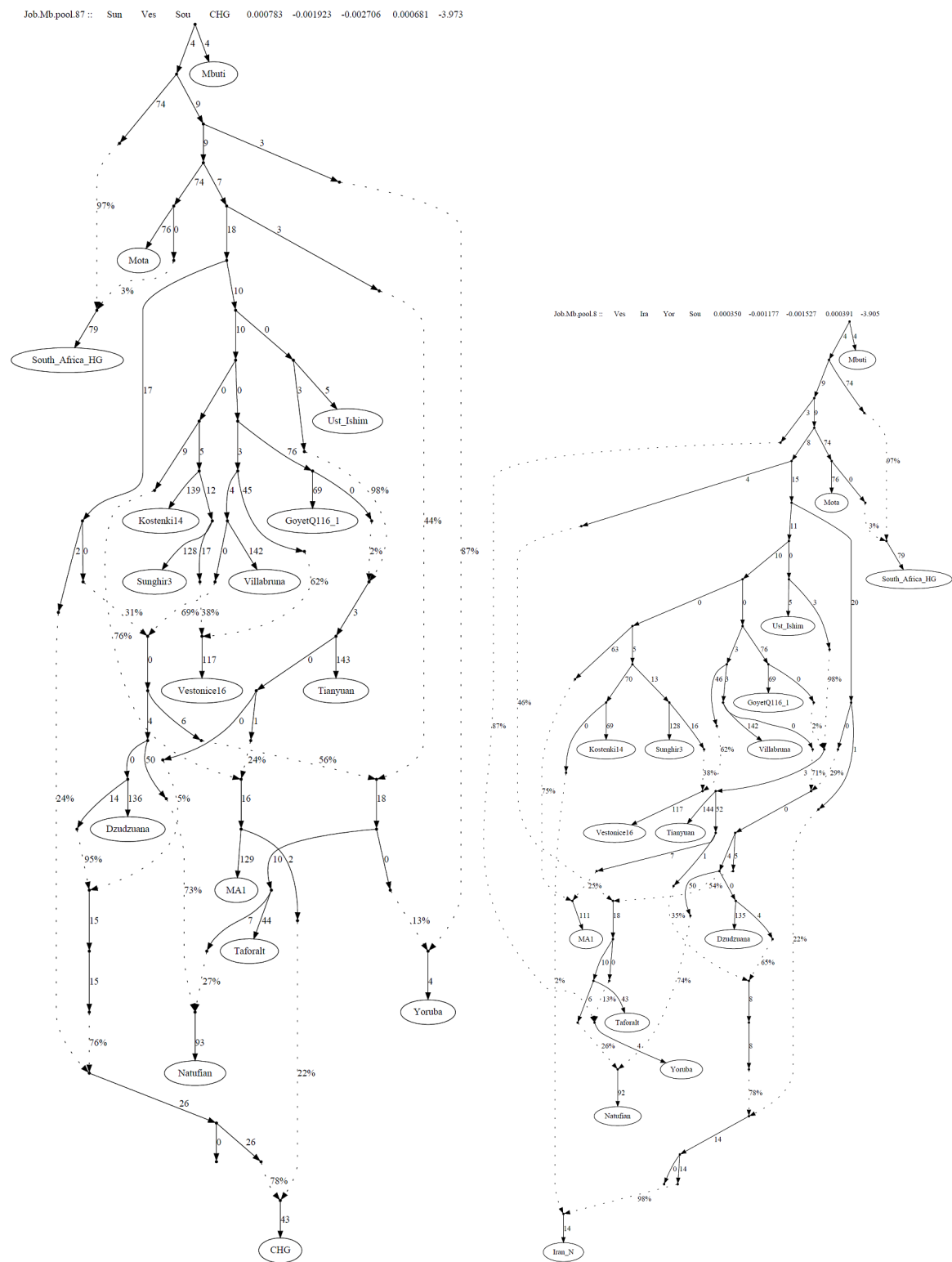


Finally, we allow for a 4th ancestry component, taking the models of Fig. S2.13 as a starting point. Both Iran_N and CHG have ancestry from Dzudzuana/Basal Eurasians/Tianyuan or MA1 and little else.

The models of Fig. S2.14 are not unique solutions due to the greedy approach we adopted to fit these populations. They agree with our inferences from *qpAdm* in Supplementary Information section 3 in having ancestry from Dzudzuana, a “Deep” source (identified with Basal Eurasians in these models), and “Ancient North Eurasians” represented by MA1. *qpAdm* in Supplementary Information section 3 also requires that both CHG/Iran_N have some eastern non-African ancestry. By contrast, the models of Fig. S2.14 do not require such ancestry. However, these models do not have more proximate sources of eastern non-African sources (such as recent East Eurasians) whose phylogeny is likely to be complex.

The models of Fig. S2.14 predict that Iran_N and CHG have $.98 \times .78 \times .65 \approx 50\%$ and $.78 \times .76 \times .95 \approx 56\%$ of Dzudzuana-related ancestry respectively, compared to 57.7% and 64.3% based on the *qpAdm* analysis (Table 1; Supplementary Information section 3). Thus, while the models of Fig. S2.14 are likely to be inaccurate in at least some of their details, they do support the idea that Dzudzuana-related ancestry forms the core component of ancient West Eurasian populations. More data from the Caucasus and Iranian plateau and Siberia/Central Asia may improve our understanding of both the Dzudzuana-related ancestors of these populations (that may have differed from Dzudzuana, e.g., in the proportion of Deep ancestry), and also of the eastern influences.

Figure S2.14: Adding a 4th source.



References

1. Patterson, N. *et al.* Ancient admixture in human history. *Genetics* **192**, 1065-1093, (2012).
2. Haak, W. *et al.* Massive migration from the steppe was a source for Indo-European languages in Europe. *Nature* **522**, 207-211, (2015).
3. Patterson, N., Price, A. L. & Reich, D. Population structure and eigenanalysis. *PLoS Genet.* **2**, e190, (2006).
4. Price, A. L. *et al.* Principal components analysis corrects for stratification in genome-wide association studies. *Nat. Genet.* **38**, 904-909, (2006).
5. Lipson, M. *et al.* Efficient moment-based inference of admixture parameters and sources of gene flow. *Mol. Biol. Evol.* **30**, 1788-1802, (2013).
6. Fu, Q. *et al.* Genome sequence of a 45,000-year-old modern human from western Siberia. *Nature* **514**, 445-449, (2014).
7. Fu, Q. *et al.* The genetic history of Ice Age Europe. *Nature* **534**, 200-205, (2016).
8. Raghavan, M. *et al.* Upper Palaeolithic Siberian genome reveals dual ancestry of Native Americans. *Nature* **505**, 87-91, (2014).
9. Sikora, M. *et al.* Ancient genomes show social and reproductive behavior of early Upper Paleolithic foragers. *Science*, (2017).
10. Yang, M. A. *et al.* 40,000-Year-Old Individual from Asia Provides Insight into Early Population Structure in Eurasia. *Curr. Biol.* **27**, 3202-3208.e3209, (2017).
11. Lipson, M. & Reich, D. A Working Model of the Deep Relationships of Diverse Modern Human Genetic Lineages Outside of Africa. *Mol. Biol. Evol.* **34**, 889-902, (2017).
12. Skoglund, P. *et al.* Genomic Diversity and Admixture Differs for Stone-Age Scandinavian Foragers and Farmers. *Science* **344**, 747-750, (2014).
13. Lazaridis, I. *et al.* Ancient human genomes suggest three ancestral populations for present-day Europeans. *Nature* **513**, 409-413, (2014).
14. van de Loosdrecht, M. *et al.* Pleistocene North African genomes link Near Eastern and sub-Saharan African human populations. *Science*, (2018).
15. Llorente, M. G. *et al.* Ancient Ethiopian genome reveals extensive Eurasian admixture in Eastern Africa. *Science* **350**, 820-822, (2015).
16. Skoglund, P. *et al.* Reconstructing Prehistoric African Population Structure. *Cell* **171**, 59-71.e21, (2017).
17. Mallick, S. *et al.* The Simons Genome Diversity Project: 300 genomes from 142 diverse populations. *Nature* **538**, 201-206, (2016).
18. Busing, F. T. A., Meijer, E. & Leeden, R. Delete-m Jackknife for Unequal m. *Statistics and Computing* **9**, 3-8, (1999).

Supplementary Information section 3

Quantifying admixture in ancient populations without an explicit phylogenetic model

We first employed *qpWave*¹/*qpAdm*² using the following **All** set of population outgroups, which includes Mbuti (an African outgroup), diverse Upper Paleolithic Europeans and Siberians, the only published Upper Paleolithic sample from East Asia (Tianyuan), eastern non-Africans (Onge, Han, Papuan), and the newly reported samples from Dzudzuana.

All: Mbuti³, Ust_Ishim⁴, Tianyuan⁵, Onge³, Han³, Papuan³, Kostenki14⁶, GoyetQ116-1⁶, Sunghir³⁷, Vestonice16⁶, MA1⁸, AG3⁶, Villabruna⁶, Dzudzuana

As in ref. 9 we take $N=1, 2, 3, 4$ sources from the **All** set to model each *Test* population, evaluating whether the $N+1$ tuple $\text{Left}=(\text{Test}, S_1, \dots, S_N)$ are consistent with descending from N streams of ancestry relative to the remaining outgroups (**All** \ *Left*).

Test is chosen from a **Test** set that includes all populations in **All** as well as additional non-African populations, including Eastern European hunter-gatherers (Karelia_HG), Neolithic Siberian hunter-gatherers from near Lake Baikal in Russia, and ancient populations from the Caucasus (Caucasus hunter-gatherers CHG), North Africa (Ibero-Maurusians from Taforalt), and the Near East: Epipaleolithic hunter-gatherers from the Levant (Natufian), early farmers from Iran (Iran_N), the Levant (PPNB), Anatolia (Anatolia_N), and the Maghreb (Morocco_EN).

Test: AG3, Anatolia_N¹⁰, CHG¹¹, Dzudzuana, ElMiron⁶, GoyetQ116-1, Han, Iran_N¹², Karelia_HG^{2,10}, Kostenki14, MA1, Morocco_EN¹³, Natufian¹², Onge, Papuan, PPNB¹², Russia_Baikal_EN¹⁴, Sunghir³, Taforalt¹⁵, Tianyuan, Ust_Ishim, Vestonice16, Villabruna

For each choice of N we identify *feasible* models^{9,12} defined as those which we cannot reject using *qpWave* (p-value for rank= $N-1$ greater than 0.05) and for which *qpAdm* produces admixture estimates within the interval $[0, 1]$. We caution that while our procedure can identify plausible models to the limits of our statistical resolution, it is identifying a minimally complex model that fits the data, the true admixture history is probably more complex, involving low level admixture from additional sources.

Simple clades ($N=1$)

We first attempt to fit each *Test* population from **Test** as a simple clade with each population of **All** (Table S3.1).

Table S3.1: Feasible models of simple clades ($N=1$). For all other populations of **Test** no source populations are feasible ($P < 0.00012$).

Test	S₁	P-value
AG3	MA1	0.107
Anatolia_N	Dzudzuana	0.286
MA1	AG3	0.107

We see that (MA1, AG3), the members of the “Mal’ta cluster”⁶ are a clade, and also that Neolithic Anatolians form a clade with Dzudzuana with respect to the diverse non-African and non-Near Eastern populations of the **All** set. Note that Neolithic Anatolians and Dzudzuana are not a clade with respect to post-glacial Near Eastern and North African populations (Extended Data Fig. 5).

2-way mixtures ($N=2$)

We next attempt to fit each *Test* population from **Test** as 2-way mixtures of populations of **All** (Table S3.2). (MA1, AG3) and (Anatolia_N, Dzudzuana) are modeled as having most ancestry from each other (and we cannot reject in the $N=1$ analysis that they are a simple clade).

ElMiron (Magdalenian culture) is modeled as a 2-way mixture of ~61% Villabruna and ~39% GoyetQ116-1, similar to those inferred using an explicit admixture graph model⁶ (~63/37%).

Han are modeled as a mixture of ~56% related to Tianyuan (a ~40,000 year old East Asian) and ~44% related to Onge (hunter-gatherers from the Andaman Islands), consistent with a recent TreeMix¹⁶ analysis¹⁷ that modeled East Asians as an admixture between the same two populations. Onge themselves are modeled as mixtures of Han and Papuan which might be tentatively suggestive of a Tianyuan→Han→Onge→Papuan cline in eastern non-Africans. However, Papuans are also modeled as a mixture of Onge and ~9.5% Mbuti; this does not mean that they have African ancestry, and this proportion likely reflects archaic Eurasian admixture from Neandertals and Denisovans¹⁸.

Both Kostenki14 and Vestonice16 are modeled by *qpAdm* as mixtures; Kostenki14 with most of its ancestry from Vestonice16, and Vestonice as a 2-way mixture of populations related to Sunghir3 and

Villabruna. The admixture graph model developed in Supplementary Information section 2 models Kostenki14 as unadmixed and models Vestonice16 as the same type of 2-way mixture as *qpAdm*. The admixture graph model of ref. 7 also models Vestonice16 as a mixture of Sunghir3 and a population related to Villabruna.

If Vestonice16 did indeed have ancestry from a Villabruna-related population then this type of ancestry was already in both Europe and the Caucasus by ~30-27 thousand years ago, and mixed (in Europe) with the earliest inhabitants represented by Sunghir3 and in the Caucasus (see below) with Basal Eurasians. The fact that it was also present in western Anatolia at the time of the Neolithic, as well as in eastern Europe by the time of the Eastern European hunter-gatherers from Karelia (see below) suggest a distribution of this type of ancestry around the Black Sea from which it could have propagated.

Finally, we model Russia_Baikal_EN as a 2-way mixture of Han and $15.7 \pm 1.6\%$ MA1-related ancestry. This set of ~7-8 thousand year old samples from Lokomotiv contrast with the ~18 thousand year old AG3 sample which as we saw above could be modeled as a clade with MA1. It appears that populations of East Asian-related ancestry appeared in the region in the intervening period¹⁴. As we will see below, mixed AG3/East Asian-related ancestry reached West Eurasia as well.

Table S3.2: Feasible models of 2-way mixtures ($N=2$).

Test			P-value	Mixture Proportions		Std. Errors	
	S₁	S₂		S₁	S₂	S₁	S₂
AG3	Mbuti	MA1	0.247	0.067	0.933	0.06	0.06
AG3	Ust_Ishim	MA1	0.218	0.096	0.904	0.068	0.068
AG3	MA1	Dzudzuana	0.109	0.812	0.188	0.187	0.187
AG3	Papuan	MA1	0.082	0.034	0.966	0.034	0.034
AG3	Onge	MA1	0.078	0.04	0.96	0.033	0.033
AG3	Han	MA1	0.077	0.044	0.956	0.035	0.035
AG3	Tianyuan	MA1	0.067	0.04	0.96	0.04	0.04
Anatolia_N	Onge	Dzudzuana	0.749	0.024	0.976	0.011	0.011
Anatolia_N	Tianyuan	Dzudzuana	0.717	0.033	0.967	0.013	0.013
Anatolia_N	Papuan	Dzudzuana	0.685	0.026	0.974	0.012	0.012
Anatolia_N	Han	Dzudzuana	0.627	0.028	0.972	0.011	0.011
Anatolia_N	Ust_Ishim	Dzudzuana	0.537	0.048	0.952	0.021	0.021
Anatolia_N	Mbuti	Dzudzuana	0.433	0.027	0.973	0.014	0.014
Anatolia_N	AG3	Dzudzuana	0.236	0.016	0.984	0.027	0.027
Dzudzuana	Mbuti	Villabruna	0.274	0.275	0.725	0.037	0.037
ElMiron	GoyetQ116-1	Villabruna	0.167	0.394	0.606	0.118	0.118
Han	Tianyuan	Onge	0.085	0.556	0.444	0.174	0.174
Kostenki14	Vestonice16	Villabruna	0.111	0.899	0.101	0.11	0.11
Kostenki14	Ust_Ishim	Vestonice16	0.066	0.16	0.84	0.032	0.032
MA1	GoyetQ116-1	AG3	0.412	0.115	0.885	0.081	0.081
MA1	Sunghir3	AG3	0.157	0.071	0.929	0.039	0.039
MA1	Kostenki14	AG3	0.097	0.021	0.979	0.034	0.034
MA1	AG3	Villabruna	0.08	0.949	0.051	0.052	0.052
MA1	Vestonice16	AG3	0.073	0.025	0.975	0.031	0.031
Morocco_EN	Mbuti	Dzudzuana	0.414	0.325	0.675	0.032	0.032
Natufian	Mbuti	Dzudzuana	0.702	0.112	0.888	0.022	0.022
Onge	Han	Papuan	0.306	0.357	0.643	0.111	0.111
Papuan	Mbuti	Onge	0.193	0.095	0.905	0.041	0.041
PPNB	Mbuti	Dzudzuana	0.729	0.071	0.929	0.018	0.018
Russia_Baikal_EN	Han	MA1	0.313	0.843	0.157	0.016	0.016
Sunghir3	Kostenki14	Vestonice16	0.366	0.842	0.158	0.266	0.266
Taforalt	Mbuti	Dzudzuana	0.556	0.272	0.728	0.024	0.024
Taforalt	Mbuti	Villabruna	0.062	0.575	0.425	0.026	0.026
Tianyuan	Ust_Ishim	Han	0.066	0.365	0.635	0.062	0.062
Vestonice16	Sunghir3	Villabruna	0.137	0.643	0.357	0.113	0.113

Deep ancestry in Dzudzuana and Taforalt

Both Dzudzuana and Taforalt are modeled as 2-way mixtures of Mbuti and Villabruna. Mbuti occupies a symmetrical phylogenetic position to all Eurasians populations—splitting off before the differentiation of western Eurasians, eastern non-Africans, and Ust’Ishim^{6,12,19} from each other—and can thus be used to quantify such ancestry¹². Similar proportions of such ancestry are inferred for Taforalt and a ~7,000 year old Early Neolithic population from the Maghreb (Morocco_EN from Ifri n’Amr or Moussa¹³). We clarify that in this section we are using the term “Deep ancestry” to represent any type of ancestry that separated from the main group of Eurasians before they differentiated from each other. This type of ancestry includes the “Basal Eurasian” lineage that was previously shown to have admixed into Near Easterners and that is inferred to have descended from same founder event / bottleneck that gave rise to the main ancestry in all non-Africans¹⁹. However, our “deep ancestry” definition also includes deeper splitting lineages as well, some of whose ancestors may not have experienced this bottleneck. Indeed, in what follows we show that “Deep Ancestry” in West Eurasians is comprised not only of Basal Eurasian ancestry but also some more deeply splitting lineages.

Dzudzuana is inferred by *qpAdm* to have ~28% deep ancestry, identical to the admixture graph model of Supplementary Information section 2. We also obtain a similar estimate of 30.3+/-8.1% when we restrict our analysis to reads with evidence of DNA damage (Methods). When we model the two Dzudzuana individuals separately, we obtain similar estimates of 26.0~4.2% for I2949 and 31.3±5.3% for I2963. Taforalt is inferred to have ~58% deep ancestry; the admixture graph model makes them a mixture of Dzudzuana and a more deeply splitting lineage, thus giving them $0.45 + 0.55 * .28 \approx 60\%$ deeply splitting ancestry, which is also a good match to the admixture graph. However, *qpAdm* can also successfully model Taforalt as a mixture of 73% Dzudzuana and 27% Mbuti, which produces a lower proportion of $0.73 * 0.28 + 0.27 \approx 47\%$ deep ancestry. It is difficult to imagine that either Villabruna or Dzudzuana are very closely related to the ancestors of Ibero-Maurusians in North Africa, however, but both *qpAdm* and *qpGraph* seem to point to them having deeply related ancestry to Villabruna and Dzudzuana plus other deep ancestry. We also observe that the Mbuti+Dzudzuana model works with Villabruna as an outgroup, which does suggest that the Villabruna-related ancestry in Taforalt was mediated by a Dzudzuana-related population. Additionally, the Mbuti+Villabruna model fits only marginally ($p=0.062$), while the Mbuti+Dzudzuana model more comfortably ($p=0.556$).

Whatever the non-African related population that admixed to form Ibero-Maurusians, we can say that it is most closely related to Dzudzuana and Villabruna, and that with Villabruna as a baseline, Dzudzuana already had some deep ancestry and Ibero-Maurusians from Taforalt even more. The admixture graph

model suggests that this deep ancestry was distinct in Taforalt and Dzudzuana, with Taforalt possessing ancestry from both an early and a later split, while Dzudzuana possessing ancestry only from the later split (the later split corresponds to the original concept of “Basal Eurasians”^{ref} indicating that it largely derives from the same bottleneck that affected other non-Africans).

Both populations from the Levant (Epipaleolithic Natufians and early Neolithic Pre-Pottery Neolithic PPNB farmers) can also be modeled as a mixture of Dzudzuana and Mbuti, with a little more deep ancestry in Natufians (~11%) than in PPNB (~7%) on top of the deep ancestry of Dzudzuana. Thus, Villabruna→Dzudzuana/Anatolia_N→PPNB→Natufian→Taforalt represents a cline of increasing deep ancestry (and decreasing Villabruna-related ancestry) in what was previously termed the South/West West Eurasian interaction sphere¹².

3-way mixtures (N=3)

The following populations of **Test** could not be modeled as either simple clades or 2-way mixtures: CHG, GoyetQ116-1, Iran_N, Karelia_HG, Ust_Ishim, Villabruna. This may be because (i) they are even more complex mixtures, or (ii) they are unadmixed, or (iii) there are no good sources for them in the **All** set.

We could model all but two of them as 3-way mixtures (Table S3.3). The affinity of Tianyuan and GoyetQ116-1 observed in ref.5 is explained by a model in which GoyetQ116-1 traces ~15% of its ancestry from a Tianyuan-related source; the admixture graph model of Supplementary Information section 2 proposed that Tianyuan traces part of its ancestry from a GoyetQ116-1-related source and the authors of ref.5 found it difficult to simultaneously fit Tianyuan and GoyetQ116-1. While both *qpAdm* and *qpGraph* require some common ancestry, the direction of gene flow remains inconclusive.

Ust’Ishim is modeled in diverse ways as a mixture of Mbuti and a combination of a western Eurasian and eastern non-African sources. This sample is approximately symmetrically related to west Eurasians and eastern non-Africans⁴ and can fit in the model without admixture. The proposed 3-way mixtures of Table S3.3 may be a balancing act preserving the symmetry by the relationship by making Ust’Ishim have ancestry from both west and east Eurasian populations. Given the lack of other lines of evidence that Ust’Ishim is admixed, we are cautious about accepting the *qpAdm* results at face value, but report them for the sake of completeness.

Villabruna, is also shown as a 3-way mixture in the model of Table S3.3, tracing about half its ancestry from Dzudzuana, and the remainder from Vestonic16 and MA1. This is not *a priori* implausible as all these sources are earlier than Villabruna. The admixture graph model presents a simpler model for Villabruna as a simple clade, and an unadmixed Villabruna acts as a plausible source for several other

simpler mixtures of (Table S3.2). We are thus cautious about accepting this *qpAdm* result at face value as well. Earlier sampling may reveal whether Villabruna-cluster⁶ populations existed earlier than ~15 thousand years ago.

Finally, Karelia_HG, a representative of Eastern European hunter-gatherers (EHG), can be modeled as a mixture of Afontova Gora 3 (AG3) and Villabruna, in agreement with previous inferences that it was a mixture of Western European hunter-gatherers (WHG) and Ancient North Eurasians (ANE)², but with an additional minor component of ~3% Han-related ancestry. We also tried separately a model with Russia_Baikal_EN (instead of Han) as a source. The p-value for this model is 0.028 with an estimated 7±1.2% Russia_Baikal_EN ancestry. A thorough sampling of Neolithic hunter-gatherers from across North Eurasia may clarify the origin of the EHG.

Table S3.3: Feasible models of 3-way mixtures (N=3).

<i>Test</i>				<i>P-value</i>	Mixture Proportions			Std. Errors		
	<i>S</i> ₁	<i>S</i> ₂	<i>S</i> ₃		<i>S</i> ₁	<i>S</i> ₂	<i>S</i> ₃	<i>S</i> ₁	<i>S</i> ₂	<i>S</i> ₃
GoyetQ116-1	Tianyuan	Sunghir3	Vestonice16	0.334	0.153	0.018	0.829	0.031	0.220	0.210
Karelia_HG	Han	AG3	Villabruna	0.060	0.032	0.628	0.340	0.015	0.029	0.028
Ust_Ishim	Mbuti	Papuan	GoyetQ116-1	0.826	0.162	0.446	0.392	0.138	0.071	0.076
Ust_Ishim	Mbuti	Onge	GoyetQ116-1	0.625	0.173	0.431	0.395	0.123	0.070	0.064
Ust_Ishim	Mbuti	Papuan	Kostenki14	0.115	0.344	0.401	0.255	0.102	0.063	0.048
Ust_Ishim	Mbuti	Tianyuan	Dzudzuana	0.085	0.866	0.076	0.059	0.215	0.088	0.146
Ust_Ishim	Mbuti	Onge	Dzudzuana	0.078	0.842	0.055	0.103	0.366	0.116	0.261
Ust_Ishim	Mbuti	Papuan	Sunghir3	0.076	0.383	0.380	0.237	0.102	0.065	0.047
Ust_Ishim	Mbuti	Onge	Kostenki14	0.060	0.287	0.430	0.283	0.113	0.073	0.049
Ust_Ishim	Mbuti	Han	GoyetQ116-1	0.059	0.238	0.406	0.355	0.140	0.080	0.070
Ust_Ishim	Mbuti	Han	Dzudzuana	0.054	0.921	0.039	0.040	0.322	0.110	0.226
Villabruna	Vestonice16	MA1	Dzudzuana	0.071	0.374	0.160	0.465	0.063	0.040	0.085

4-way mixtures (N=4)

For the two remaining populations which could not be fit as 3-way mixtures we considered 4-way mixtures (Table S3.4). Both CHG and Iran_N can fit as a 4-way mixture with Mbuti as one source, Dzudzuana as another, and a combination of eastern non-African (ENA) and Ancient North Eurasian (ANE) ancestry. >50% of the ancestry is inferred to derive from Dzudzuana in Iran_N and >64% in CHG. Previously we had shown that CHG could be modelled as a mixture of Iran_N and European hunter-gatherers¹². The Dzudzuana population clarifies the origin of these populations by showing that European affinity in the Caucasus decreased between Dzudzuana at ~26 kya and Satsurblia at ~13 kya as additional ENA/ANE ancestry arrived. Thus, Iran_N/CHG are seen as descendants of populations that existed in the

Villabruna→Basal Eurasian cline alluded to above, but with extra Basal Eurasian ancestry (compared to Dzudzuana), and also with ENA/ANE ancestry. The extra ENA/ANE ancestry also explains the affinity between Iran/Caucasus and EHG previously proposed as part of a North/East West Eurasian interaction sphere¹², which our results suggest was created by admixture of ENA/ANE ancestry on top of the Villabruna→Basal Eurasian cline. In the north, Karelia_HG traces its ancestry to a Villabruna-related source modified by ENA/ANE admixture, while CHG/Iran_N were Dzudzuana+Basal Eurasian (or, equivalently Villabruna+Basal Eurasian) derived populations also modified by ENA/ANE admixture.

As seen above, populations of mixed ENA/ANE admixture (such as Russia_Baikal_EN) already existed in Siberia by the Neolithic, although with a preponderance of ENA over ANE ancestry (the opposite of what we see in the eastern periphery of West Eurasia from Eastern Europe to Iran).

Table S3.4: Feasible models of 4-way mixtures (N=4).

Test					P-value	Mixture Proportions				Std. Errors			
	S₁	S₂	S₃	S₄		S₁	S₂	S₃	S₄	S₁	S₂	S₃	S₄
CHG	Mbuti	Tianyuan	AG3	Dzudzuana	0.685	0.054	0.081	0.222	0.643	0.040	0.028	0.031	0.041
CHG	Mbuti	Tianyuan	MA1	Dzudzuana	0.381	0.050	0.100	0.168	0.682	0.045	0.032	0.040	0.049
CHG	Mbuti	Onge	AG3	Dzudzuana	0.176	0.018	0.078	0.218	0.686	0.046	0.028	0.031	0.044
CHG	Mbuti	Onge	MA1	Dzudzuana	0.159	0.010	0.097	0.159	0.734	0.052	0.030	0.041	0.052
CHG	Mbuti	Han	AG3	Dzudzuana	0.101	0.092	0.034	0.230	0.645	0.051	0.029	0.033	0.048
CHG	Mbuti	Papuan	AG3	Dzudzuana	0.086	0.012	0.080	0.221	0.687	0.060	0.031	0.032	0.051
CHG	Mbuti	Han	MA1	Dzudzuana	0.075	0.086	0.052	0.176	0.687	0.057	0.033	0.044	0.060
Iran_N	Mbuti	Onge	AG3	Dzudzuana	0.129	0.097	0.109	0.218	0.577	0.047	0.025	0.026	0.041
Iran_N	Mbuti	Onge	MA1	Dzudzuana	0.076	0.090	0.134	0.157	0.619	0.053	0.028	0.036	0.053
Iran_N	Mbuti	Tianyuan	AG3	Dzudzuana	0.052	0.145	0.106	0.221	0.527	0.041	0.027	0.026	0.036

North African admixture in the Near East

The analysis using the **All** set showed that Levantine (Natufians and PPNB) and North African (Taforalt and Morocco_EN) populations could be modeled as a mixture of Dzudzuana with extra Basal Eurasian ancestry. The study of the Ibero-Maurusian remains from Taforalt was initially interpreted as suggesting that this population was formed by admixture between Natufians and a Sub-Saharan population¹⁵. However, the admixture graph model suggests the opposite scenario: that Natufians were formed by admixture from a Taforalt-related population and a Dzudzuana-related one.

We sought to determine the direction of admixture without a priori assumptions by forming the following set, which includes **All** plus a ~2,000BP hunter-gatherer from South Africa²⁰, a ~4,500 year old sample from East Africa (Mota), Yoruba (from present-day West Africa where no ancient genomic data is available), Taforalt and Natufians:

AllAfrican: Mbuti, South_Africa_HG²⁰, Mota²¹, Yoruba³, Ust_Ishim, Tianyuan, Onge, Han, Papuan, Kostenki14, GoyetQ116-1, Sunghir3, Vestonice16, MA1, AG3, Villabruna, Dzudzuana, Taforalt, Natufian

None of the Near Eastern populations could be modeled as simple clades of any members of the **AllAfrican** set ($p < 1e-7$). The Early Neolithic samples from Morocco could be modeled as a simple clade with Taforalt ($p = 0.06$). All the ones that could be modelled as mixtures of Villabruna/Dzudzuana+Basal Eurasian in the previous analysis using the **All** set could also be modeled using the **AllAfrican** set (Table S3.5).

Table S3.5: Feasible models of 2-way mixtures ($N=2$) using the AllAfrican set.

Test			P-value	Mixture Proportions		Std. Errors	
	S₁	S₂		S₁	S₂	S₁	S₂
Anatolia_N	Dzudzuana	Natufian	0.070	0.859	0.141	0.029	0.029
Natufian	Dzudzuana	Taforalt	0.405	0.863	0.137	0.019	0.019
PPNB	Dzudzuana	Natufian	0.910	0.409	0.591	0.042	0.042
PPNB	Villabruna	Natufian	0.187	0.163	0.837	0.024	0.024

Taforalt could not be modeled as any 2-way mixture. The best model involving Natufians and an African population (Yoruba) could still be strongly rejected ($p = 2.7e-13$). Taforalt could also not be modeled as a 3-way mixture. However, Natufians could be convincingly modeled as a 2-way mixture of ~86% Dzudzuana and ~14% Taforalt ($p = 0.405$) with small standard errors of 1.9%. Thus the affinity between Natufians and Taforalt described in ref.15 may have come about by admixture from a North African/Taforalt-related population into Natufians, rather than by admixture in the opposite direction.

The results of our analysis using the **All** set, as well as the results of the analysis of ref.15 do suggest that Taforalt can be modeled as a mixture of a West Eurasian related population (represented by Dzudzuana in our case) and a Sub-Saharan African lineage. However, when one uses only a single African population as a source without using others as outgroups, this mixture can only be interpreted as evidence of ancestry from a lineage basal to members of the **All** set, rather than as evidence of ancestry specifically

related to the chosen African population. No Sub-Saharan African populations appear to be good sources for the ancestry of Taforalt as described previously.

The admixture graph model suggests an alternative possibility: that it is West African populations like the Yoruba that may have ancestry from a North African Taforalt-like population. Under such a scenario, North Africa and the Levant were occupied by populations that experienced gene flow from each other, with more ancestry from a Basal lineage in North Africa, and more ancestry from a West Eurasian-specific lineage (represented by Dzudzuana) in the Levant, thus explaining the presence of Dzudzuana-related admixture in Taforalt and of Taforalt-related admixture in the Levant. Under this scenario, a North African-related population may have contributed some ancestry to Sub-Saharan populations to its south, perhaps during the Holocene Green Sahara period ($\sim 11\text{-}6\text{ kya}$)²² that postdates the sampled Taforalt individual which may have facilitated north→south gene flow across the Sahara.

Based on the very low presence of Neandertal admixture in Yoruba, it has been estimated that $>2.7\pm 0.9\%$ of the ancestry of Yoruba came from West Eurasia 9618 ± 1825 years ago²³. The admixture graph model predicts that 13% of the ancestry of Yoruba came from Taforalt, which in turn was 55% descended from Dzudzuana and which in turn was 72% descended from Villabruna, for a total of $0.13 \times 0.55 \times 0.72 \approx 5\%$ Villabruna-related ancestry that would have carried Neanderthal DNA. This is consistent with the $>2.7\pm 0.9\%$ estimate of ref.²³.

Two other populations fit as 2-way mixtures in Table S3.5:

Neolithic Anatolians fit as $\sim 86\%$ Dzudzuana and $\sim 14\%$ Natufians. This does not disprove that Neolithic Anatolians are approximately a clade with Dzudzuana, since Natufians trace $\sim 86\text{-}89\%$ of their ancestry to Dzudzuana (Tables S3.2, 5), and thus Neolithic Anatolians trace $>98\%$ of their ancestry from Dzudzuana, also in agreement with the 2-way models of Table S3.2. This does not mean that there was gene flow from the Levant into western Anatolia, as the (unsampled) hunter-gatherer precursors of Neolithic Anatolians may not have been identical to Dzudzuana.

Finally, PPNB can be modeled as a mixture of $\sim 41\%$ Dzudzuana and $\sim 59\%$ Natufians, consistent with them tracing a large part of their ancestry to pre-farming populations of the Levant¹². Again, we should not necessarily interpret these admixture proportions as signifying admixture into the Levant from the north during the formation of early Neolithic populations, as PPNB could be descended from a Levantine population that was not identical to the sampled Natufians.

Conclusions

We summarize our main conclusions from this section:

- “Western” Near Eastern populations, including Dzudzuana from the Caucasus, belonged to a cline of decreasing Villabruna/increasing deep ancestry: Villabruna → Dzudzuana/Anatolia_N → PPNB → Natufian → Taforalt
- “Eastern” Near Eastern populations, including Caucasus hunter-gatherers (CHG) and Neolithic Iranians (Iran_N) traced most of their ancestry from populations of this cline, but also had additional Ancient North Eurasian/Eastern non-African (ANE/ENA) admixture.
- Similar ANE/ENA admixture was represented in Eastern European hunter-gatherers (EHG) from Karelia; both Europe and the Near East was impacted by this eastern influence.
- Within the main Villabruna/Basal Eurasian cline, we can determine that there was both Dzudzuana/Villabruna-like influence in North Africa (Taforalt), but also Taforalt-like admixture in the Levant

References

1. Reich, D. *et al.* Reconstructing Native American population history. *Nature* **488**, 370-374, (2012).
2. Haak, W. *et al.* Massive migration from the steppe was a source for Indo-European languages in Europe. *Nature* **522**, 207-211, (2015).
3. Mallick, S. *et al.* The Simons Genome Diversity Project: 300 genomes from 142 diverse populations. *Nature* **538**, 201-206, (2016).
4. Fu, Q. *et al.* Genome sequence of a 45,000-year-old modern human from western Siberia. *Nature* **514**, 445-449, (2014).
5. Yang, M. A. *et al.* 40,000-Year-Old Individual from Asia Provides Insight into Early Population Structure in Eurasia. *Curr. Biol.* **27**, 3202-3208.e3209, (2017).
6. Fu, Q. *et al.* The genetic history of Ice Age Europe. *Nature* **534**, 200-205, (2016).
7. Sikora, M. *et al.* Ancient genomes show social and reproductive behavior of early Upper Paleolithic foragers. *Science*, (2017).
8. Raghavan, M. *et al.* Upper Palaeolithic Siberian genome reveals dual ancestry of Native Americans. *Nature* **505**, 87-91, (2014).
9. Lazaridis, I. *et al.* Genetic origins of the Minoans and Mycenaeans. *Nature* **548**, 214, (2017).
10. Mathieson, I. *et al.* Genome-wide patterns of selection in 230 ancient Eurasians. *Nature* **528**, 499-503, (2015).
11. Jones, E. R. *et al.* Upper Palaeolithic genomes reveal deep roots of modern Eurasians. *Nat. Commun.* **6**, 8912, (2015).
12. Lazaridis, I. *et al.* Genomic insights into the origin of farming in the ancient Near East. *Nature* **536**, 419-424, (2016).
13. Fregel, R. *et al.* Ancient genomes from North Africa evidence prehistoric migrations to the Maghreb from both the Levant and Europe. *Proceedings of the National Academy of Sciences*, (2018).

14. de Barros Damgaard, P. *et al.* The first horse herders and the impact of early Bronze Age steppe expansions into Asia. *Science*, (2018).
15. van de Loosdrecht, M. *et al.* Pleistocene North African genomes link Near Eastern and sub-Saharan African human populations. *Science*, (2018).
16. Pickrell, J. K. & Pritchard, J. K. Inference of population splits and mixtures from genome-wide Allele frequency data. *PLoS Genet.* **8**, e1002967, (2012).
17. McColl, H. *et al.* Ancient Genomics Reveals Four Prehistoric Migration Waves into Southeast Asia. *bioRxiv*, (2018).
18. Meyer, M. *et al.* A High-Coverage Genome Sequence from an Archaic Denisovan Individual. *Science* **338**, 222-226, (2012).
19. Lazaridis, I. *et al.* Ancient human genomes suggest three ancestral populations for present-day Europeans. *Nature* **513**, 409-413, (2014).
20. Skoglund, P. *et al.* Reconstructing Prehistoric African Population Structure. *Cell* **171**, 59-71.e21, (2017).
21. Llorente, M. G. *et al.* Ancient Ethiopian genome reveals extensive Eurasian admixture in Eastern Africa. *Science* **350**, 820-822, (2015).
22. Larrasoana, J. C., Roberts, A. P. & Rohling, E. J. Dynamics of Green Sahara Periods and Their Role in Hominin Evolution. *PLoS ONE* **8**, e76514, (2013).
23. Prufer, K. *et al.* The complete genome sequence of a Neanderthal from the Altai Mountains. *Nature* **505**, 43-49, (2014).

Supplementary Information section 4

Ancestral proportions of West Eurasians and North Africans

The ways in which West Eurasian populations were formed, by complex processes of differentiation and subsequent admixture, remains a mystery. In past work we derived admixture proportions in terms of the known sources of ancestry of Europeans: first as mixtures of WHG, early European farmers, and Upper Paleolithic Siberian “Ancient North Eurasians” (ANE)¹ and subsequently with the Yamnaya steppe pastoralists as a more proximate source for the eastern ANE ancestry².

It is difficult to simultaneously model the proximate history of admixture of all present-day West Eurasians, as this involves many sources, most of them unsampled. However, since the proximate sources are themselves mixtures of earlier ones, we can attempt to model West Eurasians as mixtures of earlier sources of ancestry, with the understanding that these “ultimate” sources themselves almost certainly have complex ancestry. In previous work³, we showed that diverse ancient and present-day West Eurasians are largely derived from the differentiated farmers of the Near East from Anatolia, the Levant, and Iran, and the differentiated hunter-gatherers from mainland (WHG) and eastern (EHG) Europe. Here we replace the Neolithic populations of the Near East used in the previous modeling with the hunter-gatherer ones from the region to which we now have access, thereby presenting a new model of components of West Eurasian variation entirely in terms of hunter-gatherer components.

From our analysis of Supplementary Information section 3, we showed that these sources are indeed complex, and only one of these (WHG, represented by Villabruna) appears to be a contributor to all the remaining sources. This should not be understood as showing that hunter-gatherers from mainland Europe migrated to the rest of West Eurasia, but rather that the fairly homogeneous post-15kya population of mainland Europe labeled WHG appear to represent a deep strain of ancestry that seems to have contributed to West Eurasians from the Gravettian era down to the Neolithic period.

In this section, we use the following sources to study the ancestry of West Eurasians.

Sources: Villabruna⁴, ElMiron⁴, Dzudzuana, AG3⁴, Russia_Baikal_EN⁵, Mbuti

Villabruna is representative of the WHG group. We also include ElMiron, the best sample from the Magdalenian era as we noticed that within the WHG group there were individuals that could not be modeled as a simple clade with Villabruna but also had some ElMiron-related ancestry. Dzudzuana is representative of the Ice Age Caucasus population, differentiated from Villabruna by Basal Eurasian ancestry. AG3 represents ANE/Upper Paleolithic Siberian ancestry, sampled from the vicinity of Lake

Baikal, while Russia_Baikal_EN related to eastern Eurasians and represents a later layer of ancestry from the same region of Siberia as AG3. Finally, Mbuti are a deeply diverged African population that is used here to represent deep strains of ancestry (including Basal Eurasian) prior to the differentiation between West Eurasians and eastern non-Africans that are otherwise not accounted for by the remaining five sources. Collectively, we refer to this as ‘Basal’ or ‘Deep’ ancestry, which should be understood as referring potentially to both Basal Eurasian and African ancestry.

To differentiate between the sources, we used the following set of outgroups:

Outgroups: Ust_Ishim⁶, Kostenki14⁴, GoyetQ116-1⁴, Sunghir3⁷, Vestonice16⁴, ElMiron⁴, MA1⁸, Tianyuan⁹, Clovis¹⁰, Villabruna⁴, Dzudzuana, AG3⁴, Russia_Baikal_EN⁵, Mbuti

This set includes all the **Sources** as well as early samples from Siberia (Ust_Ishim and MA1), Europe (Kostenki14, GoyetQ116-1, Sunghir3, and Vestonice16), and the Americas (Clovis).

We study the ancestry of the following *Test* populations:

Test: (*ancient*): Bichon¹¹, Loschbour¹, LaBranal¹², KO1¹³, Croatia_Mesolithic_HG¹⁴, Iberia_Canes¹⁵, Iberia_Chan¹⁵, Iron_Gates_HG¹⁴, Serbia_HG¹⁴, Latvia_HG¹⁴, Motala_HG^{1,16}, Sweden_Mesolithic¹⁷, Norway_Mesolithic¹⁷, Norway_Neolithic_HG¹⁷, Ukraine_Mesolithic¹⁴, Ukraine_Neolithic¹⁴, Karelia_HG^{2,16}, Morocco_EN¹⁸, Samara_HG^{2,16}, Russia_Popovo2¹⁹, Russia_Sidelkino⁵, Russia_UzOO77¹⁹, Taforalt²⁰, Natufian³, PPNB³, Anatolia_N¹⁶, CHG¹¹, Iran_N³

(*present-day*)^{1,3,21,22}: Abkhasian, Adygei, Albanian, Algerian, Armenian, Assyrian, Balkar, Basque, BedouinA, BedouinB, Belarusian, Bulgarian, Canary_Islander, Chechen, Chuvash, Croatian, Cypriot, Czech, Druze, Egyptian, English, Estonian, Finnish, French, Georgian, German, Greek, Hungarian, Icelandic, Iranian, Iranian_Bandari, Irish, Irish_Ulster, Italian_North, Italian_South, Jew_Ashkenazi, Jew_Georgian, Jew_Iranian, Jew_Iraqi, Jew_Libyan, Jew_Moroccan, Jew_Tunisian, Jew_Turkish, Jew_Yemenite, Jordanian, Kumyk, Lebanese, Lebanese_Christian, Lebanese_Muslim, Lezgin, Libyan, Lithuanian, Maltese, Mordovian, Moroccan, Mozabite, Norwegian, Orcadian, Ossetian, Palestinian, Polish, Romanian, Russian, Saharawi, Sardinian, Saudi, Scottish, Shetlandic, Sicilian, Sorb, Spanish, Spanish_North, Syrian, Tunisian, Turkish, Turkish_Balikesir, Ukrainian, Yemeni

The **Test** set includes all the ancient populations of Fig. 1c, and diverse present-day West Eurasian and North African populations genotyped on the Human Origins array.

For all populations in **Test** we evaluated $62 = \sum_{N=1}^5 \binom{6}{N}$ combinations of the 6 chosen **Sources**, varying the number of sources from $N=1$ to 5, and using the set of **Outgroups** as the Right set of a *qpWave/qpAdm* analysis (excluding any of the chosen sources from it).

A feasible model was defined as having *qpAdm*-inferred mixture proportions in the $[0,1]$ and we cannot reject ($P \geq 0.05$) that the *Test* population and the chosen N sources were derived by $N-1$ waves of ancestry from the Outgroups.

We first identified all feasible models. Next, for each population was identified the “best” model for each N , defined as having the highest P value. If the best model has $P < 0.05$ for $N-1$ and $P \geq 0.05$ for N , then our “conservative” estimate is the best model with N sources. The “speculative” estimate is the feasible model with the most sources. The conservative model can be seen as a minimum complexity model for each population, as models with fewer sources are rejected. The speculative model is useful because it hints at additional ancestral components for the *Test* population; this may be important because our power to detect minor ancestral component differs when dealing with populations composed of different number of individuals and (for ancient data) different data quality. Thus, a minor ancestral component may be necessary to model a high quality population in the “conservative” estimate, but simpler models cannot be rejected for a population with poor quality data.

We list all the feasible models for all considered populations in Tables S4.1-5, plot the speculative proportions for present-day populations against a map of West Eurasia in Fig. 3, and both conservative and speculative proportions for all populations of **Test** in Extended Data Fig. 6.

We begin with a couple of new observations on ancient populations revealed by our analysis.

One of the sources (ElMiron) seems to have contributed to WHG, especially in Iberia, but also in western Europe (Loschbour) and to a lesser degree (according to the speculative estimates) across Europe. It has been previously suggested⁴ that both ElMiron and Loschbour are a mixture of Villabruna and GoyetQ116-1-related ancestry (ElMiron and other Magdalenian-era hunter-gatherers appear to possess this Aurignacian-era related ancestry that was not detected in the temporally intermediate members of the Gravettian-related Vestonice cluster). Based on our analysis it seems that this shared affinity may have come about by some members of the WHG cluster having inherited ancestry from the temporally preceding Magdalenians. Note that it is possible that Villabruna itself (and other samples not shown to have ElMiron ancestry in our analysis) may have such ancestry which is not detected here since we use Villabruna as a source population.

It has been suggested that there is an Anatolia Neolithic-related affinity in hunter-gatherers from the Iron Gates¹⁴. Our analysis confirms this by showing that this population has Dzudzuana-related ancestry as do many hunter-gatherer populations from southeastern Europe, eastern Europe and Scandinavia. These populations cannot be modeled as a simple mixture of Villabruna and AG3 but require extra Dzudzuana-related ancestry even in the conservative estimates, with a positive admixture proportion inferred for several more in the speculative ones. Thus, the distinction between European hunter-gatherers and Near Eastern populations may have been gradual in pre-Neolithic times; samples from the Aegean (intermediate between those from the Balkans and Anatolia) may reveal how gradual the transition between Dzudzuana-like Neolithic Anatolians and mostly Villabruna-like hunter-gatherers was in southeastern Europe.

Turning to the present-day West Eurasians and North Africans, we discuss the distribution of the ancestral populations:

Villabruna: This type of ancestry differentiates between present-day Europeans and non-Europeans within West Eurasia, attaining a maximum of ~20% in the Baltic in accordance with previous observations¹ and with the finding of a later persistence of significant hunter-gatherer ancestry in the region^{14,23,24}. Its proportion drops to ~0% throughout the Near East. Interestingly, a hint of such ancestry is also inferred in all North African populations west of Libya in the speculative proportions, consistent with an archaeogenetic inference of gene flow from Iberia to North Africa during the Late Neolithic²⁵.

ElMiron: This type of ancestry is absent in present-day West Eurasians. This may be because most of the Villabruna-related ancestry in Europeans traces to WHG populations that lacked it (since ElMiron-related ancestry is quite variable within European hunter-gatherers). However, ElMiron ancestry makes up only a minority component of all WHG populations sampled to date and WHG-related ancestry is a minority component of present-day Europeans. Thus, our failure to detect it in present day people may be simply be too little of it to detect with our methods.

Dzudzuana: Our analysis identifies Dzudzuana-related ancestry as the most important component of West Eurasians and the one that is found across West Eurasian-North African populations at ~46-88% levels. Thus, Dzudzuana-related ancestry can be viewed as the common core of the ancestry of West Eurasian-North African populations. Its distribution reaches its minima in northern Europe and appears to be complementary to that of Villabruna, being most strongly represented in North Africa, the Near East (including the Caucasus) and Mediterranean Europe. Our results here are expected from those of Supplementary Information section 3 in which we modeled ancient Near Eastern/North African populations (the principal ancestors of present-day people from the same regions) as deriving much of their ancestry from a Dzudzuana-related source. Migrations from the Near East/Caucasus associated with the spread of the Neolithic, but also the formation of steppe populations^{2,16} introduced

most of the Dzudzuana-related ancestry present in Europe, although (as we have seen above) some such ancestry was already present in some pre-agricultural hunter-gatherers in Europe.

AG3: Ancestry related to the AG3 sample from Siberia has a northern distribution, being strongly represented in both central-northern Europe and the north Caucasus.

Russia_Baikal_EN: Ancestry related to hunter-gatherers from Lake Baikal in Siberia (postdating AG3) appears to have affected primarily northeastern European populations which have been previously identified as having East Eurasian ancestry¹; some such ancestry is also identified for a Turkish population from Balıkesir, likely reflecting the Central Asian ancestry of Turkic speakers which has been recently confirmed directly in an Ottoman sample from Anatolia⁵.

Mbuti: This is a catch-all category of ‘Basal’ ancestry defined as stemming from lineages that split off prior to the differentiation of the **Sources** and **Outgroups**. It is used to account for extra Basal Eurasian ancestry (than what is contributed by Dzudzuana), as well as other Basal ancestry (e.g., from North or Sub-Saharan Africans). Note that populations from the Levant and Iran/Caucasus have extra ‘Basal’ ancestry compared to Dzudzuana, as do North Africans from Taforalt and the Early Neolithic. We do not attempt to pinpoint the origin of this ancestry, as this will be better studied when representative samples from across Africa are available. It is clear (Extended Data Fig. 6) that some of this ancestry cannot be explained by admixture from Levantine/Iran/Caucasus populations as some of the Near Eastern and North African populations share more drift with a Sub-Saharan African population than can be explained by non-African sources alone.

Table S4.1: Feasible models with N=1 sources

Test	Source	P-value
Anatolia_N	Dzudzuana	0.685
Bichon	Villabruna	0.186
Croatia_Mesolithic_HG	Villabruna	0.108
Iberia_Canes	Villabruna	0.052

Table S4.2: Feasible models with N=2 sources

Test			P-value	Mixture Proportions		Standard Errors	
	A	B		A	B	A	B
Albanian	Dzudzuana	AG3	0.114	0.871	0.129	0.024	0.024
Anatolia_N	Dzudzuana	Russia_Baikal_EN	0.845	0.979	0.021	0.011	0.011
Anatolia_N	Dzudzuana	AG3	0.704	0.966	0.034	0.026	0.026
Anatolia_N	Dzudzuana	Mbuti	0.622	0.986	0.014	0.020	0.020
Bichon	Villabruna	ElMiron	0.545	0.995	0.005	0.088	0.088
Bichon	Villabruna	AG3	0.113	0.982	0.018	0.048	0.048
Croatia_Mesolithic_HG	Villabruna	AG3	0.219	0.865	0.135	0.062	0.062
Croatia_Mesolithic_HG	Villabruna	Dzudzuana	0.081	0.967	0.033	0.215	0.215
Croatia_Mesolithic_HG	Villabruna	Russia_Baikal_EN	0.074	0.968	0.032	0.031	0.031
Croatia_Mesolithic_HG	Villabruna	Mbuti	0.071	0.994	0.006	0.041	0.041
Iberia_Canes	Villabruna	AG3	0.104	0.913	0.087	0.047	0.047
Iberia_Chan	Villabruna	ElMiron	0.373	0.175	0.825	0.086	0.086
KO1	Villabruna	AG3	0.052	0.747	0.253	0.040	0.040
Loschbour	Villabruna	ElMiron	0.103	0.788	0.212	0.074	0.074
Moroccan	Dzudzuana	Mbuti	0.080	0.836	0.164	0.023	0.023
Morocco_EN	Dzudzuana	Mbuti	0.858	0.698	0.302	0.044	0.044
Mozabite	Dzudzuana	Mbuti	0.086	0.871	0.129	0.023	0.023
Natufian	Dzudzuana	Mbuti	0.675	0.893	0.107	0.032	0.032
Norway_Neolithic_HG	Villabruna	AG3	0.071	0.370	0.630	0.029	0.029
PPNB	Dzudzuana	Mbuti	0.681	0.955	0.045	0.025	0.025
Russia_Popovo2	Villabruna	AG3	0.800	0.213	0.787	0.050	0.050
Russia_Popovo2	ElMiron	AG3	0.209	0.154	0.846	0.060	0.060
Russia_Popovo2	Dzudzuana	AG3	0.064	0.449	0.551	0.196	0.196
Russia_UzOO77	Villabruna	AG3	0.625	0.208	0.792	0.022	0.022
Saharawi	Dzudzuana	Mbuti	0.362	0.850	0.150	0.024	0.024
Serbia_HG	Villabruna	AG3	0.365	0.793	0.207	0.050	0.050
Serbia_HG	Villabruna	Russia_Baikal_EN	0.072	0.925	0.075	0.027	0.027
Serbia_HG	Villabruna	Dzudzuana	0.070	0.701	0.299	0.104	0.104
Taforalt	Dzudzuana	Mbuti	0.938	0.740	0.260	0.034	0.034

Table S4.3: Feasible models with N=3 sources

Test				P-value	Mixture Proportions			Standard Errors		
	A	B	C		A	B	C	A	B	C
Albanian	Dzudzuana	AG3	Russia_Baikal_EN	0.060	0.872	0.120	0.009	0.024	0.027	0.012
Algerian	Dzudzuana	AG3	Mbuti	0.145	0.792	0.096	0.111	0.032	0.025	0.024
Algerian	Dzudzuana	Russia_Baikal_EN	Mbuti	0.118	0.907	0.058	0.035	0.028	0.017	0.038
Anatolia_N	Dzudzuana	AG3	Russia_Baikal_EN	0.737	0.970	0.012	0.018	0.026	0.031	0.013
Anatolia_N	Villabruna	Dzudzuana	Russia_Baikal_EN	0.698	0.009	0.969	0.022	0.026	0.033	0.012
Anatolia_N	Dzudzuana	AG3	Mbuti	0.688	0.953	0.040	0.007	0.029	0.027	0.020
Anatolia_N	Villabruna	Dzudzuana	Mbuti	0.449	0.018	0.959	0.022	0.041	0.070	0.034
Armenian	Dzudzuana	AG3	Mbuti	0.158	0.765	0.156	0.079	0.032	0.023	0.021
Assyrian	Dzudzuana	AG3	Mbuti	0.326	0.753	0.156	0.091	0.030	0.023	0.020
BedouinA	Dzudzuana	AG3	Mbuti	0.117	0.757	0.125	0.117	0.029	0.023	0.020
BedouinB	Dzudzuana	AG3	Mbuti	0.164	0.799	0.098	0.103	0.030	0.024	0.022
BedouinB	Dzudzuana	Russia_Baikal_EN	Mbuti	0.082	0.916	0.058	0.026	0.026	0.017	0.036
Bichon	Villabruna	ElMiron	AG3	0.840	0.864	0.028	0.107	0.093	0.077	0.047
Bichon	Villabruna	ElMiron	Dzudzuana	0.646	0.804	0.004	0.192	0.190	0.079	0.155
Bichon	Villabruna	ElMiron	Russia_Baikal_EN	0.563	0.954	0.020	0.026	0.090	0.084	0.026
Bichon	Villabruna	ElMiron	Mbuti	0.487	0.939	0.022	0.039	0.098	0.085	0.036
CHG	Dzudzuana	AG3	Mbuti	0.228	0.670	0.200	0.130	0.043	0.032	0.029
Croatia_Mesolithic_HG	Villabruna	ElMiron	AG3	0.110	0.844	0.016	0.140	0.128	0.106	0.070
Croatia_Mesolithic_HG	Villabruna	ElMiron	Dzudzuana	0.062	0.902	0.011	0.087	1.006	0.201	0.892
Croatian	Villabruna	Dzudzuana	AG3	0.052	0.016	0.819	0.165	0.021	0.038	0.026
Cypriot	Dzudzuana	AG3	Mbuti	0.276	0.808	0.136	0.057	0.030	0.023	0.020
Druze	Dzudzuana	AG3	Mbuti	0.286	0.798	0.132	0.070	0.029	0.023	0.020
Egyptian	Dzudzuana	AG3	Mbuti	0.110	0.773	0.095	0.133	0.030	0.023	0.021
Georgian	Dzudzuana	AG3	Mbuti	0.084	0.758	0.172	0.070	0.032	0.023	0.021
Iberia_Canes	Villabruna	ElMiron	AG3	0.540	0.651	0.188	0.160	0.094	0.074	0.046
Iberia_Chan	Villabruna	ElMiron	AG3	0.719	0.140	0.792	0.068	0.088	0.078	0.043
Iberia_Chan	Villabruna	ElMiron	Mbuti	0.484	0.092	0.842	0.066	0.101	0.085	0.038
Iberia_Chan	Villabruna	ElMiron	Russia_Baikal_EN	0.456	0.146	0.829	0.026	0.087	0.082	0.024
Iberia_Chan	Villabruna	ElMiron	Dzudzuana	0.271	0.067	0.765	0.168	0.186	0.100	0.224
Icelandic	Villabruna	Dzudzuana	AG3	0.094	0.056	0.738	0.206	0.022	0.038	0.024
Iran_N	Dzudzuana	AG3	Mbuti	0.377	0.527	0.211	0.262	0.040	0.026	0.030
Iron_Gates_HG	Villabruna	Dzudzuana	AG3	0.624	0.603	0.168	0.229	0.047	0.065	0.032
Italian_South	Dzudzuana	AG3	Mbuti	0.056	0.855	0.132	0.013	0.033	0.027	0.021
Jew_Ethiopian	Dzudzuana	AG3	Mbuti	0.605	0.602	0.076	0.322	0.031	0.021	0.026
Jew_Ethiopian	Dzudzuana	Russia_Baikal_EN	Mbuti	0.257	0.704	0.046	0.250	0.032	0.017	0.043
Jew_Georgian	Dzudzuana	AG3	Mbuti	0.368	0.765	0.160	0.075	0.031	0.023	0.021
Jew_Iranian	Dzudzuana	AG3	Mbuti	0.064	0.766	0.149	0.085	0.031	0.024	0.020
Jew_Iraqi	Dzudzuana	AG3	Mbuti	0.203	0.761	0.139	0.101	0.031	0.024	0.021
Jew_Libyan	Dzudzuana	AG3	Mbuti	0.221	0.828	0.108	0.064	0.030	0.025	0.020
Jew_Moroccan	Dzudzuana	AG3	Mbuti	0.259	0.835	0.115	0.050	0.031	0.025	0.021
Jew_Tunisian	Dzudzuana	AG3	Mbuti	0.052	0.838	0.100	0.062	0.032	0.026	0.021
Jew_Turkish	Dzudzuana	AG3	Mbuti	0.126	0.845	0.117	0.038	0.031	0.025	0.021

Jew_Yemenite	Dzudzuana	AG3	Mbuti	0.328	0.790	0.108	0.102	0.032	0.024	0.022
Jordanian	Dzudzuana	AG3	Mbuti	0.052	0.771	0.126	0.103	0.031	0.024	0.022
KO1	Villabruna	Dzudzuana	AG3	0.332	0.514	0.326	0.160	0.072	0.094	0.045
KO1	Villabruna	ElMiron	AG3	0.168	0.710	0.079	0.211	0.098	0.080	0.046
KO1	Villabruna	AG3	Mbuti	0.100	0.738	0.241	0.021	0.041	0.046	0.032
KO1	Villabruna	AG3	Russia_Baikal_EN	0.076	0.759	0.224	0.017	0.041	0.053	0.028
LaBran1	Villabruna	ElMiron	AG3	0.149	0.453	0.365	0.182	0.083	0.067	0.040
Lebanese	Dzudzuana	AG3	Mbuti	0.050	0.760	0.139	0.101	0.031	0.024	0.020
Lebanese_Christian	Dzudzuana	AG3	Mbuti	0.526	0.803	0.128	0.070	0.029	0.023	0.021
Lebanese_Muslim	Dzudzuana	AG3	Mbuti	0.173	0.772	0.136	0.092	0.029	0.023	0.020
Libyan	Dzudzuana	Russia_Baikal_EN	Mbuti	0.158	0.876	0.055	0.069	0.028	0.017	0.038
Libyan	Dzudzuana	AG3	Mbuti	0.080	0.779	0.079	0.142	0.032	0.025	0.024
Loschbour	Villabruna	ElMiron	AG3	0.504	0.654	0.233	0.113	0.082	0.065	0.041
Loschbour	Villabruna	ElMiron	Russia_Baikal_EN	0.142	0.748	0.232	0.020	0.078	0.072	0.023
Loschbour	Villabruna	ElMiron	Mbuti	0.086	0.770	0.225	0.005	0.091	0.074	0.035
Maltese	Dzudzuana	AG3	Mbuti	0.125	0.849	0.141	0.010	0.030	0.024	0.019
Moroccan	Dzudzuana	AG3	Mbuti	0.293	0.779	0.064	0.157	0.029	0.023	0.021
Moroccan	Dzudzuana	Russia_Baikal_EN	Mbuti	0.267	0.857	0.041	0.102	0.025	0.016	0.035
Morocco_EN	Dzudzuana	Russia_Baikal_EN	Mbuti	0.911	0.721	0.032	0.246	0.046	0.027	0.060
Morocco_EN	Dzudzuana	AG3	Mbuti	0.819	0.670	0.047	0.283	0.050	0.044	0.046
Morocco_EN	Villabruna	Dzudzuana	Mbuti	0.736	0.031	0.633	0.335	0.066	0.167	0.106
Morocco_EN	Villabruna	ElMiron	Mbuti	0.073	0.316	0.026	0.658	0.152	0.123	0.051
Motala_HG	Villabruna	Dzudzuana	AG3	0.101	0.446	0.086	0.469	0.045	0.074	0.039
Mozabite	Dzudzuana	Russia_Baikal_EN	Mbuti	0.481	0.895	0.048	0.057	0.025	0.017	0.035
Mozabite	Dzudzuana	AG3	Mbuti	0.236	0.819	0.062	0.119	0.029	0.024	0.022
Natufian	Dzudzuana	AG3	Mbuti	0.770	0.860	0.034	0.106	0.045	0.039	0.032
Natufian	Dzudzuana	Russia_Baikal_EN	Mbuti	0.700	0.885	0.009	0.105	0.035	0.030	0.054
Natufian	ElMiron	Dzudzuana	Mbuti	0.539	0.048	0.813	0.139	0.075	0.129	0.059
Natufian	Villabruna	Dzudzuana	Mbuti	0.529	0.012	0.860	0.128	0.054	0.097	0.052
Norway_Mesolithic	Villabruna	Dzudzuana	AG3	0.091	0.283	0.222	0.494	0.047	0.083	0.047
Norway_Neolithic_HG	Villabruna	Dzudzuana	AG3	0.649	0.264	0.217	0.519	0.046	0.086	0.052
Norway_Neolithic_HG	Villabruna	AG3	Russia_Baikal_EN	0.255	0.379	0.564	0.056	0.029	0.039	0.023
Norway_Neolithic_HG	Villabruna	AG3	Mbuti	0.101	0.353	0.604	0.043	0.030	0.033	0.024
Norway_Neolithic_HG	Villabruna	ElMiron	AG3	0.076	0.397	0.001	0.602	0.085	0.074	0.034
Palestinian	Dzudzuana	AG3	Mbuti	0.457	0.780	0.120	0.099	0.029	0.022	0.020
PPNB	Villabruna	Dzudzuana	Mbuti	0.774	0.071	0.826	0.103	0.052	0.090	0.044
PPNB	ElMiron	Dzudzuana	Mbuti	0.589	0.022	0.915	0.063	0.052	0.090	0.043
PPNB	Dzudzuana	AG3	Mbuti	0.491	0.954	0.001	0.045	0.037	0.035	0.026
Russia_Popovo2	Villabruna	AG3	Russia_Baikal_EN	0.811	0.217	0.725	0.058	0.048	0.077	0.058
Russia_Popovo2	Villabruna	Dzudzuana	AG3	0.772	0.148	0.209	0.643	0.073	0.189	0.139
Russia_Popovo2	Villabruna	AG3	Mbuti	0.730	0.201	0.767	0.032	0.056	0.059	0.059
Russia_Popovo2	ElMiron	Dzudzuana	AG3	0.179	0.048	0.361	0.592	0.111	0.331	0.238
Russia_Popovo2	ElMiron	AG3	Mbuti	0.144	0.153	0.814	0.033	0.063	0.071	0.055
Russia_Popovo2	ElMiron	AG3	Russia_Baikal_EN	0.139	0.165	0.829	0.007	0.059	0.090	0.061
Russia_Sidelkino	Villabruna	Dzudzuana	AG3	0.307	0.083	0.330	0.587	0.037	0.077	0.049
Russia_Sidelkino	Villabruna	AG3	Mbuti	0.118	0.184	0.762	0.054	0.027	0.025	0.025

Russia_Sidelkino	Villabruna	AG3	Russia_Baikal_EN	0.099	0.212	0.721	0.067	0.022	0.030	0.023
Russia_UzOO77	Villabruna	Dzudzuana	AG3	0.761	0.151	0.146	0.703	0.046	0.115	0.076
Russia_UzOO77	Villabruna	AG3	Russia_Baikal_EN	0.750	0.205	0.750	0.045	0.022	0.032	0.025
Russia_UzOO77	Villabruna	AG3	Mbuti	0.628	0.189	0.773	0.038	0.026	0.026	0.028
Saharawi	Dzudzuana	AG3	Mbuti	0.614	0.802	0.056	0.142	0.031	0.026	0.023
Saharawi	Dzudzuana	Russia_Baikal_EN	Mbuti	0.470	0.867	0.030	0.102	0.027	0.017	0.037
Samara_HG	Villabruna	AG3	Russia_Baikal_EN	0.122	0.245	0.652	0.103	0.022	0.034	0.026
Saudi	Dzudzuana	AG3	Mbuti	0.231	0.809	0.095	0.096	0.031	0.024	0.022
Saudi	Dzudzuana	Russia_Baikal_EN	Mbuti	0.122	0.921	0.054	0.024	0.026	0.018	0.036
Serbia_HG	Villabruna	Dzudzuana	AG3	0.738	0.662	0.155	0.183	0.083	0.104	0.054
Serbia_HG	Villabruna	AG3	Mbuti	0.286	0.788	0.182	0.030	0.051	0.058	0.035
Serbia_HG	Villabruna	AG3	Russia_Baikal_EN	0.273	0.793	0.186	0.021	0.051	0.064	0.030
Serbia_HG	Villabruna	Dzudzuana	Russia_Baikal_EN	0.109	0.742	0.207	0.051	0.121	0.141	0.032
Shetlandic	Villabruna	Dzudzuana	AG3	0.081	0.052	0.744	0.204	0.022	0.040	0.025
Sicilian	Dzudzuana	AG3	Mbuti	0.087	0.871	0.117	0.012	0.031	0.025	0.020
Sweden_Mesolithic	Villabruna	Dzudzuana	AG3	0.531	0.364	0.235	0.401	0.041	0.067	0.037
Syrian	Dzudzuana	AG3	Mbuti	0.233	0.771	0.133	0.096	0.031	0.024	0.021
Tunisian	Dzudzuana	AG3	Mbuti	0.173	0.786	0.089	0.125	0.030	0.024	0.021
Tunisian	Dzudzuana	Russia_Baikal_EN	Mbuti	0.143	0.894	0.055	0.051	0.026	0.017	0.035
Ukraine_Mesolithic	Villabruna	Dzudzuana	AG3	0.202	0.282	0.217	0.501	0.034	0.063	0.037
Ukraine_Neolithic	Villabruna	Dzudzuana	AG3	0.277	0.319	0.250	0.432	0.032	0.056	0.032
Yemeni	Dzudzuana	AG3	Mbuti	0.075	0.703	0.117	0.180	0.031	0.024	0.023
Chechen	Dzudzuana	AG3	Russia_Baikal_EN	0.006	0.820	0.132	0.049	0.025	0.028	0.013
German	Villabruna	Dzudzuana	AG3	0.029	0.035	0.782	0.183	0.023	0.040	0.025
Orcadian	Villabruna	Dzudzuana	AG3	0.024	0.044	0.758	0.198	0.023	0.041	0.026
Karelia_HG	Villabruna	AG3	Russia_Baikal_EN	0.011	0.226	0.710	0.063	0.022	0.032	0.022
Karelia_HG	Villabruna	Dzudzuana	AG3	0.001	0.149	0.159	0.693	0.046	0.100	0.062

Table S4.4: Feasible models with N=4 sources

Test					P-value	Mixture Proportions				Standard Errors			
	A	B	C	D		A	B	C	D	A	B	C	D
Abkhasian	Dzudzuana	AG3	Russia_Baikal_EN	Mbuti	0.207	0.779	0.150	0.036	0.035	0.042	0.031	0.019	0.033
Albanian	Villabruna	Dzudzuana	AG3	Mbuti	0.198	0.044	0.748	0.174	0.034	0.037	0.087	0.031	0.031
Algerian	Dzudzuana	AG3	Russia_Baikal_EN	Mbuti	0.194	0.834	0.068	0.033	0.065	0.044	0.032	0.020	0.039
Algerian	Villabruna	Dzudzuana	AG3	Mbuti	0.119	0.020	0.720	0.110	0.151	0.039	0.102	0.029	0.049
Anatolia_N	Villabruna	Dzudzuana	AG3	Mbuti	0.675	0.053	0.856	0.054	0.037	0.040	0.078	0.027	0.031
Anatolia_N	Villabruna	Dzudzuana	AG3	Russia_Baikal_EN	0.533	0.009	0.959	0.011	0.020	0.026	0.039	0.031	0.015
Armenian	Dzudzuana	AG3	Russia_Baikal_EN	Mbuti	0.167	0.795	0.134	0.024	0.046	0.042	0.031	0.020	0.035
Assyrian	Dzudzuana	AG3	Russia_Baikal_EN	Mbuti	0.436	0.792	0.128	0.030	0.050	0.040	0.030	0.019	0.033
Assyrian	Villabruna	Dzudzuana	AG3	Mbuti	0.186	0.014	0.712	0.167	0.108	0.032	0.085	0.030	0.036
Basque	Villabruna	Dzudzuana	AG3	Mbuti	0.081	0.147	0.594	0.202	0.057	0.045	0.097	0.032	0.031
BedouinA	Dzudzuana	AG3	Russia_Baikal_EN	Mbuti	0.206	0.799	0.098	0.032	0.072	0.040	0.029	0.019	0.035
BedouinB	Dzudzuana	AG3	Russia_Baikal_EN	Mbuti	0.203	0.836	0.073	0.030	0.061	0.042	0.031	0.020	0.037
Bichon	Villabruna	ElMiron	Dzudzuana	AG3	0.732	0.776	0.025	0.118	0.081	0.189	0.077	0.171	0.054
Bichon	Villabruna	ElMiron	AG3	Mbuti	0.691	0.855	0.032	0.101	0.012	0.098	0.078	0.050	0.037
Bichon	Villabruna	ElMiron	Dzudzuana	Russia_Baikal_EN	0.522	0.822	0.009	0.162	0.006	0.210	0.079	0.197	0.031
Bichon	Villabruna	ElMiron	Russia_Baikal_EN	Mbuti	0.390	0.954	0.020	0.021	0.006	0.101	0.085	0.047	0.069
Bulgarian	Villabruna	Dzudzuana	AG3	Mbuti	0.089	0.065	0.682	0.196	0.057	0.039	0.095	0.033	0.034
Bulgarian	Villabruna	Dzudzuana	AG3	Russia_Baikal_EN	0.065	0.016	0.830	0.128	0.025	0.023	0.039	0.027	0.013
Canary_Islander	Villabruna	Dzudzuana	AG3	Mbuti	0.569	0.157	0.548	0.177	0.119	0.059	0.133	0.038	0.049
Croatian	Villabruna	Dzudzuana	AG3	Mbuti	0.063	0.071	0.681	0.210	0.037	0.039	0.098	0.036	0.033
Cypriot	Dzudzuana	AG3	Russia_Baikal_EN	Mbuti	0.350	0.844	0.109	0.030	0.018	0.040	0.031	0.020	0.034
Cypriot	Villabruna	Dzudzuana	AG3	Mbuti	0.175	0.020	0.751	0.150	0.080	0.034	0.085	0.029	0.034
Druze	Dzudzuana	AG3	Russia_Baikal_EN	Mbuti	0.316	0.832	0.108	0.027	0.034	0.040	0.030	0.020	0.034
Druze	Villabruna	Dzudzuana	AG3	Mbuti	0.170	0.013	0.755	0.143	0.088	0.033	0.083	0.029	0.034
Egyptian	Dzudzuana	AG3	Russia_Baikal_EN	Mbuti	0.116	0.802	0.076	0.023	0.099	0.040	0.029	0.019	0.035
Finnish	Villabruna	Dzudzuana	AG3	Russia_Baikal_EN	0.149	0.079	0.635	0.228	0.057	0.024	0.042	0.024	0.013
French	Villabruna	Dzudzuana	AG3	Mbuti	0.063	0.124	0.583	0.234	0.059	0.041	0.098	0.034	0.030
Georgian	Dzudzuana	AG3	Russia_Baikal_EN	Mbuti	0.211	0.803	0.140	0.036	0.021	0.042	0.031	0.020	0.035
Georgian	Villabruna	Dzudzuana	AG3	Mbuti	0.066	0.005	0.718	0.184	0.092	0.037	0.102	0.033	0.042
Greek	Villabruna	Dzudzuana	AG3	Mbuti	0.053	0.045	0.723	0.176	0.056	0.037	0.091	0.032	0.033
Iberia_Canes	Villabruna	ElMiron	Dzudzuana	AG3	0.674	0.560	0.223	0.030	0.187	0.171	0.072	0.176	0.050
Iberia_Chan	Villabruna	ElMiron	AG3	Mbuti	0.685	0.100	0.805	0.052	0.044	0.098	0.080	0.045	0.039
Iberia_Chan	Villabruna	ElMiron	AG3	Russia_Baikal_EN	0.639	0.140	0.797	0.056	0.007	0.087	0.078	0.052	0.028
Iberia_Chan	Villabruna	ElMiron	Dzudzuana	AG3	0.529	0.085	0.761	0.093	0.060	0.159	0.091	0.186	0.045
Iberia_Chan	Villabruna	ElMiron	Dzudzuana	Russia_Baikal_EN	0.259	0.121	0.812	0.045	0.023	0.189	0.116	0.265	0.032
Icelandic	Villabruna	Dzudzuana	AG3	Russia_Baikal_EN	0.189	0.080	0.703	0.193	0.024	0.023	0.038	0.024	0.012
Icelandic	Villabruna	Dzudzuana	AG3	Mbuti	0.076	0.103	0.616	0.241	0.040	0.041	0.096	0.035	0.029
Iranian	Dzudzuana	AG3	Russia_Baikal_EN	Mbuti	0.236	0.734	0.171	0.037	0.058	0.039	0.029	0.018	0.031
Iranian_Bandari	Dzudzuana	AG3	Russia_Baikal_EN	Mbuti	0.509	0.669	0.167	0.045	0.119	0.040	0.028	0.018	0.034
Iran_N	Dzudzuana	AG3	Russia_Baikal_EN	Mbuti	0.278	0.553	0.195	0.017	0.236	0.053	0.036	0.024	0.046
Irish	Villabruna	Dzudzuana	AG3	Russia_Baikal_EN	0.062	0.076	0.700	0.197	0.027	0.022	0.039	0.024	0.012
Iron_Gates_HG	Villabruna	ElMiron	Dzudzuana	AG3	0.504	0.520	0.039	0.211	0.230	0.090	0.041	0.087	0.029

Italian_North	Villabruna	Dzudzuana	AG3	Mbuti	0.152	0.064	0.724	0.169	0.042	0.038	0.088	0.031	0.031
Italian_North	Villabruna	Dzudzuana	AG3	Russia_Baikal_EN	0.061	0.010	0.863	0.108	0.019	0.023	0.039	0.027	0.013
Italian_South	Villabruna	Dzudzuana	AG3	Mbuti	0.066	0.042	0.736	0.160	0.061	0.041	0.095	0.032	0.037
Jew_Ethiopian	Dzudzuana	AG3	Russia_Baikal_EN	Mbuti	0.744	0.629	0.064	0.019	0.287	0.040	0.025	0.019	0.040
Jew_Ethiopian	Villabruna	Dzudzuana	AG3	Mbuti	0.456	0.016	0.551	0.081	0.352	0.029	0.085	0.022	0.053
Jew_Georgian	Dzudzuana	AG3	Russia_Baikal_EN	Mbuti	0.584	0.808	0.129	0.034	0.029	0.042	0.031	0.020	0.035
Jew_Georgian	Villabruna	Dzudzuana	AG3	Mbuti	0.234	0.015	0.714	0.174	0.096	0.037	0.098	0.033	0.040
Jew_Iranian	Dzudzuana	AG3	Russia_Baikal_EN	Mbuti	0.160	0.803	0.124	0.030	0.043	0.040	0.030	0.020	0.034
Jew_Iraqi	Dzudzuana	AG3	Russia_Baikal_EN	Mbuti	0.200	0.796	0.112	0.029	0.062	0.042	0.031	0.021	0.036
Jew_Iraqi	Villabruna	Dzudzuana	AG3	Mbuti	0.130	0.012	0.715	0.150	0.123	0.036	0.096	0.032	0.040
Jew_Libyan	Dzudzuana	AG3	Russia_Baikal_EN	Mbuti	0.335	0.873	0.074	0.036	0.017	0.042	0.033	0.021	0.035
Jew_Libyan	Villabruna	Dzudzuana	AG3	Mbuti	0.279	0.039	0.716	0.135	0.110	0.034	0.083	0.029	0.033
Jew_Moroccan	Dzudzuana	AG3	Russia_Baikal_EN	Mbuti	0.367	0.876	0.084	0.034	0.006	0.043	0.033	0.021	0.036
Jew_Moroccan	Villabruna	Dzudzuana	AG3	Mbuti	0.193	0.015	0.778	0.130	0.077	0.039	0.096	0.031	0.040
Jew_Tunisian	Villabruna	Dzudzuana	AG3	Mbuti	0.094	0.060	0.668	0.142	0.130	0.040	0.102	0.033	0.041
Jew_Turkish	Villabruna	Dzudzuana	AG3	Mbuti	0.172	0.048	0.708	0.151	0.093	0.037	0.093	0.031	0.038
Jew_Yemenite	Dzudzuana	AG3	Russia_Baikal_EN	Mbuti	0.224	0.808	0.096	0.014	0.082	0.044	0.032	0.021	0.038
Jew_Yemenite	Villabruna	Dzudzuana	AG3	Mbuti	0.175	0.014	0.754	0.116	0.116	0.036	0.091	0.030	0.040
Jordanian	Dzudzuana	AG3	Russia_Baikal_EN	Mbuti	0.155	0.819	0.093	0.039	0.049	0.041	0.031	0.020	0.036
KO1	Villabruna	ElMiron	AG3	Russia_Baikal_EN	0.229	0.709	0.088	0.198	0.005	0.095	0.079	0.053	0.028
KO1	Villabruna	AG3	Russia_Baikal_EN	Mbuti	0.213	0.757	0.238	0.004	0.000	0.049	0.052	0.047	0.056
Kumyk	Dzudzuana	AG3	Russia_Baikal_EN	Mbuti	0.154	0.782	0.165	0.052	0.001	0.043	0.032	0.020	0.033
Latvia_HG	Villabruna	ElMiron	Dzudzuana	AG3	0.090	0.386	0.108	0.146	0.360	0.077	0.036	0.089	0.034
Lebanese	Dzudzuana	AG3	Russia_Baikal_EN	Mbuti	0.189	0.812	0.105	0.039	0.044	0.043	0.031	0.020	0.036
Lebanese_Christian	Dzudzuana	AG3	Russia_Baikal_EN	Mbuti	0.628	0.823	0.115	0.016	0.045	0.039	0.030	0.020	0.034
Lebanese_Muslim	Dzudzuana	AG3	Russia_Baikal_EN	Mbuti	0.343	0.815	0.105	0.035	0.045	0.040	0.030	0.020	0.034
Lebanese_Muslim	Villabruna	Dzudzuana	AG3	Mbuti	0.079	0.002	0.760	0.139	0.099	0.035	0.091	0.031	0.038
Libyan	Dzudzuana	AG3	Russia_Baikal_EN	Mbuti	0.130	0.827	0.046	0.038	0.089	0.044	0.032	0.021	0.039
Maltese	Villabruna	Dzudzuana	AG3	Mbuti	0.254	0.049	0.708	0.178	0.065	0.036	0.086	0.029	0.032
Mordovian	Villabruna	Dzudzuana	AG3	Russia_Baikal_EN	0.084	0.067	0.652	0.219	0.062	0.022	0.041	0.024	0.013
Moroccan	Villabruna	Dzudzuana	AG3	Mbuti	0.371	0.026	0.692	0.080	0.202	0.033	0.083	0.025	0.040
Moroccan	Dzudzuana	AG3	Russia_Baikal_EN	Mbuti	0.254	0.808	0.045	0.023	0.124	0.040	0.029	0.019	0.036
Morocco_EN	Dzudzuana	AG3	Russia_Baikal_EN	Mbuti	0.801	0.698	0.029	0.023	0.250	0.062	0.054	0.033	0.059
Morocco_EN	Villabruna	Dzudzuana	Russia_Baikal_EN	Mbuti	0.799	0.024	0.682	0.033	0.261	0.060	0.146	0.028	0.106
Morocco_EN	Villabruna	Dzudzuana	AG3	Mbuti	0.649	0.024	0.621	0.048	0.306	0.063	0.159	0.045	0.101
Morocco_EN	Villabruna	ElMiron	Russia_Baikal_EN	Mbuti	0.073	0.360	0.012	0.000	0.627	0.164	0.124	0.051	0.098
Motala_HG	Villabruna	ElMiron	Dzudzuana	AG3	0.303	0.269	0.109	0.180	0.442	0.089	0.041	0.097	0.036
Motala_HG	Villabruna	Dzudzuana	AG3	Russia_Baikal_EN	0.118	0.486	0.018	0.472	0.025	0.057	0.097	0.041	0.021
Mozabite	Dzudzuana	AG3	Russia_Baikal_EN	Mbuti	0.389	0.861	0.033	0.036	0.070	0.039	0.030	0.020	0.036
Mozabite	Villabruna	Dzudzuana	AG3	Mbuti	0.313	0.047	0.691	0.083	0.179	0.034	0.083	0.025	0.040
Mozabite	Villabruna	Dzudzuana	Russia_Baikal_EN	Mbuti	0.313	0.020	0.850	0.048	0.082	0.035	0.074	0.017	0.049
Natufian	ElMiron	Dzudzuana	AG3	Mbuti	0.676	0.061	0.745	0.051	0.144	0.073	0.143	0.042	0.056
Natufian	Villabruna	Dzudzuana	AG3	Mbuti	0.645	0.027	0.797	0.042	0.135	0.052	0.109	0.040	0.049
Natufian	Villabruna	Dzudzuana	Russia_Baikal_EN	Mbuti	0.546	0.003	0.863	0.005	0.129	0.052	0.098	0.032	0.075
Natufian	ElMiron	Dzudzuana	Russia_Baikal_EN	Mbuti	0.526	0.040	0.817	0.005	0.137	0.075	0.133	0.033	0.086
Natufian	Villabruna	ElMiron	Dzudzuana	Mbuti	0.365	0.075	0.062	0.669	0.194	0.284	0.095	0.523	0.174

Norway_Mesolithic	Villabruna	Dzudzuana	AG3	Russia_Baikal_EN	0.244	0.318	0.153	0.500	0.028	0.051	0.095	0.048	0.021
Norway_Mesolithic	Villabruna	ElMiron	Dzudzuana	AG3	0.057	0.244	0.053	0.205	0.498	0.108	0.051	0.127	0.054
Norway_Neolithic_HG	Villabruna	Dzudzuana	AG3	Russia_Baikal_EN	0.678	0.319	0.113	0.532	0.036	0.073	0.138	0.059	0.031
Norway_Neolithic_HG	Villabruna	ElMiron	Dzudzuana	AG3	0.532	0.189	0.049	0.261	0.502	0.097	0.054	0.119	0.057
Norway_Neolithic_HG	Villabruna	ElMiron	AG3	Russia_Baikal_EN	0.170	0.380	0.016	0.554	0.050	0.073	0.065	0.040	0.023
Norway_Neolithic_HG	Villabruna	ElMiron	AG3	Mbuti	0.053	0.341	0.030	0.593	0.036	0.090	0.073	0.034	0.029
Norwegian	Villabruna	Dzudzuana	AG3	Russia_Baikal_EN	0.080	0.071	0.717	0.183	0.030	0.023	0.041	0.026	0.012
Ossetian	Dzudzuana	AG3	Russia_Baikal_EN	Mbuti	0.204	0.776	0.158	0.063	0.003	0.041	0.030	0.019	0.032
Palestinian	Dzudzuana	AG3	Russia_Baikal_EN	Mbuti	0.470	0.807	0.102	0.021	0.069	0.039	0.029	0.019	0.034
Palestinian	Villabruna	Dzudzuana	AG3	Mbuti	0.306	0.009	0.747	0.129	0.116	0.030	0.078	0.027	0.035
PPNB	Villabruna	Dzudzuana	Russia_Baikal_EN	Mbuti	0.905	0.079	0.833	0.038	0.050	0.050	0.086	0.024	0.055
PPNB	ElMiron	Dzudzuana	Russia_Baikal_EN	Mbuti	0.693	0.027	0.923	0.039	0.012	0.050	0.087	0.025	0.055
PPNB	Villabruna	ElMiron	Dzudzuana	Mbuti	0.624	0.233	0.013	0.576	0.178	0.209	0.047	0.310	0.099
PPNB	Villabruna	Dzudzuana	AG3	Mbuti	0.598	0.076	0.803	0.018	0.103	0.053	0.101	0.034	0.043
PPNB	ElMiron	Dzudzuana	AG3	Mbuti	0.374	0.025	0.902	0.009	0.063	0.055	0.107	0.036	0.043
Russia_Popovo2	Villabruna	Dzudzuana	AG3	Russia_Baikal_EN	0.720	0.163	0.169	0.635	0.033	0.075	0.194	0.126	0.059
Russia_Popovo2	Villabruna	Dzudzuana	AG3	Mbuti	0.575	0.154	0.180	0.656	0.010	0.095	0.317	0.204	0.068
Russia_Sidelkino	Villabruna	Dzudzuana	AG3	Russia_Baikal_EN	0.358	0.111	0.259	0.597	0.033	0.041	0.091	0.050	0.022
Russia_Sidelkino	Villabruna	ElMiron	Dzudzuana	AG3	0.246	0.010	0.017	0.420	0.552	0.108	0.058	0.125	0.064
Russia_UzOO77	Villabruna	Dzudzuana	AG3	Russia_Baikal_EN	0.754	0.175	0.074	0.716	0.035	0.054	0.139	0.078	0.030
Russia_UzOO77	Villabruna	ElMiron	AG3	Russia_Baikal_EN	0.652	0.215	0.005	0.742	0.039	0.062	0.058	0.033	0.026
Russia_UzOO77	Villabruna	Dzudzuana	AG3	Mbuti	0.613	0.146	0.140	0.698	0.016	0.077	0.256	0.145	0.048
Russia_UzOO77	Villabruna	ElMiron	Dzudzuana	AG3	0.559	0.157	0.008	0.122	0.713	0.137	0.057	0.235	0.127
Russia_UzOO77	Villabruna	AG3	Russia_Baikal_EN	Mbuti	0.538	0.204	0.749	0.045	0.002	0.033	0.034	0.046	0.051
Russia_UzOO77	Villabruna	ElMiron	AG3	Mbuti	0.473	0.200	0.007	0.765	0.028	0.076	0.061	0.027	0.034
Saharawi	Dzudzuana	AG3	Russia_Baikal_EN	Mbuti	0.456	0.818	0.046	0.013	0.124	0.043	0.032	0.021	0.038
Saharawi	Villabruna	Dzudzuana	AG3	Mbuti	0.399	0.011	0.775	0.060	0.154	0.037	0.089	0.028	0.044
Samara_HG	Villabruna	Dzudzuana	AG3	Russia_Baikal_EN	0.255	0.234	0.019	0.645	0.102	0.066	0.165	0.084	0.037
Samara_HG	Villabruna	ElMiron	AG3	Russia_Baikal_EN	0.070	0.183	0.060	0.655	0.102	0.069	0.067	0.035	0.026
Sardinian	Villabruna	Dzudzuana	AG3	Mbuti	0.314	0.105	0.711	0.127	0.056	0.039	0.083	0.027	0.030
Saudi	Dzudzuana	AG3	Russia_Baikal_EN	Mbuti	0.261	0.839	0.075	0.024	0.062	0.042	0.032	0.021	0.037
Serbia_HG	Villabruna	Dzudzuana	AG3	Russia_Baikal_EN	0.639	0.649	0.168	0.177	0.006	0.094	0.117	0.057	0.030
Serbia_HG	Villabruna	Dzudzuana	AG3	Mbuti	0.595	0.725	0.052	0.193	0.030	0.232	0.350	0.077	0.078
Shetlandic	Villabruna	Dzudzuana	AG3	Russia_Baikal_EN	0.143	0.074	0.710	0.192	0.024	0.023	0.040	0.025	0.012
Shetlandic	Villabruna	Dzudzuana	AG3	Mbuti	0.093	0.111	0.593	0.253	0.044	0.041	0.099	0.037	0.030
Sicilian	Villabruna	Dzudzuana	AG3	Mbuti	0.135	0.051	0.727	0.154	0.068	0.038	0.093	0.031	0.035
Sorb	Villabruna	Dzudzuana	AG3	Russia_Baikal_EN	0.113	0.090	0.678	0.203	0.029	0.023	0.039	0.024	0.012
Sorb	Villabruna	Dzudzuana	AG3	Mbuti	0.066	0.125	0.555	0.264	0.055	0.039	0.093	0.032	0.030
Spanish	Villabruna	Dzudzuana	AG3	Mbuti	0.107	0.105	0.659	0.180	0.056	0.039	0.089	0.030	0.029
Spanish_North	Villabruna	Dzudzuana	AG3	Mbuti	0.064	0.163	0.564	0.193	0.081	0.051	0.113	0.036	0.036
Sweden_Mesolithic	Villabruna	ElMiron	Dzudzuana	AG3	0.685	0.259	0.069	0.275	0.396	0.070	0.041	0.084	0.037
Sweden_Mesolithic	Villabruna	Dzudzuana	AG3	Russia_Baikal_EN	0.384	0.377	0.209	0.399	0.015	0.048	0.082	0.038	0.019
Syrian	Dzudzuana	AG3	Russia_Baikal_EN	Mbuti	0.412	0.810	0.106	0.031	0.053	0.041	0.031	0.020	0.035
Tunisian	Dzudzuana	AG3	Russia_Baikal_EN	Mbuti	0.213	0.825	0.063	0.031	0.082	0.041	0.031	0.020	0.036
Tunisian	Villabruna	Dzudzuana	AG3	Mbuti	0.113	0.023	0.715	0.103	0.159	0.038	0.100	0.028	0.047
Turkish	Dzudzuana	AG3	Russia_Baikal_EN	Mbuti	0.159	0.811	0.122	0.056	0.011	0.040	0.030	0.019	0.032

Ukraine_Mesolithic	Villabruna	ElMiron	Dzudzuana	AG3	0.192	0.335	0.017	0.124	0.525	0.093	0.040	0.117	0.047
Ukraine_Mesolithic	Villabruna	Dzudzuana	AG3	Russia_Baikal_EN	0.117	0.292	0.196	0.499	0.013	0.040	0.072	0.036	0.017
Ukraine_Neolithic	Villabruna	Dzudzuana	AG3	Russia_Baikal_EN	0.324	0.345	0.204	0.427	0.024	0.038	0.067	0.032	0.015
Ukraine_Neolithic	Villabruna	ElMiron	Dzudzuana	AG3	0.209	0.248	0.033	0.300	0.419	0.067	0.032	0.079	0.033
Ukraine_Neolithic	Villabruna	Dzudzuana	AG3	Mbuti	0.141	0.330	0.227	0.439	0.005	0.091	0.203	0.080	0.039
Ukrainian	Villabruna	Dzudzuana	AG3	Russia_Baikal_EN	0.059	0.070	0.707	0.194	0.030	0.025	0.041	0.025	0.013
Yemeni	Dzudzuana	AG3	Russia_Baikal_EN	Mbuti	0.160	0.745	0.093	0.029	0.133	0.043	0.030	0.020	0.038
German	Villabruna	Dzudzuana	AG3	Mbuti	0.029	0.087	0.662	0.226	0.025	0.047	0.113	0.040	0.033
German	Villabruna	Dzudzuana	AG3	Russia_Baikal_EN	0.017	0.049	0.762	0.174	0.015	0.024	0.042	0.026	0.013
Orcadian	Villabruna	Dzudzuana	AG3	Mbuti	0.034	0.117	0.583	0.256	0.044	0.050	0.119	0.042	0.035
Orcadian	Villabruna	Dzudzuana	AG3	Russia_Baikal_EN	0.024	0.064	0.726	0.188	0.021	0.024	0.042	0.026	0.012
Romanian	Villabruna	Dzudzuana	AG3	Russia_Baikal_EN	0.007	0.009	0.815	0.149	0.027	0.023	0.041	0.027	0.014
Romanian	Villabruna	Dzudzuana	AG3	Mbuti	0.006	0.064	0.653	0.225	0.058	0.049	0.122	0.042	0.039
Karelia_HG	Villabruna	ElMiron	AG3	Russia_Baikal_EN	0.014	0.195	0.054	0.693	0.058	0.064	0.057	0.032	0.022

Table S4.5: Feasible models with N=5 sources

Test						P-value	Mixture Proportions					Standard Errors				
	A	B	C	D	E		A	B	C	D	E	A	B	C	D	E
Abkhasian	Villabruna	Dzudzuana	AG3	Russia_Baikal_EN	Mbuti	0.149	0.041	0.656	0.190	0.031	0.082	0.035	0.106	0.043	0.019	0.049
Adygei	Villabruna	Dzudzuana	AG3	Russia_Baikal_EN	Mbuti	0.087	0.030	0.689	0.189	0.055	0.036	0.035	0.107	0.044	0.019	0.047
Albanian	Villabruna	Dzudzuana	AG3	Russia_Baikal_EN	Mbuti	0.456	0.070	0.737	0.160	0.032	0.001	0.039	0.096	0.039	0.020	0.043
Algerian	Villabruna	Dzudzuana	AG3	Russia_Baikal_EN	Mbuti	0.122	0.034	0.726	0.093	0.025	0.122	0.043	0.120	0.039	0.020	0.065
Anatolia_N	Villabruna	ElMiron	Dzudzuana	AG3	Mbuti	0.410	0.129	0.002	0.735	0.066	0.068	0.177	0.039	0.299	0.038	0.082
Armenian	Villabruna	Dzudzuana	AG3	Russia_Baikal_EN	Mbuti	0.060	0.013	0.766	0.142	0.024	0.055	0.036	0.103	0.042	0.021	0.051
Assyrian	Villabruna	Dzudzuana	AG3	Russia_Baikal_EN	Mbuti	0.243	0.024	0.733	0.144	0.029	0.071	0.032	0.092	0.038	0.020	0.047
Balkar	Villabruna	Dzudzuana	AG3	Russia_Baikal_EN	Mbuti	0.431	0.047	0.643	0.194	0.063	0.053	0.033	0.097	0.039	0.017	0.042
Basque	Villabruna	Dzudzuana	AG3	Russia_Baikal_EN	Mbuti	0.133	0.160	0.602	0.184	0.027	0.027	0.047	0.109	0.041	0.018	0.042
BedouinA	Villabruna	Dzudzuana	AG3	Russia_Baikal_EN	Mbuti	0.077	0.003	0.794	0.099	0.032	0.072	0.035	0.099	0.038	0.020	0.052
BedouinB	Villabruna	Dzudzuana	AG3	Russia_Baikal_EN	Mbuti	0.077	0.005	0.831	0.073	0.031	0.060	0.036	0.097	0.037	0.021	0.052
Belarusian	Villabruna	Dzudzuana	AG3	Russia_Baikal_EN	Mbuti	0.195	0.169	0.498	0.271	0.038	0.024	0.047	0.119	0.046	0.018	0.043
Bulgarian	Villabruna	Dzudzuana	AG3	Russia_Baikal_EN	Mbuti	0.381	0.093	0.672	0.177	0.036	0.021	0.038	0.094	0.038	0.018	0.040
Canary_Islander	Villabruna	Dzudzuana	AG3	Russia_Baikal_EN	Mbuti	0.397	0.169	0.534	0.176	0.009	0.112	0.068	0.163	0.052	0.024	0.069
Chuvash	Villabruna	Dzudzuana	AG3	Russia_Baikal_EN	Mbuti	0.121	0.109	0.456	0.272	0.149	0.013	0.038	0.116	0.046	0.017	0.039
Croatian	Villabruna	Dzudzuana	AG3	Russia_Baikal_EN	Mbuti	0.137	0.102	0.645	0.209	0.022	0.023	0.041	0.105	0.043	0.019	0.043
Cypriot	Villabruna	Dzudzuana	AG3	Russia_Baikal_EN	Mbuti	0.215	0.035	0.751	0.135	0.024	0.054	0.037	0.099	0.039	0.020	0.049
Czech	Villabruna	Dzudzuana	AG3	Russia_Baikal_EN	Mbuti	0.053	0.130	0.593	0.230	0.036	0.011	0.047	0.125	0.050	0.018	0.047
Druze	Villabruna	Dzudzuana	AG3	Russia_Baikal_EN	Mbuti	0.163	0.024	0.764	0.127	0.023	0.061	0.034	0.095	0.038	0.020	0.047
English	Villabruna	Dzudzuana	AG3	Russia_Baikal_EN	Mbuti	0.249	0.151	0.576	0.233	0.031	0.008	0.044	0.111	0.045	0.018	0.043
Estonian	Villabruna	Dzudzuana	AG3	Russia_Baikal_EN	Mbuti	0.295	0.181	0.487	0.279	0.040	0.012	0.047	0.122	0.049	0.018	0.044
Finnish	Villabruna	Dzudzuana	AG3	Russia_Baikal_EN	Mbuti	0.391	0.134	0.531	0.259	0.073	0.003	0.045	0.118	0.045	0.017	0.042
French	Villabruna	Dzudzuana	AG3	Russia_Baikal_EN	Mbuti	0.260	0.142	0.589	0.214	0.031	0.025	0.041	0.102	0.040	0.017	0.040
Georgian	Villabruna	Dzudzuana	AG3	Russia_Baikal_EN	Mbuti	0.135	0.026	0.710	0.171	0.028	0.064	0.037	0.108	0.042	0.020	0.052
Greek	Villabruna	Dzudzuana	AG3	Russia_Baikal_EN	Mbuti	0.145	0.066	0.721	0.158	0.032	0.023	0.037	0.097	0.039	0.018	0.043
Hungarian	Villabruna	Dzudzuana	AG3	Russia_Baikal_EN	Mbuti	0.239	0.128	0.608	0.216	0.037	0.011	0.041	0.105	0.042	0.017	0.041
Iberia_Chan	Villabruna	ElMiron	Dzudzuana	AG3	Russia_Baikal_EN	0.379	0.099	0.771	0.072	0.056	0.003	0.164	0.102	0.210	0.053	0.032
Icelandic	Villabruna	ElMiron	Dzudzuana	AG3	Russia_Baikal_EN	0.479	0.018	0.003	0.772	0.188	0.018	0.050	0.032	0.052	0.025	0.013
Icelandic	Villabruna	Dzudzuana	AG3	Russia_Baikal_EN	Mbuti	0.300	0.126	0.612	0.223	0.032	0.007	0.042	0.105	0.043	0.020	0.042
Iranian	Villabruna	Dzudzuana	AG3	Russia_Baikal_EN	Mbuti	0.116	0.016	0.674	0.192	0.033	0.085	0.031	0.098	0.041	0.018	0.047
Iranian_Bandari	Villabruna	Dzudzuana	AG3	Russia_Baikal_EN	Mbuti	0.317	0.003	0.639	0.178	0.041	0.138	0.032	0.108	0.041	0.019	0.056
Irish	Villabruna	Dzudzuana	AG3	Russia_Baikal_EN	Mbuti	0.300	0.146	0.547	0.249	0.033	0.025	0.039	0.101	0.042	0.017	0.039
Irish_Ulster	Villabruna	Dzudzuana	AG3	Russia_Baikal_EN	Mbuti	0.186	0.160	0.541	0.236	0.042	0.020	0.044	0.112	0.047	0.019	0.042
Italian_South	Villabruna	Dzudzuana	AG3	Russia_Baikal_EN	Mbuti	0.191	0.072	0.723	0.143	0.034	0.028	0.041	0.100	0.039	0.020	0.047
Jew_Ashkenazi	Villabruna	Dzudzuana	AG3	Russia_Baikal_EN	Mbuti	0.244	0.063	0.761	0.115	0.042	0.019	0.042	0.108	0.043	0.020	0.049
Jew_Ethiopian	Villabruna	Dzudzuana	AG3	Russia_Baikal_EN	Mbuti	0.729	0.036	0.521	0.079	0.014	0.349	0.030	0.095	0.027	0.019	0.065
Jew_Georgian	Villabruna	Dzudzuana	AG3	Russia_Baikal_EN	Mbuti	0.423	0.033	0.718	0.155	0.032	0.062	0.036	0.101	0.040	0.020	0.048
Jew_Iranian	Villabruna	Dzudzuana	AG3	Russia_Baikal_EN	Mbuti	0.064	0.021	0.739	0.144	0.026	0.070	0.044	0.126	0.047	0.021	0.059
Jew_Iraqi	Villabruna	Dzudzuana	AG3	Russia_Baikal_EN	Mbuti	0.087	0.015	0.743	0.129	0.025	0.088	0.040	0.113	0.043	0.022	0.056
Jew_Libyan	Villabruna	Dzudzuana	AG3	Russia_Baikal_EN	Mbuti	0.373	0.055	0.717	0.119	0.024	0.084	0.038	0.099	0.039	0.020	0.049
Jew_Moroccan	Villabruna	Dzudzuana	AG3	Russia_Baikal_EN	Mbuti	0.236	0.032	0.781	0.112	0.027	0.049	0.042	0.111	0.042	0.022	0.055
Jew_Tunisian	Villabruna	Dzudzuana	AG3	Russia_Baikal_EN	Mbuti	0.159	0.070	0.695	0.118	0.032	0.085	0.043	0.120	0.045	0.022	0.059

Jew_Turkish	Villabruna	Dzudzuana	AG3	Russia_Baikal_EN	Mbuti	0.232	0.058	0.727	0.131	0.028	0.057	0.038	0.105	0.041	0.020	0.051
Jew_Yemenite	Villabruna	Dzudzuana	AG3	Russia_Baikal_EN	Mbuti	0.096	0.024	0.748	0.112	0.010	0.106	0.041	0.117	0.043	0.022	0.061
Jordanian	Villabruna	Dzudzuana	AG3	Russia_Baikal_EN	Mbuti	0.060	0.021	0.762	0.108	0.036	0.073	0.038	0.106	0.040	0.021	0.054
Kumyk	Villabruna	Dzudzuana	AG3	Russia_Baikal_EN	Mbuti	0.054	0.016	0.734	0.181	0.051	0.017	0.043	0.131	0.054	0.020	0.054
Latvia_HG	Villabruna	ElMiron	Dzudzuana	AG3	Russia_Baikal_EN	0.069	0.419	0.115	0.089	0.354	0.023	0.092	0.037	0.119	0.036	0.019
Lebanese	Villabruna	Dzudzuana	AG3	Russia_Baikal_EN	Mbuti	0.109	0.037	0.702	0.137	0.033	0.091	0.040	0.116	0.043	0.020	0.056
Lebanese_Christian	Villabruna	Dzudzuana	AG3	Russia_Baikal_EN	Mbuti	0.365	0.011	0.798	0.122	0.016	0.054	0.035	0.095	0.039	0.021	0.048
Lebanese_Muslim	Villabruna	Dzudzuana	AG3	Russia_Baikal_EN	Mbuti	0.156	0.016	0.776	0.116	0.033	0.060	0.036	0.100	0.039	0.020	0.050
Lezgin	Villabruna	Dzudzuana	AG3	Russia_Baikal_EN	Mbuti	0.264	0.049	0.599	0.266	0.034	0.053	0.032	0.098	0.044	0.019	0.044
Lithuanian	Villabruna	Dzudzuana	AG3	Russia_Baikal_EN	Mbuti	0.113	0.189	0.466	0.291	0.032	0.023	0.048	0.125	0.051	0.020	0.048
Maltese	Villabruna	Dzudzuana	AG3	Russia_Baikal_EN	Mbuti	0.475	0.061	0.723	0.156	0.030	0.030	0.037	0.096	0.038	0.020	0.045
Mordovian	Villabruna	Dzudzuana	AG3	Russia_Baikal_EN	Mbuti	0.162	0.119	0.534	0.260	0.071	0.016	0.040	0.113	0.046	0.017	0.043
Moroccan	Villabruna	Dzudzuana	AG3	Russia_Baikal_EN	Mbuti	0.230	0.030	0.704	0.071	0.013	0.183	0.037	0.103	0.034	0.019	0.058
Morocco_EN	ElMiron	Dzudzuana	AG3	Russia_Baikal_EN	Mbuti	0.607	0.007	0.686	0.031	0.024	0.252	0.087	0.220	0.059	0.036	0.129
Morocco_EN	Villabruna	Dzudzuana	AG3	Russia_Baikal_EN	Mbuti	0.598	0.029	0.644	0.031	0.023	0.272	0.060	0.163	0.056	0.035	0.108
Morocco_EN	Villabruna	ElMiron	Dzudzuana	Russia_Baikal_EN	Mbuti	0.574	0.230	0.025	0.239	0.024	0.482	0.402	0.085	0.875	0.034	0.450
Motala_HG	Villabruna	ElMiron	Dzudzuana	AG3	Russia_Baikal_EN	0.393	0.327	0.111	0.089	0.454	0.020	0.100	0.041	0.128	0.040	0.020
Mozabite	Villabruna	Dzudzuana	AG3	Russia_Baikal_EN	Mbuti	0.520	0.062	0.696	0.068	0.026	0.149	0.036	0.094	0.032	0.018	0.051
Natufian	Villabruna	ElMiron	Dzudzuana	AG3	Mbuti	0.466	0.035	0.059	0.682	0.053	0.171	0.185	0.078	0.354	0.043	0.114
Norway_Mesolithic	Villabruna	ElMiron	Dzudzuana	AG3	Russia_Baikal_EN	0.291	0.303	0.065	0.088	0.515	0.030	0.104	0.052	0.138	0.054	0.022
Norway_Neolithic_HG	Villabruna	ElMiron	Dzudzuana	AG3	Russia_Baikal_EN	0.503	0.270	0.047	0.124	0.525	0.034	0.145	0.057	0.219	0.073	0.036
Norwegian	Villabruna	Dzudzuana	AG3	Russia_Baikal_EN	Mbuti	0.421	0.143	0.565	0.233	0.040	0.018	0.043	0.110	0.044	0.017	0.041
Ossetian	Villabruna	Dzudzuana	AG3	Russia_Baikal_EN	Mbuti	0.114	0.030	0.679	0.190	0.059	0.042	0.038	0.112	0.043	0.018	0.049
Palestinian	Villabruna	Dzudzuana	AG3	Russia_Baikal_EN	Mbuti	0.288	0.023	0.739	0.121	0.017	0.100	0.032	0.091	0.035	0.019	0.048
Polish	Villabruna	Dzudzuana	AG3	Russia_Baikal_EN	Mbuti	0.279	0.161	0.518	0.259	0.036	0.025	0.041	0.104	0.042	0.017	0.040
PPNB	Villabruna	ElMiron	Dzudzuana	Russia_Baikal_EN	Mbuti	0.976	0.274	0.017	0.538	0.042	0.129	0.191	0.048	0.273	0.027	0.087
PPNB	Villabruna	ElMiron	Dzudzuana	AG3	Mbuti	0.424	0.207	0.020	0.581	0.025	0.167	0.193	0.049	0.308	0.035	0.095
Russian	Villabruna	Dzudzuana	AG3	Russia_Baikal_EN	Mbuti	0.122	0.140	0.497	0.273	0.074	0.017	0.042	0.117	0.047	0.016	0.041
Saharawi	Villabruna	Dzudzuana	AG3	Russia_Baikal_EN	Mbuti	0.228	0.015	0.782	0.052	0.011	0.139	0.040	0.109	0.038	0.022	0.062
Samara_HG	Villabruna	ElMiron	Dzudzuana	AG3	Russia_Baikal_EN	0.351	0.071	0.083	0.181	0.585	0.081	0.098	0.057	0.182	0.081	0.033
Sardinian	Villabruna	Dzudzuana	AG3	Russia_Baikal_EN	Mbuti	0.501	0.123	0.706	0.116	0.022	0.033	0.040	0.091	0.034	0.019	0.042
Saudi	Villabruna	Dzudzuana	AG3	Russia_Baikal_EN	Mbuti	0.106	0.010	0.809	0.082	0.021	0.077	0.043	0.118	0.042	0.023	0.062
Scottish	Villabruna	Dzudzuana	AG3	Russia_Baikal_EN	Mbuti	0.188	0.138	0.580	0.231	0.035	0.016	0.041	0.106	0.044	0.018	0.041
Shetlandic	Villabruna	Dzudzuana	AG3	Russia_Baikal_EN	Mbuti	0.546	0.133	0.593	0.232	0.035	0.008	0.038	0.096	0.041	0.018	0.038
Sicilian	Villabruna	Dzudzuana	AG3	Russia_Baikal_EN	Mbuti	0.354	0.068	0.738	0.132	0.033	0.029	0.037	0.097	0.038	0.019	0.045
Sorb	Villabruna	Dzudzuana	AG3	Russia_Baikal_EN	Mbuti	0.512	0.158	0.528	0.251	0.034	0.028	0.037	0.090	0.036	0.018	0.036
Spanish	Villabruna	Dzudzuana	AG3	Russia_Baikal_EN	Mbuti	0.243	0.116	0.678	0.156	0.031	0.019	0.039	0.094	0.037	0.018	0.040
Spanish_North	Villabruna	Dzudzuana	AG3	Russia_Baikal_EN	Mbuti	0.592	0.204	0.526	0.185	0.030	0.055	0.050	0.114	0.042	0.021	0.047
Sweden_Mesolithic	Villabruna	ElMiron	Dzudzuana	AG3	Russia_Baikal_EN	0.486	0.275	0.069	0.247	0.396	0.012	0.077	0.041	0.102	0.038	0.018
Syrian	Villabruna	Dzudzuana	AG3	Russia_Baikal_EN	Mbuti	0.328	0.017	0.738	0.130	0.023	0.092	0.035	0.099	0.039	0.020	0.050
Tunisian	Villabruna	Dzudzuana	AG3	Russia_Baikal_EN	Mbuti	0.112	0.035	0.724	0.087	0.026	0.128	0.042	0.116	0.038	0.019	0.060
Turkish	Villabruna	Dzudzuana	AG3	Russia_Baikal_EN	Mbuti	0.086	0.026	0.722	0.151	0.052	0.049	0.034	0.101	0.040	0.018	0.046
Turkish_Balikesir	Villabruna	Dzudzuana	AG3	Russia_Baikal_EN	Mbuti	0.096	0.062	0.597	0.178	0.085	0.077	0.048	0.156	0.057	0.020	0.069
Ukraine_Mesolithic	Villabruna	ElMiron	Dzudzuana	AG3	Russia_Baikal_EN	0.137	0.362	0.023	0.066	0.525	0.023	0.100	0.041	0.140	0.048	0.020
Ukraine_Neolithic	Villabruna	ElMiron	Dzudzuana	AG3	Russia_Baikal_EN	0.214	0.289	0.034	0.234	0.420	0.022	0.071	0.032	0.094	0.033	0.016
Ukrainian	Villabruna	Dzudzuana	AG3	Russia_Baikal_EN	Mbuti	0.529	0.163	0.491	0.266	0.033	0.046	0.043	0.111	0.044	0.018	0.044

Yemeni	Villabruna Dzudzuana AG3	Russia_Baikal_EN Mbuti	0.070	0.005 0.711 0.104 0.024 0.156	0.040 0.121 0.041 0.021 0.066
Chechen	Villabruna Dzudzuana AG3	Russia_Baikal_EN Mbuti	0.036	0.030 0.690 0.195 0.046 0.040	0.040 0.125 0.053 0.021 0.054
Romanian	Villabruna Dzudzuana AG3	Russia_Baikal_EN Mbuti	0.046	0.089 0.649 0.201 0.041 0.020	0.047 0.123 0.048 0.019 0.048

References

1. Lazaridis, I. *et al.* Ancient human genomes suggest three ancestral populations for present-day Europeans. *Nature* **513**, 409-413, (2014).
2. Haak, W. *et al.* Massive migration from the steppe was a source for Indo-European languages in Europe. *Nature* **522**, 207-211, (2015).
3. Lazaridis, I. *et al.* Genomic insights into the origin of farming in the ancient Near East. *Nature* **536**, 419-424, (2016).
4. Fu, Q. *et al.* The genetic history of Ice Age Europe. *Nature* **534**, 200-205, (2016).
5. de Barros Damgaard, P. *et al.* The first horse herders and the impact of early Bronze Age steppe expansions into Asia. *Science*, (2018).
6. Fu, Q. *et al.* Genome sequence of a 45,000-year-old modern human from western Siberia. *Nature* **514**, 445-449, (2014).
7. Sikora, M. *et al.* Ancient genomes show social and reproductive behavior of early Upper Paleolithic foragers. *Science*, (2017).
8. Raghavan, M. *et al.* Upper Palaeolithic Siberian genome reveals dual ancestry of Native Americans. *Nature* **505**, 87-91, (2014).
9. Yang, M. A. *et al.* 40,000-Year-Old Individual from Asia Provides Insight into Early Population Structure in Eurasia. *Curr. Biol.* **27**, 3202-3208.e3209, (2017).
10. Rasmussen, M. *et al.* The genome of a Late Pleistocene human from a Clovis burial site in western Montana. *Nature* **506**, 225-229, (2014).
11. Jones, E. R. *et al.* Upper Palaeolithic genomes reveal deep roots of modern Eurasians. *Nat. Commun.* **6**, 8912, (2015).
12. Olalde, I. *et al.* Derived immune and ancestral pigmentation alleles in a 7,000-year-old Mesolithic European. *Nature* **507**, 225-228, (2014).
13. Gamba, C. *et al.* Genome flux and stasis in a five millennium transect of European prehistory. *Nat. Commun.* **5**, 5257 (2014).
14. Mathieson, I. *et al.* The genomic history of southeastern Europe. *Nature* **555**, 197, (2018).
15. González-Fortes, G. *et al.* Paleogenomic Evidence for Multi-generational Mixing between Neolithic Farmers and Mesolithic Hunter-Gatherers in the Lower Danube Basin. *Curr. Biol.* **27**, 1801-1810.e1810, (2017).
16. Mathieson, I. *et al.* Genome-wide patterns of selection in 230 ancient Eurasians. *Nature* **528**, 499-503, (2015).
17. Günther, T. *et al.* Population genomics of Mesolithic Scandinavia: Investigating early postglacial migration routes and high-latitude adaptation. *PLoS Biol.* **16**, e2003703, (2018).
18. Fregel, R. *et al.* Ancient genomes from North Africa evidence prehistoric migrations to the Maghreb from both the Levant and Europe. *Proceedings of the National Academy of Sciences*, (2018).
19. Mitnik, A. *et al.* The Genetic History of Northern Europe. *bioRxiv*, (2017).
20. van de Loosdrecht, M. *et al.* Pleistocene North African genomes link Near Eastern and sub-Saharan African human populations. *Science*, (2018).
21. Patterson, N. *et al.* Ancient admixture in human history. *Genetics* **192**, 1065-1093, (2012).
22. Broushaki, F. *et al.* Early Neolithic genomes from the eastern Fertile Crescent. *Science* **353**, 499-503, (2016).
23. Jones, E. R. *et al.* The Neolithic Transition in the Baltic Was Not Driven by Admixture with Early European Farmers. *Curr. Biol.* **27**, 576-582, (2017).

24. Mittnik, A. *et al.* The genetic prehistory of the Baltic Sea region. *Nat. Commun.* **9**, 442, (2018).
25. Fregel, R. *et al.* Neolithization of North Africa involved the migration of people from both the Levant and Europe. *bioRxiv*, (2017).

Supplementary Information section 5

Dilution of Neandertal ancestry in West Eurasians

We have previously shown¹ that Basal Eurasian ancestry is associated with reduced Neandertal ancestry by showing that an estimate of Basal Eurasian ancestry is anti-correlated with the statistic $f_4(\textit{Test}, \textit{Mbuti}, \textit{Altai}, \textit{Denisova})$ which quantifies allele sharing between the *Test* population and the Altai Neandertal².

Here we provide further evidence for this phenomenon, taking into account a few developments since the original analysis. First, a second high quality Neandertal genome, closer to the Neandertal population that introgressed to non-Africans was published from Vindija Cave³. Second, it was shown⁴ that an f_4 -ratio estimate of Neandertal ancestry in a previous study⁵ which uses two African populations produces inconsistent answers in comparison to a new “direct” f_4 -ratio that uses only a single African population and the two published high quality Neandertal genomes. The discrepancy between the two ratios is interpreted in ref. 4 as a consequence of West Eurasian-related gene flow into Sub-Saharan Africa. Third, the analysis of the present study (Supplementary Information section 2) suggests that West Eurasian populations may have ancestry from at least two “deep” sources of ancestry, defined as lineages that split off from other non-Africans prior to the differentiation of Ust’Ishim and Tianyuan, thus raising the question whether one or both of these sources had reduced Neandertal ancestry.

Neandertal ancestry

We first present a new method of estimating Neandertal ancestry using $qpWave^6/qpAdm^7$ which has three advantages: unlike a simple f_4 -ratio, it formally tests whether an admixture model fits the data, it allows for the simultaneous use of all high quality genomes, including that of the Denisovan⁸, and it makes no use of African populations, thus not relying on any assumptions about the phylogeny of these populations or their relationship to or gene flow with non-Africans).

The model has Ust’Ishim and Vindija as sources and Altai, Chimp, and Denisova as outgroups and we show its application in Table S5.1, which shows that it cannot be rejected ($p > 0.05$) for most non-African populations, while it fails for Sub-Saharan African populations and also Papuans (who have substantial Denisovan-related ancestry). We also tried an alternative model in which the sources were Mbuti and Vindija (with the same outgroups); this allows us to also estimate the mixture proportion of Ust’Ishim, using Mbuti as a source, a population that has negligible Neandertal ancestry². The estimated proportions

of Neandertal ancestry (for the Mbuti+Vindija model) are strongly correlated with those of the Ust'Ishim+Vindija model (Fig. S5.1) with the estimates using Ust'Ishim as a baseline being 2% lower, reflecting the Neandertal ancestry in Ust'Ishim itself, which is estimated as $2.2 \pm 0.4\%$. However, the model of Mbuti+Vindija fails ($p < 0.05$) for most populations suggesting that even though the Mbuti+Vindija model largely captures the same information as the Ust'Ishim+Vindija one (Fig. S5.1), a phylogeny similar to that of ref. 4 in which non-African populations are a simple mix of Vindija- and African-related lineages is not a good fit to the data.

To understand why this is so, we examined the “dscore” output of qpAdm¹ which correspond to the statistic $f_4(\text{Test}, \text{Fitted Test}; \text{Altai}, O)$ and thus quantifies asymmetries between the actual *Test* population, its modeled version (*Fitted Test*) as a mixture of Mbuti+Vindija, with respect to an outgroup *O*; since we have three outgroups, *O* can be Chimp or Denisova. For *Test*=Ust'Ishim, the symmetry for *O*=Chimp is good ($|Z|=1.2$), and less so for Denisova ($Z=2.7$), suggesting that Denisova may not be correctly taken to be an outgroup. This population has been modeled as a 3-way mixture before² and resolving its phylogenetic relationship to the other populations is beyond the scope of this paper (we note that it was also not used in ref. 4). We thus obtain a separate estimate of the Vindija-related ancestry in Ust'Ishim using the direct ratio of ref. 4 of $\frac{f_4(\text{Altai}, \text{Chimp}; \text{Ust}'\text{Ishim}, \text{Mbuti})}{f_4(\text{Altai}, \text{Chimp}; \text{Vindija}, \text{Mbuti})}$ which is $1.6 \pm 0.4\%$

In the remainder of this section, we will use the Ust'Ishim+Vindija model (which fits most populations using Denisova as an outgroup). To convert these proportions of Neandertal ancestry (relative to Ust'Ishim) to proportions relative to Sub-Saharan Africans like Mbuti, we can either use the ratio estimate ($1.6 \pm 0.4\%$), the qpAdm estimate ($2.2 \pm 0.4\%$) or the inferred intercept from Fig. S5.1 (2%).

Basal Eurasian ancestry

The statistic $f_4(\text{Test}, \text{Tianyuan}; \text{Ust}'\text{Ishim}, \text{Chimp})$ quantifies allele sharing between *Test* and Ust'Ishim. If a population has “Deep” ancestry then it will share fewer alleles with Ust'Ishim than Tianyuan does. The value of the statistic depends on how deeply diverged the “Deep” ancestry is and also on the amount of this ancestry in *Test*. In Fig S5.2 we show the value of this statistic for all populations of Table S5.1 (except Tianyuan, which is used in the statistic). It is clear that Sub-Saharan African populations lack shared genetic drift between North African and West Eurasian populations, usually interpreted as the Out-of-Africa bottleneck.

Table S5.1 and Fig. S5.2 suggest that Near Eastern/North African populations both have reduced Ust’Ishim allele sharing (consistent with “Deep” ancestry) and reduced Neandertal ancestry. To formally test this association, we study the relationship of the Fig. S5.2 statistic against the Table S5.1 estimated proportion of Neandertal ancestry in Extended Data Fig. 8. We perform linear regression of the statistic on the proportion of Neandertal ancestry; all points of Table S5.2 for which the corresponding models of Table S5.1 fit are shown in Extended Data Fig. 8. The regression is performed on all “color” points of Extended Data Fig. 8 except Taforalt, Morocco_EN (which are outliers and also possess substantial ancestry from a different “Deep” lineage not present to the same extent in the Basal Eurasians; Fig. 2), and Russia_Popovo2 (a single individual which is an outlier and also has large standard errors). We also show present-day West Eurasian and North African populations (shotgun sequenced in the Simons Genetic Diversity Project⁹) in Extended Data Fig. 8 (small grey points); these are variable in terms of these two statistics and are largely included within the variation of the ancient samples; the present-day West Eurasians are not used in the regression as their dilution of Neandertal ancestry/Ust’Ishim affinity is in some cases due to African admixture (Extended Data Fig. 7).

To assess the variability of the inferred slope and intercept of the regression we repeat it 100 times deleting equally sized blocks of the genome. The estimated intercept is 0.001 ± 0.001 , suggesting that a population with as much Vindija-related ancestry as Ust’Ishim is symmetrically related with Tianyuan to Ust’Ishim (and thus has no “Deep” ancestry). However, the estimated slope is 0.436 ± 0.066 (>6 standard errors greater than zero), which confirms that reduced Neandertal ancestry is associated with the presence of “Deep” ancestry.

Thus, for a *Deep* population with 0% absolute Vindija-related ancestry (hence -2.2% relative to Ust’Ishim, taking this estimate from Table S5.2), we estimate that $f_4(\text{Deep}, \text{Tianyuan}; \text{Ust’Ishim}, \text{Chimp}) = -0.022 * 0.436 \approx -0.0096$. This is similar to the drift length of $11/1000 = 0.011$ estimated for the drift length shared by Ust’Ishim/Tianyuan to the exclusion of Basal Eurasians in the *qpGraph* model (Supplementary Information section 2; Fig. 2). Note also that $f_4(\text{Sub-Saharan African}, \text{Tianyuan}, \text{Ust’Ishim}, \text{Chimp})$ is maximized for *Sub-Saharan African*=Mota (Fig. S5.2) with a value of -0.031 ± 0.0008 . Thus, we can estimate that Basal Eurasians share $0.031 - 0.0096 \approx \sim 0.021$ units of genetic drift with other non-Africans after their split from eastern Africans like Mota; this is estimated as $(15+8)/1000 = 0.023$ by the *qpGraph* model.

The fact that the genetic drift before and after the Basal Eurasian split is estimated similarly by the admixture graph model of Fig. 2 (which uses no archaic samples or Chimp) and Extended Data Fig. 8

(which uses archaic ancestry estimated using Altai, Chimp, and Denisova as outgroups) provides two independent lines of evidence for our estimates of these quantities, suggesting that $\sim 2/3$ of the drift since the split from East Africans is shared by Basal Eurasians and an additional $\sim 1/3$ is shared by non-Basal Eurasian non-Africans. This suggests that the Basal Eurasians (so named because they occupy a basal position in the phylogeny of Eurasians¹⁰) did in fact experience most of the common bottleneck shared by Eurasians. (Note also, that if we used the lower (1.6%) estimate of absolute Neandertal ancestry in Ust’Ishim from the f_4 -ratio, this would imply even more shared genetic drift between Basal Eurasians and other non-Africans, since then $f_4(\text{Deep}, \text{Tianyuan}; \text{Ust’Ishim}, \text{Chimp}) = -0.016 * 0.436 \approx -0.007$.)

The other “Deep” lineage found in Taforalt (Fig. 2) experienced only 0.008 units of genetic drift with non-Africans (Fig. 2) and could be plausibly interpreted as having deep presence in (North) Africa. Note that Taforalt and the Neolithic of the Maghreb are well below the regression line (Extended Data Fig. 8) and thus lack more genetic drift with Ust’Ishim than is predicted by their level of archaic ancestry; this is expected if they trace their ancestry from a lineage that is even more deeply diverged than the Basal Eurasians.

The accumulation of genetic drift depends on elapsed time and the demography of the population. The f_2 -statistic (which measures genetic drift in the f -statistics framework) is analogous to F_{ST} for which the expression¹¹ $1 - F_{ST} = \left(1 - \frac{1}{2N_e}\right)^t$ relates time t in generations with the effective population size N_e . Thus, $t = \frac{\ln(1-F_{ST})}{\ln(1-\frac{1}{2N_e})}$. Assuming a conventional $N_e=10,000$ and taking $F_{ST} \approx 0.022$ (the mean of the f -statistic and $qpGraph$ estimates of 0.021 and 0.023) of the we obtain $t=445$ generations; with a generation length of 28.1 years¹², this corresponds to ~ 12.5 ky. Given the age of ~ 45 kya for Ust’Ishim¹³, it implies that Basal Eurasians split from other non-Africans >57.5 kya and also prior to the Neandertal admixture into Ust’Ishim¹³. We note that while anatomically modern humans were present in the Levant¹⁴ since at least ~ 177 kya, the region was also occupied by Neandertals intermittently and especially during 53-70kya (Amud Cave)¹⁵, although anatomically modern humans were certainly present there by ~ 55 kya (Manot Cave)¹⁶. We note, however, that there is uncertainty about the effective population size of humans of this period. For example, a point estimate of 1,203 for Ust’Ishim (ref.¹⁷) or a range of estimates using PSMC on modern genomes from around $\sim 2,000$ for ~ 45 kya increasing further back in time⁹.

With these caveats in mind, we propose a scenario in which

- (i) Basal Eurasians split from other non-Africans, and may have plausibly not participated in the Neandertal admixture of Ust’Ishim and other non-Africans. Their divergence from other non-

Africans has been recently estimated as having occurred 67.4-101kya using an independent method.¹⁸

- (ii) The Basal Eurasian split from other Eurasians may have involved migration of the ancestors of non-Basal Eurasians that brought them into contact with Levantine Neandertal populations followed by admixture.
- (iii) Subsequently, this mixed population dispersed across Eurasia established a relatively homogeneous ~2%-admixed set of Eurasian populations outside the Near East
- (iv) Admixture between Basal and non-Basal Eurasians in the Near East occurred at some time prior to our samples from Dzudzuana Cave.

Regardless of the accuracy of this scenario, our results provide additional evidence that Basal Eurasians did not experience Neandertal admixture and through Near Eastern populations such as Dzudzuana diluted this type of ancestry in later West Eurasians.

Table S5.1: Fitting the model Vindija+Ust'Ishim. Left=(*Test*, Vindija, Ust'Ishim), Right=(Altai, Denisova, Chimp).

Test	P-value for rank=1	Vindija-related ancestry	Std. error
Yoruba	2.40E-03	-0.022	0.004
Mbuti	9.47E-07	-0.022	0.004
Mota	1.41E-03	-0.021	0.005
Russia_Popovo2	4.89E-01	-0.017	0.011
Morocco_EN	5.38E-01	-0.015	0.005
Taforalt	3.98E-01	-0.015	0.004
PPNB	3.91E-01	-0.012	0.005
Dzudzuana	6.19E-01	-0.012	0.006
South_Africa_HG	3.92E-06	-0.011	0.005
Natufian	2.60E-01	-0.009	0.005
Iran_N	4.09E-01	-0.009	0.004
Jordanian.DG	8.68E-01	-0.008	0.004
Samaritan.DG	3.31E-01	-0.008	0.004
CHG	5.74E-01	-0.007	0.004
Ostuni1	8.03E-01	-0.007	0.006
AG3	2.47E-01	-0.007	0.007
Spanish.DG	2.60E-01	-0.006	0.004
Druze.DG	1.33E-01	-0.006	0.004
Iranian.DG	4.35E-01	-0.006	0.004
Abkhasian.DG	1.29E-01	-0.006	0.004
KO1	9.85E-01	-0.006	0.005
Serbia_HG	2.99E-01	-0.005	0.005
English.DG	5.40E-01	-0.005	0.004
Norway_Neolithic_HG	6.19E-01	-0.005	0.005
Chechen.DG	8.25E-01	-0.005	0.004
Anatolia_N	2.98E-01	-0.005	0.004
Mozabite.DG	9.88E-01	-0.005	0.004
Orcadian.DG	1.20E-01	-0.004	0.004
Palestinian.DG	1.85E-02	-0.004	0.004
Iraqi_Jew.DG	3.55E-01	-0.004	0.004
Estonian.DG	7.75E-01	-0.004	0.004
Vestonice16	2.88E-01	-0.004	0.005
Yemenite_Jew.DG	5.70E-01	-0.004	0.004
North_Ossetian.DG	5.12E-01	-0.004	0.004
BedouinB.DG	3.95E-01	-0.004	0.004
Croatia_Mesolithic_HG	7.47E-01	-0.004	0.006
French.DG	1.80E-01	-0.003	0.004
Crete.DG	2.83E-01	-0.003	0.004
Tuscan.DG	8.08E-01	-0.003	0.004
Turkish.DG	3.47E-01	-0.003	0.004
Kostenki14	6.92E-01	-0.003	0.005
MA1	1.02E-02	-0.003	0.005
Russia_Baikal_EN	3.38E-01	-0.003	0.004
Armenian.DG	4.20E-01	-0.003	0.004
Ukraine_Mesolithic	4.68E-02	-0.003	0.004
Russia_UzOO77	9.50E-01	-0.003	0.006
Greek.DG	9.26E-02	-0.002	0.004
Finnish.DG	4.81E-01	-0.002	0.004
Sweden_Mesolithic	7.39E-01	-0.002	0.004
Ukraine_Neolithic	8.08E-02	-0.002	0.004
Bichon	7.19E-01	-0.002	0.005
Georgian.DG	8.17E-02	-0.002	0.004
Karitiana	8.44E-02	-0.002	0.004
Polish.DG	2.87E-01	-0.002	0.004
Loschbour	4.35E-01	-0.001	0.005
Karelia_HG	5.04E-01	-0.001	0.005
Bulgarian.DG	5.24E-01	-0.001	0.004
Sunghir3	2.70E-01	-0.001	0.005
Russian.DG	6.10E-02	-0.001	0.004
Iron_Gates_HG	2.79E-01	-0.001	0.004
Icelandic.DG	7.67E-01	-0.001	0.004
Bergamo.DG	2.29E-01	-0.001	0.004
Sardinian.DG	8.09E-01	-0.001	0.004
Samara_HG	4.30E-01	-0.001	0.005
Basque.DG	2.49E-01	-0.001	0.004
Lezgin.DG	1.23E-01	0.000	0.004
Villabruna	6.46E-01	0.000	0.005
Han	1.78E-01	0.000	0.004
Hungarian.DG	5.59E-01	0.000	0.004
Czech.DG	4.35E-02	0.000	0.004
Motala_HG	3.24E-01	0.000	0.004
Adygei.DG	8.39E-01	0.001	0.004
Papuan	1.84E-22	0.001	0.004
Latvia_HG	7.38E-02	0.001	0.004
ElMiron	4.56E-01	0.001	0.006
Saami.DG	3.42E-01	0.001	0.004
Iberia_Canes	3.86E-03	0.001	0.005
Norway_Mesolithic	5.90E-01	0.001	0.005
Onge	1.65E-01	0.002	0.004
Albanian.DG	7.31E-01	0.002	0.005
Iberia_Chan	3.78E-01	0.002	0.005
Russia_Sidelkino	4.25E-01	0.002	0.005
LaBranca1	5.32E-01	0.003	0.005
GoyetQ116-1	2.55E-02	0.009	0.006

Table S5.2: Fitting the model Vindija+Mbuti. Left=(*Test*, Mbuti, Ust’Ishim), Right=(Altai, Denisova, Chimp).

Test	P-value for rank=1	Vindija-related ancestry	Std. error
Yoruba	1.33E-03	-0.001	0.002
Mota	2.94E-01	0.000	0.003
Taforalt	5.70E-06	0.006	0.003
Morocco_EN	3.83E-04	0.008	0.004
PPNB	2.75E-07	0.009	0.003
Russia_Popovo2	9.40E-03	0.009	0.011
South_Africa_HG	2.36E-01	0.009	0.003
Iran_N	7.45E-05	0.012	0.003
Jordanian.DG	1.49E-08	0.012	0.003
Samaritan.DG	3.12E-04	0.012	0.003
Dzudzuana	1.61E-03	0.013	0.006
CHG	1.20E-05	0.013	0.003
Druze.DG	2.40E-04	0.014	0.003
Spanish.DG	3.41E-05	0.014	0.003
Iranian.DG	3.06E-06	0.014	0.003
English.DG	2.89E-06	0.014	0.003
Natufian	8.81E-03	0.015	0.004
Abkhasian.DG	2.55E-04	0.015	0.003
Iraqi_Jew.DG	6.03E-06	0.015	0.003
Chechen.DG	8.27E-07	0.015	0.003
Mozabite.DG	1.70E-08	0.015	0.003
Yemenite_Jew.DG	5.01E-07	0.015	0.003
Norway_Neolithic_HG	3.24E-03	0.015	0.004
Orcadian.DG	1.75E-04	0.015	0.003
North_Ossetian.DG	4.35E-06	0.016	0.003
Anatolia_N	1.79E-06	0.016	0.003
Palestinian.DG	9.62E-04	0.016	0.003
BedouinB.DG	5.88E-06	0.016	0.003
Estonian.DG	1.29E-06	0.016	0.003
Crete.DG	2.72E-05	0.016	0.003
Tuscan.DG	3.86E-07	0.016	0.003
French.DG	1.33E-04	0.016	0.003
Turkish.DG	9.22E-06	0.017	0.003
KO1	2.69E-04	0.017	0.004
Armenian.DG	5.11E-06	0.017	0.003
Greek.DG	2.64E-04	0.017	0.003
Kostenki14	1.26E-04	0.017	0.004
Finnish.DG	1.87E-06	0.017	0.003
Georgian.DG	4.88E-04	0.018	0.003
Russia_UzOO77	6.51E-04	0.018	0.005
Bichon	1.57E-04	0.018	0.004
Ostuni1	1.85E-03	0.018	0.006
Tianyuan	1.48E-03	0.018	0.005
Karitiana	9.25E-04	0.018	0.003
Ukraine_Neolithic	1.36E-03	0.018	0.003
Ukraine_Mesolithic	5.38E-03	0.018	0.003
Vestonice16	1.28E-02	0.018	0.005
Bulgarian.DG	3.72E-06	0.018	0.003
Serbia_HG	3.34E-05	0.018	0.005
Sweden_Mesolithic	6.33E-06	0.019	0.003
Lezgin.DG	2.17E-04	0.019	0.003
Russian.DG	1.08E-03	0.019	0.003
Icelandic.DG	4.72E-07	0.019	0.003
Polish.DG	3.33E-04	0.019	0.003
Hungarian.DG	5.21E-06	0.019	0.003
Bergamo.DG	6.93E-05	0.019	0.003
Russia_Baikal_EN	1.55E-04	0.019	0.003
Iron_Gates_HG	1.03E-05	0.019	0.003
Sunghir3	8.16E-04	0.019	0.004
Sardinian.DG	3.46E-08	0.019	0.003
MA1	2.59E-01	0.019	0.004
Karelia_HG	1.88E-03	0.019	0.004
Han	1.58E-05	0.019	0.003
Czech.DG	1.17E-02	0.020	0.004
Basque.DG	5.29E-05	0.020	0.003
Loschbour	3.24E-04	0.020	0.004
Adygei.DG	5.83E-08	0.020	0.003
Norway_Mesolithic	2.44E-04	0.021	0.004
Motala_HG	1.85E-04	0.021	0.003
Croatia_Mesolithic_HG	7.78E-03	0.021	0.005
Latvia_HG	4.26E-04	0.021	0.003
Saami.DG	1.88E-05	0.021	0.003
Russia_Sidelkino	2.20E-04	0.021	0.004
Albanian.DG	6.37E-06	0.022	0.004
Onge	2.09E-04	0.022	0.003
Ust_Ishim	1.14E-06	0.022	0.004
AG3	2.96E-02	0.022	0.006
Villabruna	1.09E-03	0.022	0.004
Papuan	1.30E-07	0.022	0.003
Iberia_Canes	2.47E-01	0.023	0.004
Iberia_Chan	3.32E-03	0.024	0.004
LaBranca1	9.75E-04	0.024	0.004
Samara_HG	3.88E-01	0.025	0.005
EIMiron	6.15E-04	0.027	0.005
GoyetQ116-1	1.44E-01	0.029	0.005

Figure S5.1: Correlation of Vindija-related ancestry relative to Ust'Ishim and Mbuti. We plot estimates of Vindija-related ancestry from Tables S5.1 and S5.2

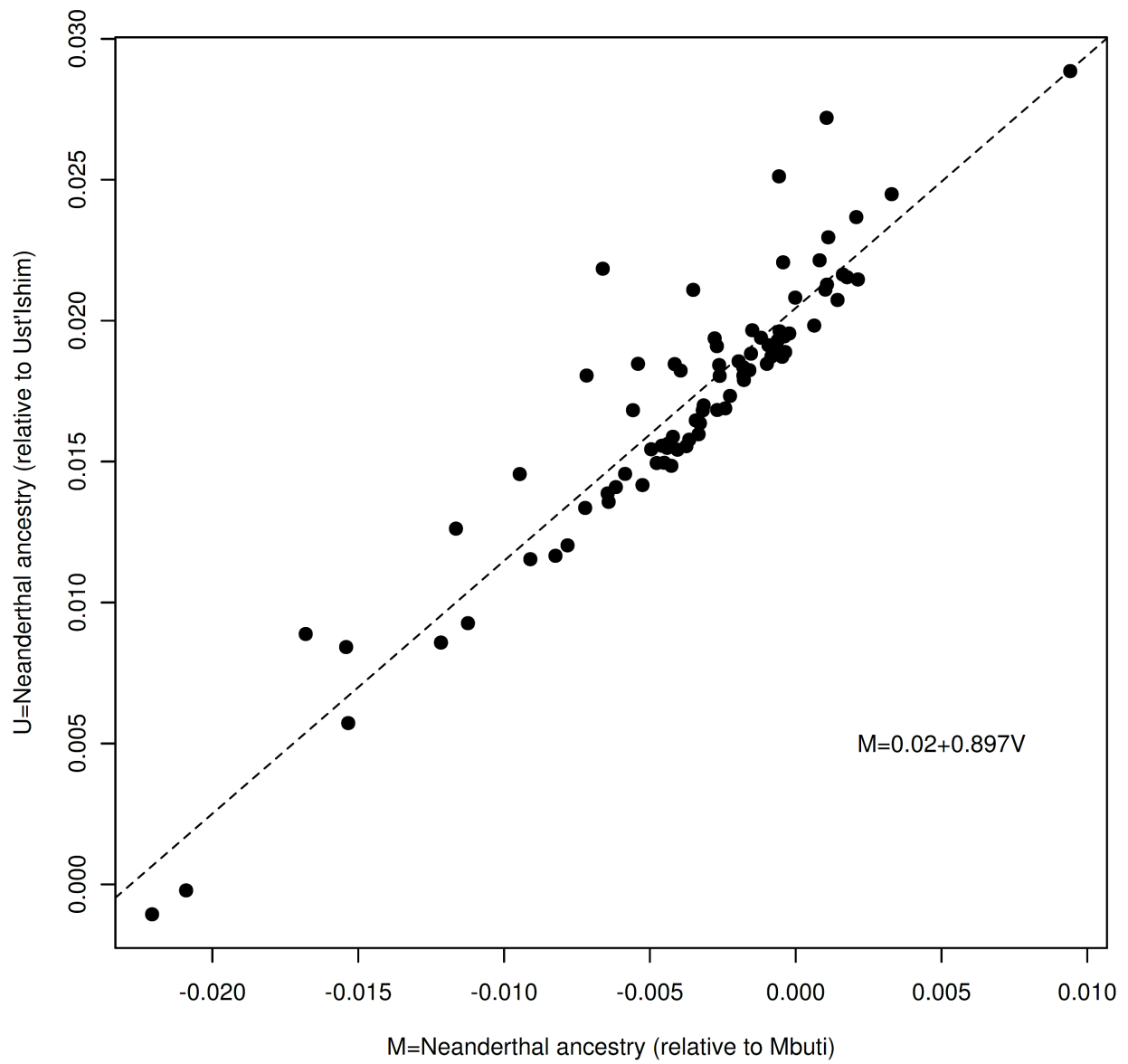
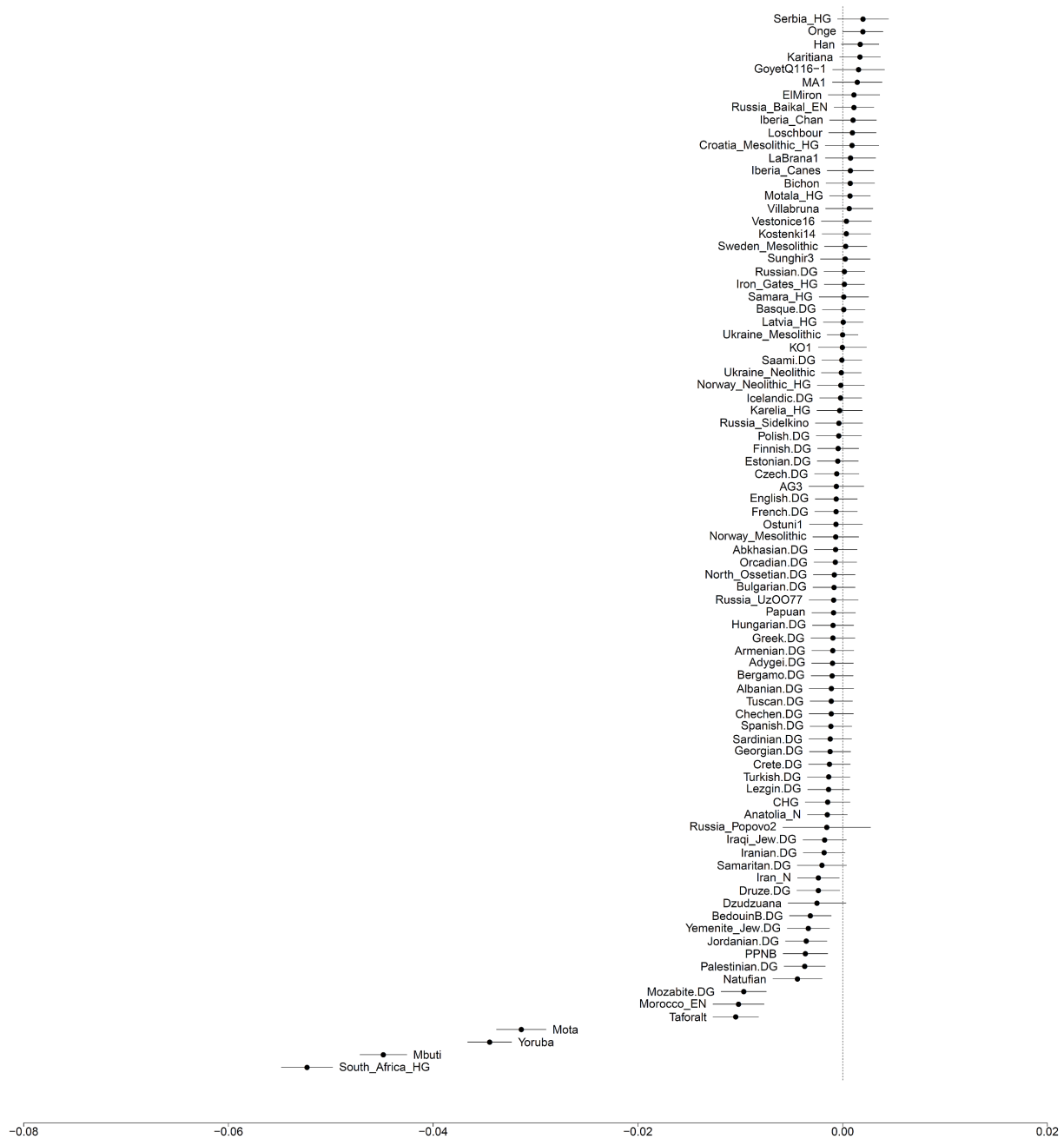


Figure S5.2: Allele sharing between *Test* and Ust’Ishim. We show the value of the statistic $f_4(\text{Test}, \text{Tianyuan}; \text{Ust’Ishim}, \text{Chimp})$ with 3 standard errors



References

1. Lazaridis, I. *et al.* Genomic insights into the origin of farming in the ancient Near East. *Nature* **536**, 419-424, (2016).
2. Prufer, K. *et al.* The complete genome sequence of a Neanderthal from the Altai Mountains. *Nature* **505**, 43-49, (2014).
3. Prüfer, K. *et al.* A high-coverage Neandertal genome from Vindija Cave in Croatia. *Science*, (2017).
4. Petr, M., Pääbo, S., Kelso, J. & Vernot, B. The limits of long-term selection against Neandertal introgression. *bioRxiv*, (2018).
5. Fu, Q. *et al.* The genetic history of Ice Age Europe. *Nature* **534**, 200-205, (2016).
6. Reich, D. *et al.* Reconstructing Native American population history. *Nature* **488**, 370-374, (2012).
7. Haak, W. *et al.* Massive migration from the steppe was a source for Indo-European languages in Europe. *Nature* **522**, 207-211, (2015).
8. Meyer, M. *et al.* A High-Coverage Genome Sequence from an Archaic Denisovan Individual. *Science* **338**, 222-226, (2012).
9. Mallick, S. *et al.* The Simons Genome Diversity Project: 300 genomes from 142 diverse populations. *Nature* **538**, 201-206, (2016).
10. Lazaridis, I. *et al.* Ancient human genomes suggest three ancestral populations for present-day Europeans. *Nature* **513**, 409-413, (2014).
11. Holsinger, K. E. & Weir, B. S. Genetics in geographically structured populations: defining, estimating and interpreting F_{ST} . *Nat. Rev. Genet.* **10**, 639, (2009).
12. Moorjani, P. *et al.* A genetic method for dating ancient genomes provides a direct estimate of human generation interval in the last 45,000 years. *Proceedings of the National Academy of Sciences* **113**, 5652, (2016).
13. Fu, Q. *et al.* Genome sequence of a 45,000-year-old modern human from western Siberia. *Nature* **514**, 445-449, (2014).
14. HersHKovitz, I. *et al.* The earliest modern humans outside Africa. *Science* **359**, 456, (2018).
15. Hallin, K. A., Schoeninger, M. J. & Schwarcz, H. P. Paleoclimate during Neandertal and anatomically modern human occupation at Amud and Qafzeh, Israel: the stable isotope data. *J. Hum. Evol.* **62**, 59-73, (2012).
16. HersHKovitz, I. *et al.* Levantine cranium from Manot Cave (Israel) foreshadows the first European modern humans. *Nature* **520**, 216-219, (2015).
17. Sikora, M. *et al.* Ancient genomes show social and reproductive behavior of early Upper Paleolithic foragers. *Science*, (2017).
18. Kamm, J. A., Terhorst, J., Durbin, R. & Song, Y. S. Efficiently inferring the demographic history of many populations with allele count data. *bioRxiv*, (2018).